

**Design, Synthesis and Biological Evaluation of
Cu(I) and Cu(II) Complexes with
bis(pyrazolyl)acetates and related Bioconjugated
Ligands**

Francesco Scorcelletti

Thesis to obtain the Master of Science
Degree in

Chemistry

Supervisors

Orientadores: Prof^a. Luísa Margarida Martins

Prof^a. Maura Pellei

Examination Committee

Chairperson: Prof^a. Maria Matilde Soares Duarte Marques

Supervisor: Prof^a. Luísa Margarida Martins

Member of the committee: Prof^a. Maria de Fátima Costa Guedes da Silva

Novembro de 2018

Acknowledgements

I would like to thank my tutors Unicam Prof. Maura Pellei and Prof. Carlo Santini to guide and support me in the thesis work. Especially I want to underline the importance that they put in the safety condition of the laboratory, particularly in cleaning, in the differentiation of the laboratory waste, and in the healthiness of the laboratory, allowing me to be safe in every moment.

I also want to acknowledge Prof. Fabio Del Bello, for the kind collaboration in the development of the bioconjugated ligands, and Prof. Luciano Marchiò for the X-Ray analyses on the crystals.

I sincerely want to acknowledge Prof. Matilda Marques, Prof. Fatima Guedes and Prof. Luísa Martins and all the other academic for what learned during the month spent in Lisbon.

This thesis was supported by the University of Camerino (FAR 2014-2015).

Resumo

Devido ao sucesso da cisplatina no tratamento de diferentes tipos de tumores, o desenvolvimento de complexos baseados em metais de transição como fármacos ganhou um impulso relevante. Os fenómenos de toxicidade e de resistência a fármacos de cisplatina limitam seu uso clínico, portanto a atenção tem sido focada em outros metais de transição. Especialmente fármacos à base de cobre têm sido investigadas na suposição de que um metal endógeno deverá ser menos tóxico em relação a outros fármacos metálicos e os investigadores têm dado grande atenção ao estudo do mecanismo de adsorção, distribuição, metabolismo e excreção de compostos à base de cobre.

Os ligandos polidentados doadores de nitrogénio derivados de poli(pirazol-1-il)metanos que possuem grupos funcionais orgânicos no carbono de ligação atraíram recentemente atenção considerável e a sua química de coordenação em relação ao grupo principal e de metais de transição tem sido extensivamente estudada. Neste trabalho foram sintetizados dois ligandos heteroescorpionatos carboxilados, $[\text{HC}(\text{CO}_2\text{H})(\text{pz}^{\text{Me}_2})_2]$ e $[\text{HC}(\text{CO}_2\text{H})(\text{pz})_2]$ e estudada a sua química de coordenação relativamente a aceitadores de cobre(II), a partir de cloreto de cobre ou perclorato, e aceitadores de cobre(I) na presença de coligandos de fosfano (trifenilfosfina e PTA). Os ligandos bis(pirazolil)acetatos também foram funcionalizados com o potente antagonista do recetor de NMDA (6,6-difenil-1,4-dioxan-2-il)metanamina, que mostrou uma atividade citotóxica significativa nas linhagens celulares de cancro da mama humano MCF7, expressando intensamente recetores de NMDA. Alguns complexos de cobre, bem como os correspondentes pro-ligandos não coordenados, foram avaliados quanto à sua atividade citotóxica relativamente a um painel de várias linhas celulares de tumores humanos.

Palavras-chave: Complexos de cobre (I/II), fármacos anticancerígenos, complexos baseados em metais de transição, ligandos heteroescorpionados, ligandos bioconjugados.

Abstract

Due to the success of cisplatin in the treatment of different type of tumors, the development of transition metal-based complexes as drugs have gained a relevant boost. Toxicity and drug resistance phenomena of cisplatin limit its clinical use, so the attention has been focused on other transition metals. Especially copper-based drugs have been investigated on the assumption that an endogenous metal should be less toxic with respect to other metallodrugs and researchers have putted great attention in the study of mechanism of adsorption, distribution, metabolism and excretion of copper-based compounds.

Polydentate nitrogen-containing donor ligands derived from poly(pyrazol-1-yl)methanes bearing organic functional groups on the bridging carbon have recently attracted considerable attention and their coordination chemistry towards main group and transition metals have been extensively studied. I have synthesized two carboxylated heteroscorpionate ligands, $[\text{HC}(\text{CO}_2\text{H})(\text{pz}^{\text{Me}_2})_2]$ and $[\text{HC}(\text{CO}_2\text{H})(\text{pz})_2]$ and I have studied their coordination chemistry towards copper(II) acceptors starting from copper chloride or perchlorate and copper(I) acceptors in the presence of phosphane coligands (triphenylphosphine and PTA). The bis(pyrazolyl)acetates ligands have also been functionalized with the potent NMDA receptor antagonist (6,6-diphenyl-1,4-dioxan-2-yl)methanamine, which showed a significant cytotoxic activity on MCF7 human breast cancer cell lines, highly expressing NMDA receptors. Some copper complexes as well as the corresponding uncoordinated ligands were evaluated for their cytotoxic activity towards a panel of several human tumour cell lines.

Key words: Copper(I/II) complexes, anticancer drugs, transition metal-based complexes, heteroscorpionate ligands, bioconjugated ligands.

Index

Acknowledgements	2
Resumo	3
Abstract	4
Index of figures	6
Index of tables	7
Abbreviation list	7
I. Introduction	9
THE BEGIN OF ANTICANCER THERAPY	9
ESSENTIAL ELEMENTS	10
COPPER CHEMISTRY	12
COPPER COMPLEXES AS ANTICANCER AGENTS	13
<i>N-donor systems, pyrazoles</i>	14
<i>P-donor phosphine ligands</i>	15
MECHANISTIC APPROACHES AND PROPOSED BIOLOGICAL TARGETS: STATE OF THE ART.....	17
<i>Copper complexes as DNA targeting drugs</i>	17
<i>Copper complexes as Topoisomerase I,II inhibitors</i>	19
<i>Copper Complexes as Proteasome Inhibitors</i>	20
<i>IN VIVO</i> ANTITUMOR STUDIES	22
HETEROSCORPIONATE LIGANDS: POLY(PYRAZOLYL)ACETATE AND THEIR APPLICATIONS	24
NMDA RECEPTORS	26
II. Experimental section	28
METHODS AND MATERIALS	28
SYNTHESIS OF THE LIGANDS.....	29
SYNTHESIS OF THE COMPLEXES.....	32
III. Results and discussion	38
SYNTHESIS AND CHARACTERIZATION OF THE LIGANDS	39
SYNTHESIS AND CHARACTERIZATION OF THE COMPLEXES	41
IV Appendix	51
V. References	76

Index of figures

Fig. 1.1. Structure of cis-diamminedichloroplatinum(II) and cisplatin bottle.....	9
Fig. 1.2. From left to right: Barnett Rosenberg (1926-2009), Michele Peyrone (1813-1883), Alfred Werner (1866-1916).....	10
Fig. 1.3. Structure of carboplatin and oxaliplatin.....	10
Fig. 1.4. Dose-response curve for essential elements in human body.....	11
Fig. 1.5. Number of articles in Web of Science on the topic “copper and anticancer” from 2000 to 2012.....	12
Fig. 1.6. Coordination geometry: square planar (C.N. 4), trigonal bipyramidal (C.N. 5), octahedral (C.N. 6).....	13
Fig. 1.7. Structure of: a) 2,2-bis(3,5-dimethyl-1H-pyrazol-1-yl)-N-(2-(2-methyl-5-nitro-1H-imidazol-1-yl)ethyl)acetamide ligand (HL ^{MN}); b) 1,3,4,6-tetra-O-acetyl-2-[[bis(3,5-dimethyl-1H-pyrazol-1-yl)acetyl]amino]-2-deoxy-β-D-glucopyranose ligand (HL ^{DAC}); c) the copper(II) cores [(L ^{MN}) ₂ Cu] ²⁺ and [(L ^{DAC}) ₂ Cu] ²⁺	14
Fig. 1.8. Structure of water soluble monodentate phosphines thp, thpp, and PTA.....	16
Fig. 1.9. Structure of [Cu(thp) ₄] ⁺ (a) and [Cu(PCN) ₂] ⁺ (b).....	16
Fig. 1.10. Schematic representation of intercalative (left) and groove (right) binding.....	18
Fig. 1.11. Schematic representation of Topoisomerase I and II mode of action.....	19
Fig. 1.12. Schematic diagrams of cellular pathways involved in proteasome inhibition induced by copper compounds. a) Apoptosis triggered by DTC copper(II) complexes; b) paraptosis caused by phosphine copper(I) and thioxotriazole copper(II) complexes.....	20
Fig. 1.13. Structure of: a) [TiCl ₃ (κ ³ -bis(3,5-dimethylpyrazol-1-yl)acetate)]; b) [TiCl ₂ (κ ³ -bis(3,5-dimethylpyrazol-1-yl)acetate){O(CH ₂) ₄ Cl}.....	25
Fig. 1.14. Structure of: a) {RuCl[κ ³ -bis(pyrazol-1-yl)acetate](CHPh)(PCy ₃)} and {RuCl[κ ³ -bis(3,5-dimethylpyrazol-1-yl)acetate](CHPh)(PCy ₃)}; b) of [RuCl(bis(pyrazol-1-yl)acetate)(CO) ₂] and [RuCl(2,2-bis(3,5-dimethylpyrazol-1-yl)propionate)(CO) ₂].....	26
Fig. 1.15. Structure of Phencyclidine (PCP).....	27
Fig. 1.16. Structure of: a) 1,4- dioxane scaffold; b) (±)-(6,6-Diphenyl-1,4-dioxan-2-yl)methanamine.....	27
Fig. 3.1. Reaction scheme of the synthesis of 1 and 2	39
Fig. 3.2. Reaction scheme of the synthesis of 3 : (a) NaH, (CH ₃) ₃ Si, DMSO (b) Na, CH ₂ =CHCH ₂ OH; (c) <i>m</i> -CPBA, CH ₂ Cl ₂ ; (d) (1 <i>S</i>)-(+)-CSA, CH ₂ Cl ₂ ; (e) <i>p</i> -TsCl, pyridine; (f) NaN ₃ , DMF; (g) LiAlH ₄ , Et ₂ O.....	40
Fig. 3.3. Reaction scheme of the synthesis of 4 and 5	40
Fig. 3.4. Reaction scheme of the syntheses of 6 and 7	42
Fig. 3.5. Crystal structure of [(L ²) ₂ Cu].....	42

Fig. 3.6. Reaction scheme of the syntheses of 8 and 9	43
Fig. 3.7. Crystal structure of [(L) ₂ Cu].....	44
Fig. 3.8. Reaction scheme of the syntheses of complexes 10 and 11	47
Fig. 3.9. Reaction scheme of the syntheses of 12 and 13	48
Fig. 3.10. Reaction scheme of the syntheses of 14 and 15	50

Index of tables

Table 1.1. Percentage (by weight) of composition of selected elements in human body... 11
Table 1.2. Copper complexes recently tested in <i>in vivo</i> experiments ⁴¹ 24
Table 3.1. Crystal data and structure refinement for [(L) ₂ Cu]..... 45
Table 3.2. Atomic coordinates (x 10 ⁴) and equivalent isotropic displacement parameters (Å ² x 10 ³) for [(L) ₂ Cu]. U(eq) is defined as one third of the trace of the orthogonalized U ^{ij} tensor..... 46

Abbreviation list

AB q – AB quartet
ADME – Absorption, Distribution, Metabolism, Excretion
bhpe – (bis[bis(hydroxymethyl)phosphino]ethane
br – broad
C.N. – Coordination Number
CDI – Carbonyldiimidazole
CNS – Central Nervous System
Cp – Cyclopentadienyl
Cp* - 1,2,3,4,5-pentamethylcyclopentadiene
CPBA – Chloroperoxybenzoic acid
CSA – Camphorsulfonic acid
Ctr – Copper transporter protein
Cy – Cyclohexyl
d – doublet
dd – doublet of doublets
DMF – Dimethylformamide
DMSO – Dimethyl sulfoxide
DNA – Deoxyribonucleic acid
DTC – Dithiocarbamate
EDTA – Ethylenediaminetetraacetic acid
ER – Endoplasmic Reticulum
ESIMS – Electrospray Ionization Mass Spectrometry
FT-IR – Fourier Transform Infrared spectroscopy
HPLC – High Performance Liquid Chromatography

IC₅₀ – half maximal inhibitory concentration
IR – Infrared spectroscopy
m – multiplet
Mp – Melting point
NCI – National Cancer Institute
NHC – N-Heterocyclic Carbene
NMR – Nuclear Magnetic Resonance
PCD – Programmed Cell Death
PCN – tris-(cyanoethyl)phospine
PCP – Phencyclidine
Pcy – Tricyclohexylphospine
phen – phenantroline
PTA – 1,3,5-Triaza-7-phosphaadamantane
Pz – Pyrazole
s – singlet
s br – broad singlet
TBAB – Tetra-n-butylammonium bromide
THF – Tetrahydrofuran
thp – tris-(hydroxymethyl)phospine
thpp – tris-(hydroxypropyl)phospine
Topo I – Topoisomerase I
Topo II – Topoisomerase II
UPR – Unfolded Protein Response
v br – very broad
XAS – X-ray Absorption Spectroscopy

I. Introduction

The begin of anticancer therapy

In medicinal chemistry organic compounds and natural products were almost the entirety of the drug used. During the past three decades metal complexes have gained a growing interest as pharmaceuticals for the use as diagnostic agents or as chemotherapeutic drugs¹⁻⁷. The widespread success of cisplatin (cis-diamminedichloroplatinum(II), Fig. 1.1) in the clinical treatment of various types of neoplasias has placed coordination chemistry of metal-based drugs in the frontline in the fight against cancer in the 20th century^{1, 8-10}.



Fig. 1.1. Structure of cis-diamminedichloroplatinum(II) and cisplatin bottle.

The anticancer property of cis-diamminedichloroplatinum(II) was discovered accidentally in 1965 by the American chemist Barnett Rosenberg¹¹ during an experiment on the influence of electric fields in cellular growth. However, the first who synthesized cisplatin was the Italian chemist Michele Peyrone in 1845¹², with the historical name of "Peyrone's chloride"; the Nobel Prize Alfred Werner first elucidated the structure only in 1893.

The goodness of cisplatin is the high efficacy in treating a wide range of cancers, especially testicular cancer, for which the overall cure rate exceeds 90%².



Fig. 1.2. From left to right: Barnett Rosenberg (1926-2009), Michele Peyrone (1813-1883), Alfred Werner (1866-1916).

Unfortunately the cure with cisplatin is limited by the drawbacks, such as the dose limiting effects¹³, nephrotoxicity, emetogenesis and neurotoxicity² and by inherited or acquired resistance phenomena, only partially overcome by the development of new platinum drugs, such as carboplatin and oxaliplatin (Fig. 1.3.)¹⁴⁻¹⁷.

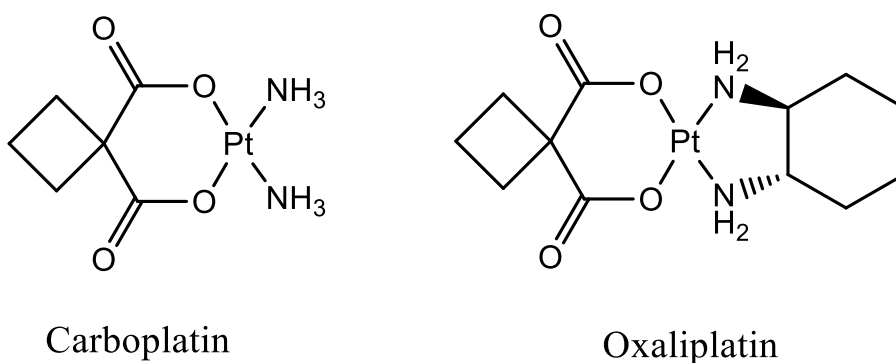


Fig. 1.3. Structure of carboplatin and oxaliplatin.

The side effects have encouraged an extensive research in this field, and rapidly chemists developed alternative antitumor-active inorganic complexes, based on different metals, with improved pharmacological properties and pointed to different targets¹⁸.

Essential elements

One of the research strategies is focused on the use of biologically active complexes formed by essential ions, based on the assumption that endogenous metals may be less toxic for normal cells with respect to cancer cells. All the biological systems tend to concentrate some elements and to reject others, like a natural selection.

Element	Percentage (by weight)	Element	Percentage (by weight)
Oxygen	53.6	Silicon, Magnesium	0.04
Carbon	16.0	Iron, fluorine	0.005
Hydrogen	13.4	Zinc	0.003
Nitrogen	2.4	Copper, bromine	2×10^{-4}
Sodium, potassium, sulfur	0.10	Selenium, manganese, arsenic, nickel	2×10^{-5}
Chlorine	0.09	Lead, cobalt	9×10^{-6}

Table 1.1. Percentage (by weight) of composition of selected elements in human body.

The base elements are four and represent more than the 99% of the number of the atoms: hydrogen, oxygen, carbon and nitrogen. Other seven represent the 0.9% of the number of the atoms and are considered essentials: sodium, potassium, calcium, magnesium, phosphorus, sulphur and chlorine. In addition, some elements are essential only for some species, like manganese, iron, cobalt, nickel, copper and zinc (Table 1.1.).

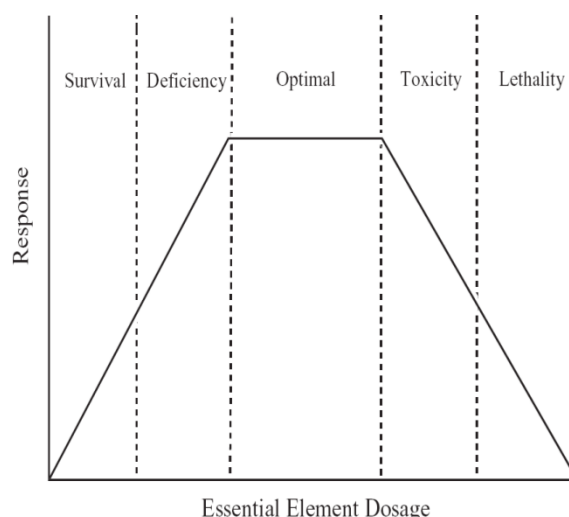


Fig. 1.4. Dose-response curve for essential elements in human body.

These element are considered essentials because with a deficit in concentration take place a disease, a surplus cause toxicity, and because to each element is associated a specific function. This is well represented with the dose-response curve (Fig. 1.4.).

The design of copper complexes could be an interesting strategy¹⁹; the interest in this field has rapidly grown in the last years, as illustrated by the increasing number of publications reported since 2000 (Fig. 1.5.).

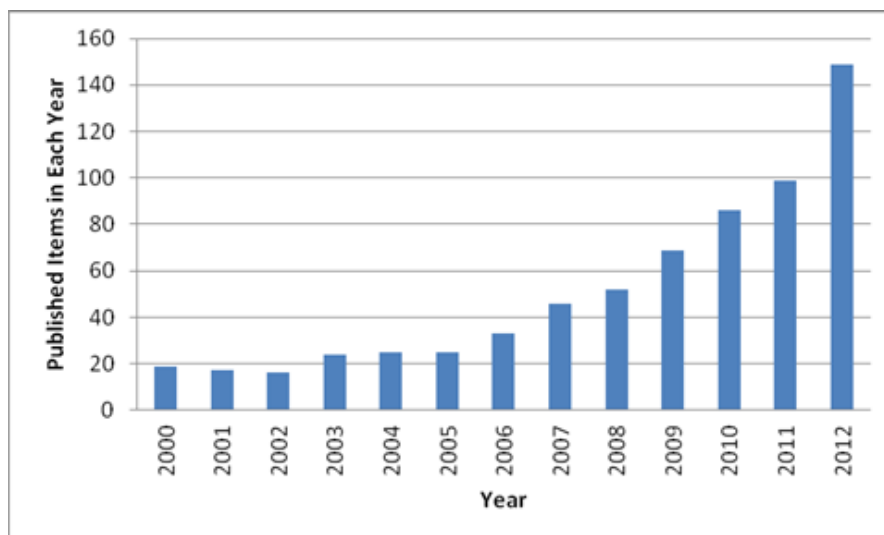


Fig. 1.5. Number of articles in Web of Science on the topic “copper and anticancer” from 2000 to 2012.

Copper-based complexes showed encouraging perspectives in this field²⁰⁻²⁴, even if copper could show toxicity due to its redox activity and its affinity for binding sites that should be occupied by other metals. The basis for the progress of copper complexes is the different response between tumour and normal cells to copper and the change in metabolism of cancer cells.

Copper is a micronutrient essential for most of the aerobic organisms, employed as a structural and catalytic cofactor, and consequently it is involved in many biological pathways^{14, 15, 25}. Take it into account it's reasonable that researchers have put lot of attention on the mechanisms of ADME (absorption¹⁶⁻¹⁸, distribution²⁰⁻²², metabolism, and excretion) of copper^{23, 24, 26}, as well as on its role in the development of cancer and other diseases²⁷⁻²⁹. Interesting examples are Menkes syndrome and Wilson disease²³, which are of genetic origin, in which altered levels of copper (overload or deficiency respectively³⁰) are associated with diseases such as rheumatoid arthritis, gastrointestinal ulcers, epilepsy, diabetes and cancer.

Copper chemistry

Copper forms a rich variety of coordination complexes with oxidation states Cu(II) and Cu(I), and very few examples of Cu(III) compounds are reported³¹. Coordination chemistry of copper is dominated by Cu(II) derivatives with little, but important examples of Cu(I) compounds. Since copper(I/II) complexes are redox active, frequently labile, and atypical in their preference for distorted coordination geometries, they are much less structurally predictable than other first row transition metal complexes. Copper(I) strongly prefers ligands having soft donor atoms such as P, C, thioether S and aromatic amines. Although two-coordinated linear and three-coordinated trigonal arrangements are known, Cu(I) complexes are mostly four-coordinated species adopting a tetrahedral geometry. In Cu(II)

complexes the coordination number (C.N.) varies from four to six, including four-coordinate square planar, five-coordinate trigonal bipyramidal and six-coordinate octahedral geometries (Fig. 1.6.).

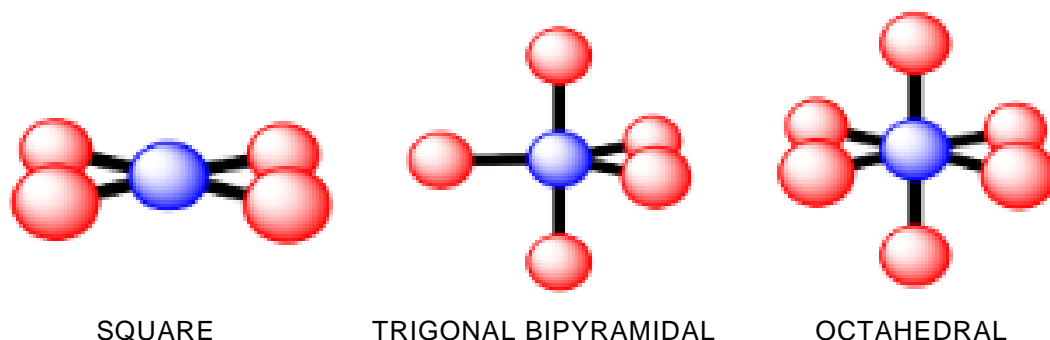


Fig. 1.6. Coordination geometry: square planar (C.N. 4), trigonal bipyramidal (C.N. 5), octahedral (C.N. 6).

The variety of accessible arrays allows for a great assortment in the choice of the ligands (from mono- to hexa-dentate chelates), and of the donor atoms (N, O, S and halides)³². The redox potential of the physiologically accessible Cu(I)/Cu(II) couple varies dramatically depending upon the ligand environment due to the donor set, geometry, substituents, electronic and steric effects, and chelation³³. For example, in the one electron oxidation of Cu(I) complexes toward dioxygen, a wide range of reduction potentials (from -1.5 to +1.3 vs standard hydrogen electrode)³³ is known for copper complexes. In addition, such an electron transfer always involves important modifications of the stereochemistry of the pertinent oxidized/reduced complexes. This feature, together with the possibility to release coordinating groups ongoing, for example, from octahedral Cu(II) to tetrahedral Cu(I) species, are chemical factors that illustrate the complexity of the Cu(I)/Cu(II) system in physiological media³⁴.

Copper complexes as anticancer agents

In review papers about copper complexes as antitumor agents, ligands are generally classified discriminating by the donor atom(s) involved in the bond with the metal in organometallic compounds. Following this rule most of the ligands are classified as S-donor, O-donor, N-donor, P-donor, C-donor, N,O-donor, N-N diimide, C-donor N-heterocyclic, but also as Schiff bases, polydentate and macrocyclic ones.

Starting from the tris(pyrazolyl)borates, a very useful class of monoanionic, nitrogen-based, auxiliary ligands, some ligands take the name of “heteroscorpionate” because of the shape that they take in the coordination to the metal centre, like the scorpion when attack his prey with the two chelae in the horizontal plane and the tale on the top. They

readily coordinate usually as face-capping tridentate ligands to a wide variety of metal ions affording stable metal complexes³⁵.

N-donor systems, pyrazoles

Polydentate nitrogen-containing donor ligands derived from poly(pyrazol-1-yl) methanes with $[\text{RR}'\text{C}(\text{Az})_2]$ (Az = azolyl groups; R = H or Az) as general structure and bearing organic functional groups (R') on the central carbon have attracted considerable attention and their coordination chemistry towards main group and transition metals have been extensively studied³⁶⁻³⁸. These intriguing heteroscorpionate ligands^{35, 39} present different types of functional groups, which successfully broaden the scope of their applications.

Nitroimidazole and glucosamine conjugated heteroscorpionate ligands, namely 2,2-bis(3,5-dimethyl-1H-pyrazol-1-yl)-N-(2-(2-methyl-5-nitro-1H-imidazol-1-yl)ethyl) acetamide (HL^{MN} , Fig. 1.7.) and 1,3,4,6-tetra-O-acetyl-2-[[bis(3,5-dimethyl-1H-pyrazol-1-yl)acetyl]amino]-2-deoxy- β -D-glucopyranose (HL^{DAC} , Fig. 1.7.), were synthesized by direct coupling of preformed side chain acid and amine components. In the related copper(II) complexes $\{[\text{L}^{\text{MN}}]_2\text{Cu}\}\text{Cl}_2$, and $\{[\text{L}^{\text{DAC}}]_2\text{Cu}\}\text{Cl}_2$, the local structure $[\text{Cu}(\text{L})_2]^{2+}$ was described by four Cu-N and two Cu-O interactions to form a pseudo-octahedron core (Fig. 1.7.). X-Ray Absorption Spectroscopy (XAS) has been used to probe the local structure of the copper complexes⁴⁰.

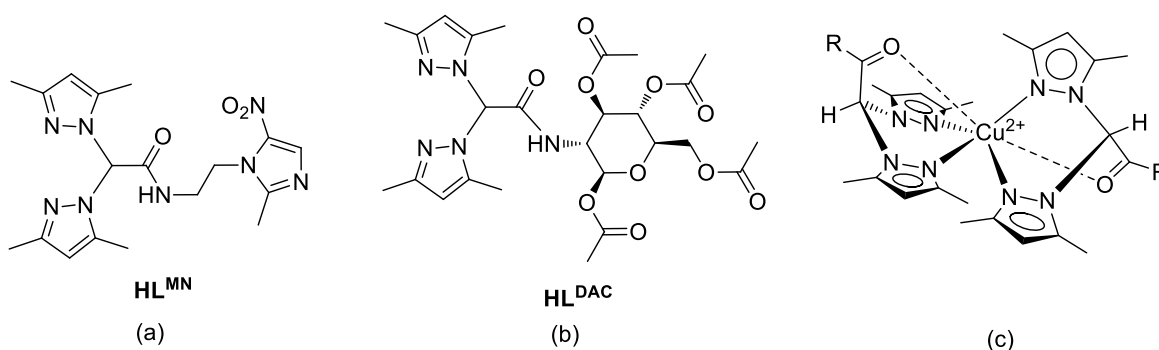


Fig. 1.7. Structure of: a) 2,2-bis(3,5-dimethyl-1H-pyrazol-1-yl)-N-(2-(2-methyl-5-nitro-1H-imidazol-1-yl)ethyl)acetamide ligand (HL^{MN}); b) 1,3,4,6-tetra-O-acetyl-2-[[bis(3,5-dimethyl-1H-pyrazol-1-yl)acetyl]amino]-2-deoxy- β -D-glucopyranose ligand (HL^{DAC}); c) the copper(II) cores $[\text{L}^{\text{MN}}]_2\text{Cu}^{2+}$ and $[\text{L}^{\text{DAC}}]_2\text{Cu}^{2+}$.

$[\text{L}^{\text{MN}}]_2\text{Cu}^{2+}$ and $[\text{L}^{\text{DAC}}]_2\text{Cu}^{2+}$ as well as the corresponding uncoordinated ligands were evaluated for their cytotoxic activity towards a panel of six tumour cell lines (A431, HCT-15, A549, Capan-1, MCF-7 and A375). Uncoordinated ligands proved to be ineffective against all cell lines, whereas copper complexes displayed a similar growth inhibitory potency in the micromolar range (7-14 μM), slightly lower than that shown by cisplatin. Interestingly, in HCT-15 colon adenocarcinoma cells, the cytotoxicity of copper(II) complexes exceeded that of the reference drug by a factor of about 3. Moreover, both copper(II) complexes overcame acquired resistance to cisplatin.

P-donor phosphine ligands

The distinctive characteristic of the complexes bearing phosphine ligands is the +1 oxidation state of the metal, which is mostly comprised in a four-coordinated tetrahedral environment. Copper coordination sphere is either partially or totally filled by phosphine ligands that efficiently bind the electron-rich d^{10} metal ion. Although Cu(I) is the chemical form generally accepted by the bioinorganic community to describe the active internalization of physiological copper in mammalian cells through copper transporter (Ctr) proteins, still very few studies report on the action of Cu(I) complexes as antitumor agents. This is likely related to the intrinsic difficulty to stabilize copper(I) species, especially in aqueous media. Only the formation of quite robust metal-ligand interactions, as those displayed in the case of copper-phosphine (and copper-NHC) species, prevents hydrolysis and the activation of the redox machinery⁴⁰.

Two different coordination spheres have been particularly investigated in the field of copper-phosphine compounds, with the corresponding tetrahedral complexes showing both easy synthesis and appealing biological properties: the homoleptic, mono-cationic $[\text{Cu}(\text{P})_4]^+$ arrangement and the mixed-ligand, neutral $[\text{Cu}(\text{N-N})(\text{P})(\text{X})]$ assembly, where P represents a monodentate phosphine, N-N an aromatic diimine and X a halide⁴¹.

The work by Berners-Price on 1:2 hydrophilic adducts of copper(I) halides with 1,2-bis(di-2-pyridylphosphino)ethane (P-P)⁴² joined the extensive studies performed in the eighties^{43, 44} on group 11 metals including lipophilic bis-aryldiphosphines. The lack of selectivity toward tumorigenic and non-tumorigenic cells, and the robustness toward dissociation of these copper adducts made them more promising candidates in the radiopharmaceutical field⁴⁵.

The above conclusion was in agreement with experimental evidences illustrated by other authors on a similar bis-chelated 'P-P' complex including hydrophilic, alkyl bis[bis(hydroxymethyl)phosphine]ethane (bhpe)⁴⁶. The negligible cytotoxic activity shown by $[\text{Cu}(\text{bhpe})_2]^+$ was attributed to its robust inertness toward dissociation, whereas complexes of similar 'CuP₄' stoichiometry, but containing mono-dentate phosphines, exhibited moderate to high antiproliferative activity. In these species, the original $[\text{Cu}(\text{P})_4]^+$ complexes underwent dissociation to coordinative unsaturated $[\text{Cu}(\text{P})_3]^+$ and $[\text{Cu}(\text{P})_2]^+$ adducts at micromolar concentration⁴⁶. The more favoured was the displacement of P from the $[\text{Cu}(\text{P})_4]^+$ parent complex, the more favoured was in turn the ability of the metal ion to interact with a pharmacological target, thereby promoting the antiproliferative effect. Several $[\text{Cu}(\text{P})_4]^+$ -type complexes including hydrophilic phosphines such as tris-(hydroxymethyl)phosphine (thp)⁴⁷, tris-(hydroxypropyl)phosphine (thpp)⁴⁸, and 1,3,5-triaza-7-phosphaadamantane (PTA)⁴⁹ were prepared (Fig. 1.8.).

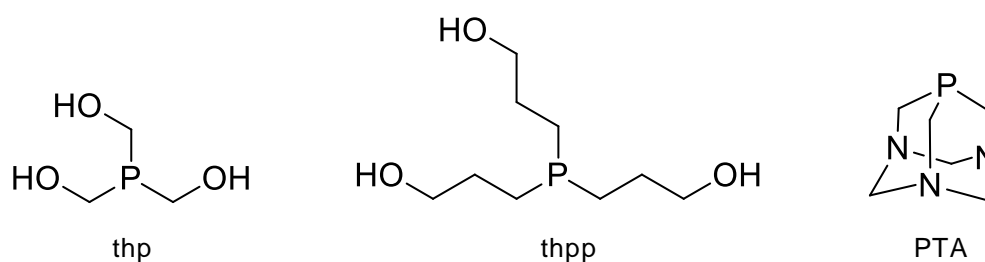


Fig. 1.8. Structure of water soluble monodentate phosphines thp, thpp, and PTA.

The most promising complex of the series, $[\text{Cu}(\text{thp})_4]^+$, (Fig. 1.9.) was tested *in vitro* against a wide panel of human tumour cell lines showing remarkable cytotoxic activity⁴⁷, roughly one order of magnitude higher than that shown by the cisplatin reference drug. In particular, on a panel of selected human colon carcinoma cell lines corresponding to different stages of disease progression (LoVo, DLD-1, SW480, HCT-15 and Caco-2 cells) $[\text{Cu}(\text{thp})_4]^+$ killed these tumour cells more efficiently than cisplatin and oxaliplatin and it overcame platinum drug resistance⁵⁰. $[\text{Cu}(\text{thp})_4]^+$ preferentially reduced cancer cell viability whereas non-tumour cells were poorly affected. Colon cancer cells died via a programmed cell death whose transduction pathways were characterized by the absence of hallmarks of apoptosis.

Looking for coordinative unsaturated assemblies, the same authors described the linear, di-substituted $[\text{Cu}(\text{PCN})_2]^+$ (Fig. 1.9.) (PCN = tris-(cyanoethyl)phosphine). Although appealing from the coordination point-of-view, the cytotoxic activity shown by PCN was moderate because of the peculiar intramolecular 'umbrella-shaped' coordination of the two PCN ligands causing low availability of the metal to interact with biological substrates⁵¹.

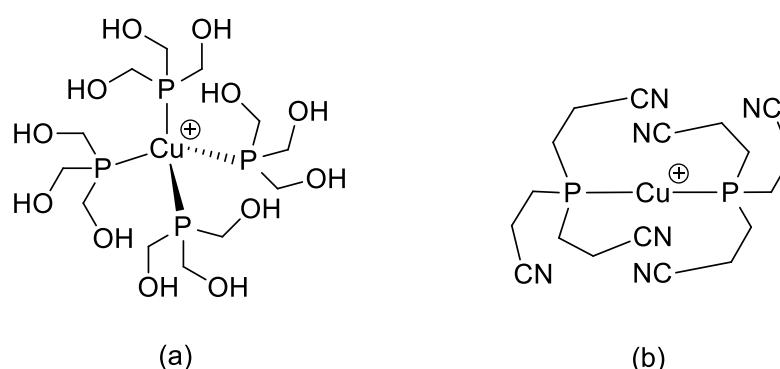


Fig. 1.9. Structure of $[\text{Cu}(\text{thp})_4]^+$ (a) and $[\text{Cu}(\text{PCN})_2]^+$ (b).

Mononuclear and dinuclear copper(I) chloride complexes $[\text{CuCl}(\text{PPh}_3)_3](\text{CH}_3\text{CN})$ and $[\text{Cu}_2(\mu\text{-Cl})_2(\text{PPh}_3)_3]$ comprising triphenylphosphine (PPh_3) have been tested against LMS and MCF-7 cells showing remarkable cytotoxic activity IC_{50} values (half maximal inhibitory concentration, represent the concentration of a drug necessary to inhibit the 50% of the target) in the 5-6 μM range)⁵².

Two distorted tetrahedral complexes $[\text{Cu}(\text{Fchy})(\text{PPh}_3)_2]$ including ferrocene containing bidentate hydrazone ligands were synthesized from the bivalent copper precursor $[\text{CuCl}_2(\text{PPh}_3)_2]$. These compounds showed moderate *in vitro* cytotoxicity against HeLa and A431 tumour cells and little damage to NIH 3T3 non-tumour cells^{53, 54}.

Mechanistic approaches and proposed biological targets: state of the art

Copper species possess a broader spectrum of activity and a lower toxicity than platinum drugs, and are suggested to be able to overcome inherited and/or acquired resistance to cisplatin. These features are consistent with the hypothesis that copper complexes possess mechanism(s) of action different from platinum drugs that covalently bind to DNA. Moreover, DNA damaging agents, the drugs that promote DNA dysfunction, can induce as drawback gene mutations and chromosomal modification. Hence development of antitumor drugs that act through different pathway than DNA is preferred. Anyway, little information is available on the molecular basis for the mode of action of copper complexes. At present, most investigations still focus on the ability of these complexes, or fragments thereof, to interact with DNA. However, other cellular constituents such as topoisomerases or the proteasome multi-protein complex are emerging as new putative targets⁴¹.

The last studies are confirming that copper-based complexes could be a solution to overcome the problem of toxicity and acquired resistance to platinum drugs, especially for Cu(I) complexes, the chemical form nowadays accepted for internalization of physiological copper in mammalian cells.

Copper complexes as DNA targeting drugs

Since 1969 copper has been found to possess high DNA binding affinity⁵⁵. Analogously to what has been widely illustrated for cisplatin⁵⁶, a crystal structure describing the formation of an adduct between CuCl_2 and DNA was published in 1991⁵⁷. The binding was dependent on copper complex size, electron affinity and geometry of the formed adduct inducing an irreversible modification of the DNA conformational structure.

According to these observations, a high number of copper complexes have been and are still being tested as DNA-targeting metal-based drugs. For some classes of copper derivatives, the ability to bind DNA has been well established and documented. Copper derivatives have been found capable of non-covalently interact with DNA double helix, rather than forming coordinated covalent adducts with DNA. The non-covalent DNA interactions included intercalative, electrostatic and groove binding (Fig. 1.10.) of metal complexes, along major or minor DNA groove.



Fig. 1.10. Schematic representation of intercalative (left) and groove (right) binding.

In most cases, the metal acted as an inorganic modifier of the organic backbone of the bio-active molecule and ligands granted DNA affinity and specificity. In this frame, a particular attention has been focused on copper(II) complexes including N-donor ligands, due to their high DNA interaction ability and *in vitro* antitumor efficiency. Copper derivatives containing 1,10-phen (phen = phenanthroline) and related di-imine chelates had been described as potent cytotoxic agents, eliciting IC_{50} values in the sub-micromolar range⁴¹.

Overall, it has been demonstrated that physico-chemical features, such as the planarity, hydrophobicity and size of the di-imine, the nature of the coligand as well as the coordination geometry of the metal complex, all played important roles in determining the binding/intercalating mode of copper complexes to DNA.

Despite many copper complexes have been found able to trigger apoptotic cell death because of DNA damage, very few papers report elucidations on signal transduction molecular determinants activated in copper-complexes treated cells. In some cases, copper complexes determined an upregulation of proapoptotic proteins or a downregulation of antiapoptotic proteins, which were consistent with the induction of apoptosis⁴¹.

In addition, the involvement of caspase activation in copper complex mediated cell death has not been fully elucidated. Only few copper derivatives have been reported to induce apoptosis in cancer cells through the involvement of caspase-3^{58, 59} and/or caspase-9 activation⁶⁰.

Copper complexes as Topoisomerase I,II inhibitors

Recent research into the ability of copper complexes to inhibit topoisomerases has served not only to reinforce the significant potential of this class of metal complexes in cancer research but also to expand the array of possible biochemical targets for these molecules. Topoisomerases are essential nuclear enzymes that regulate the overwinding or underwinding of DNA and so they play essential functions in DNA replication and transcription. Topoisomerases create transient nicks (Topo I) or breaks (Topo II) (Fig. 1.11.) in the double-stranded DNA polymer, allowing DNA to be converted between topological isomers⁶¹.

Nuclear Topo I and Topo II have been identified as clinically important targets for cancer chemotherapy, and their inhibitors are central components in many therapeutic regimens. These topo-targeting agents are broadly classified in two groups, *viz.* topo poisons and catalytic inhibitors. Topo poisons are able to stabilize the reversible covalent topo-DNA complex termed the cleavage complex, whereas catalytic inhibitors, most of which target Topo II, act on the other steps in the catalytic cycle without trapping the covalent complex.

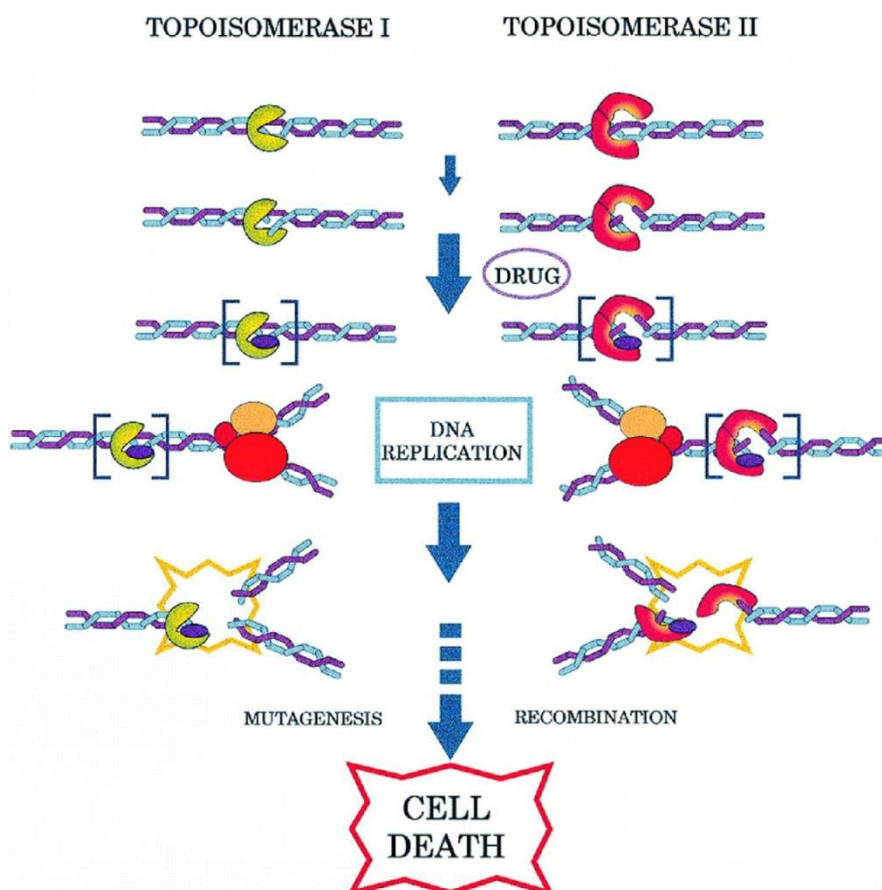


Fig. 1.11. Schematic representation of Topoisomerase I and II mode of action.

Currently there is still an increasing interest focusing on the development of new kinds of drugs targeting human topoisomerases and the development of metal complexes as

Topo I,II inhibitors fits just in this therapeutic niche. However, unlike that involving DNA, interaction of copper complexes with topoisomerases is a relatively new field of research. The first observations regarded oxime copper complexes as Topo II poisons⁶².

Once more, among copper complexes containing the pharmacophoric planar heterocyclic phen, a series of mixed copper (II)-phen complexes with glycine and methylated glycine has been developed with the aim to investigate the effect of the position and number of methyl substituent(s) in the auxiliary ligand on the biological activity, including the inhibition of Topo I. It has been found that the replacement of metal coordinated glycine with methylated glycine affected the DNA binding properties of the ternary complexes whereas there was no significant difference in the antiproliferative activity promoted against HK1 cancer cells as well as in the degree of Topo I inhibition. The Topo I inhibitory property was very similar to that induced by some anticancer organic compounds targeting topoisomerases⁴¹.

Copper Complexes as Proteasome Inhibitors

The proteasome is a large multiprotein complex located in both the nucleus and the cytoplasm that selectively modulates and degrades intracellular proteins. The proteasome is part of a major mechanism by which cells regulate the concentration and the stability of particular proteins (e.g. cyclins, bcl-2 family members, and p53) and decompose unfolded proteins. The ubiquitin proteasome-dependent degradation system is essential for many cellular functions, including processes of primary importance for carcinogenesis such as proliferation, apoptosis, angiogenesis and metastasis formation⁶³.

It has been shown that cancer cells are more sensitive to proteasome inhibition than normal cells. Thus, targeting the ubiquitin-proteasome pathway has emerged as a favourable anticancer strategy^{64, 65} and currently the development of proteasome inhibitors as novel anti-cancer agents is under intensive investigation.

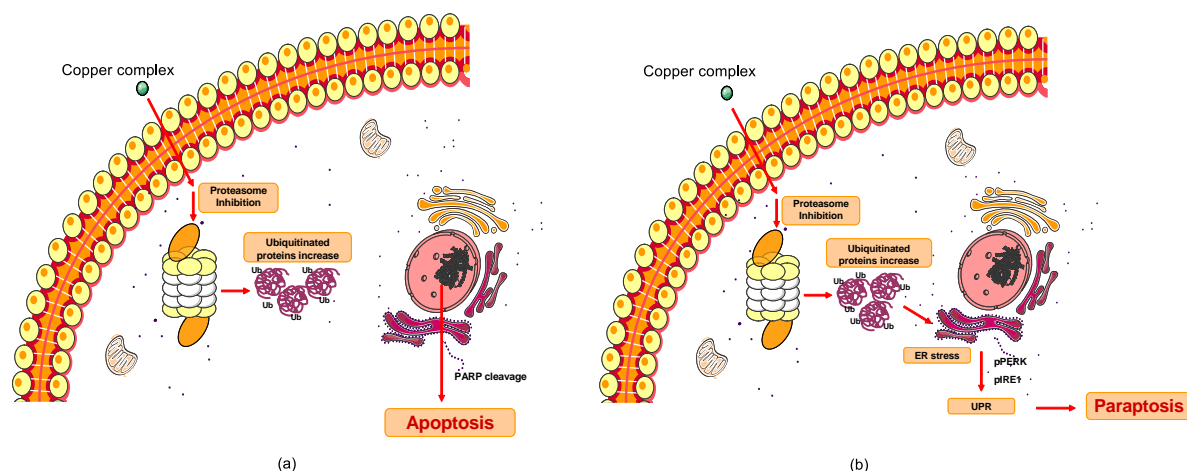


Fig. 1.12. Schematic diagrams of cellular pathways involved in proteasome inhibition induced by copper compounds. a) Apoptosis triggered by DTC copper(II) complexes; b) paraptosis caused by phosphine copper(I) and thioxotriazole copper(II) complexes.

The first case of copper complexes inhibiting proteasome function has been reported by Dou and co-workers⁶⁶. In 2004 they described some 'copper mixtures', derived from mixtures of copper(II) salts (CuCl_2 or CuBr_2) and bidentate ligands (the family of 8-hydroxyquinolone including clioquinol, phen, and the family of dithiocarbamates (DTCs)) as potent inhibitors of the chymotrypsin-like proteasome activity⁶⁵. Owing to proteasome inhibitory activity, these "copper mixtures" could selectively induce apoptotic cell death in cancer cells (Fig. 1.12.) but not in non-transformed cells and were effective in *in vivo* tumour models⁶⁷. These studies established that elevated proteasome activity and high concentration of copper are unique features in human tumour cells that can be used as targets by "copper mixtures" that act as potent tumour cell killers⁶⁸⁻⁷³.

Proteasome has been identified as the main molecular target for a series of copper(I) complexes with hydrophilic phosphine ligands⁴⁸. The monocationic copper(I) complex $[\text{Cu}(\text{thp})_4][\text{PF}_6]$, highly soluble and stable in water solution, gained special attention because of its strong antiproliferative effects selectively directed toward human cancer cells⁴⁷. $[\text{Cu}(\text{thp})_4][\text{PF}_6]$ was found to inhibit both *in vitro* and in human colon cancer cells, causing intracellular accumulation of polyubiquitinated proteins and the functional suppression of the ubiquitin-proteasome pathway thus triggering endoplasmic reticulum (ER) stress. The latter one was paralleled by a strong increase in the levels of phosphorylated ER sensors, proving the concomitant induction of unfolded protein response (UPR). The irreversible ER stress was accompanied with a massive cytoplasmatic vacuolization and a programmed cell death (PCD) termed paraptosis⁵⁰. Paraptosis, a PCD morphologically and biochemically different from apoptosis, has been observed in cancer cells treated with other class of copper complexes⁷⁴. In particular, the thioxotriazole copper(II) complex $[\text{Cu}(4\text{-amino-3-(pyridin-2-yl)-1H-1,2,4-triazole-5(4H)-thione)Cl}_2]$, induced paraptotic like cell death in a wide panel of human cancer cell lines (Fig. 1.12.).

Interestingly, all these studies suggested that copper ion played a fundamental role in the mixture for conferring the proteasome inhibitory activity but limited information was available about the composition of the coordination species generated. Copper-mediated proteasome-inhibitory activity could be enhanced by the choice of appropriate bidentate ligands but blocked by stronger copper polydentate chelators such as EDTA. This feature denoted that substitution-inert copper complexes, in which copper was totally sequestered by the ligand framework, could not act as proteasome inhibitors because the metal was likely incapable to interact with cell substrates at molecular level²⁰.

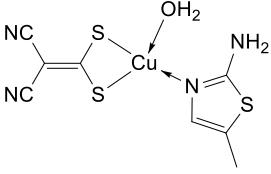
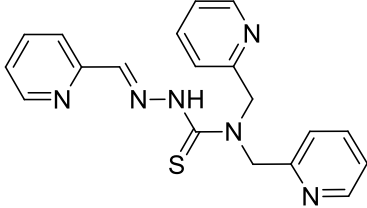
Furthermore, Xiao and co-workers recently investigated the effect of the oxidation status of copper Cu(I) and Cu(II) on inhibition of proteasome activity⁷⁵. Mixing neocuproine, a copper-binding compound, with Cu(I) or Cu(II), both copper mixtures could inhibit proteasome chymotrypsin-like activity and induce apoptosis in tumour cells even if Cu(I) mixture was more potent. Actually, purified 20S proteasome protein was able to directly reduce Cu(II) to Cu(I), suggesting that Cu(I) is the oxidation state of copper that directly

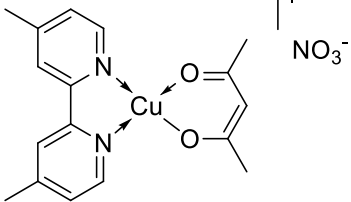
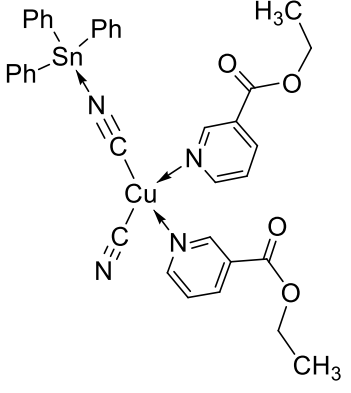
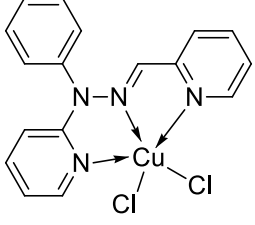
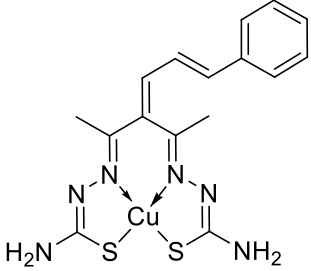
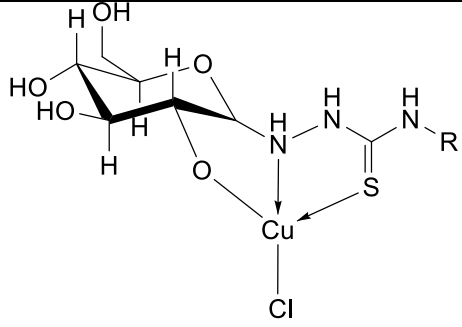
reacts with proteasome. However, little is known about the mode of interaction/inhibition of these copper derivatives with the catalytic subunits of 26S proteasome.

***In vivo* antitumor studies**

Although many different *in vitro* assays, both cell-based and molecular-target driven, have been used to identify lead compounds, the most common step following *in vitro* assays is efficacy assessments in animal tumour models. Actually, there are series of reports in literature describing *in vitro* cytotoxic activity investigations as no predictive assays of *in vivo* antitumor efficacy. Animal models have several advantages over *in vitro* cell cultures as tumours develop vasculature and interact with the stroma; therefore, they allow evaluation of toxicity and provide pharmacokinetic data of the agent. The typical development plan for a cancer agent also requires studies on preclinical models in which critically important measures of antitumor effectiveness (i.e. the increase in the life time and/or tumour growth delay in tumour bearing mice) can be monitored according to the standard protocol of the experimental evaluation of antitumor drugs (National Cancer Institute or NCI, USA).

Despite huge interest in the development of copper based compounds that are poorly toxic and highly active as antitumor drugs, nowadays there is still a paucity of studies investigating the *in vivo* antitumor activity of copper(I,II) complexes. Actually, although several classes of copper(I,II) complexes have been proposed as very promising cytotoxic agents, for very few of them a remarkable *in vivo* activity has been demonstrated so far (Table 1.2.).

Compound	Tumor type
	Leukemia P380
	HL60 human xenografts

 <p>Chemical structure of a copper complex. The copper atom is coordinated to a bis-imidazole ligand (two imidazole rings linked at their 2-positions), a methylacrylate ligand (CH₂=CHCOOCH₃), and a methylammonium cation (CH₃NH₃⁺). A nitrate counterion (NO₃⁻) is also present.</p>	<p>HCT-15 colorectal xenografts</p>
 <p>Chemical structure of a copper complex. The copper atom is coordinated to a tin(IV) complex (Ph₃Sn-N≡C-C≡N), two ethyl acrylate ligands (CH₂=CHCOOCH₂CH₃), and two imidazole ligands.</p>	<p>MNU induced rat mammary carcinoma</p>
 <p>Chemical structure of a copper complex. The copper atom is coordinated to a bis-imidazole ligand (two imidazole rings linked at their 2-positions), two phenyl rings (Ph), and two chlorine atoms (Cl).</p>	<p>MNU induced rat breast cancer</p>
 <p>Chemical structure of a copper complex. The copper atom is coordinated to a bis-thioamide ligand (two thioamide groups linked at their 2-positions), two amino groups (H₂N), and a chalcone ligand (trans-stilbene derivative).</p>	<p>Erich ascites carcinoma</p>
 <p>Chemical structure of a copper complex. The copper atom is coordinated to a thioamide ligand (H₂N-C(=S)-NH-R), a chlorine atom (Cl), and a sugar derivative (a pyranose ring with multiple hydroxyl groups).</p>	<p>Erich ascites carcinoma</p>

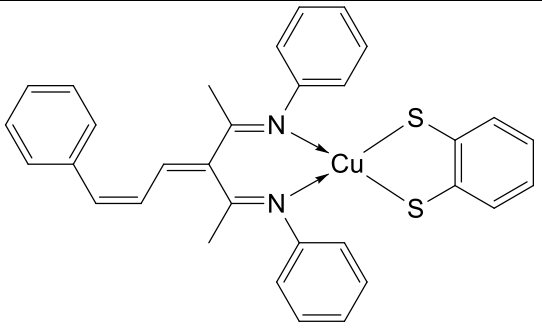
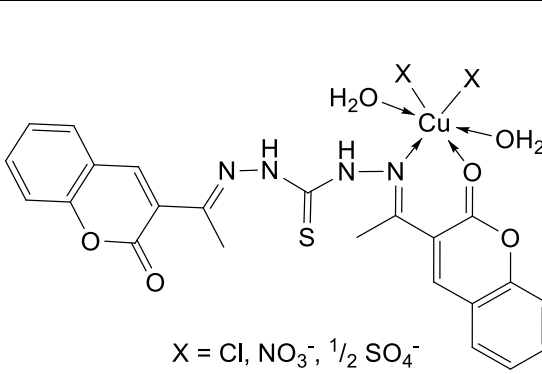
	Erlch ascites carcinoma
 <p style="text-align: center;">X = Cl, NO₃⁻, 1/2 SO₄⁻</p>	Erlch ascites carcinoma

Table. 1.2. Copper complexes recently tested in *in vivo* experiments⁴¹.

Heteroscorpionate ligands: poly(pyrazolyl)acetate and their applications

Bis(pyrazol-1-yl)carboxylic acids belong to a versatile class of N,N,O-donor ligands, which are useful in the field of enzyme modelling. They are particularly interesting, due to the k^3 -N,N,O coordination behaviour, in the field of model complexes, regarding zinc and iron enzymes with a 2-histidine-1-carboxylate metal bonding topic⁷⁶⁻⁷⁹.

Burzlaff *et al.* have identified the heteroscorpionate ligand bis(3,5-dimethylpyrazol-1-yl)acetic acid as suitable as model for the active sites of the facial 2-histidine-1-carboxylate triad in iron and zinc containing enzymes⁴¹.

Otero and coworkers first synthesized in 1999 a bis(pyrazol-1-yl)acetate ligand; they studied the coordination ability of bis(3,5-dimethylpyrazol-1-yl)acetate ligands towards group IV and group V metals. The synthesis of the ligand was performed starting from 3,5-dimethylpyrazole to achieve (3,5-dimethylpyrazol-1-yl)methane by reaction with CH₂Cl₂. The deprotonation with BuⁿLi at the bridging CH₂ in presence of CO₂ gives the lithium bis(3,5-dimethylpyrazol-1-yl)acetate salt.

In addition to this multistep synthesis Burzlaff *et al.* have designed a synthesis starting from commercially available dibromo- or dichloro-acetic acid and 2 equivalents of 3,5-dimethylpyrazole, with an excess of potassium hydroxide and potassium carbonate, using tetra-n-butylammonium bromide as phase-transfer catalyst. After acidification and

extraction with diethyl ether the synthesis affords bis(3,5-dimethylpyrazol-1-yl)acetic acid with reasonable yield. This procedure works as well using pyrazole.

Due to their characteristics and the catalytic activity shown in different reactions (like olefin polymerization, olefin oxidation, hydrogen/deuterium exchange and metathesis reaction), several studies have been carried out on transition metal complexes with bis(pyrazol-1-yl)acetate ligands.

In the polymerization of olefins group IV metal complexes are useful catalyst precursors, and one of the strategies in the design of new catalysts was the development of non-cyclopentadienyl ligands, with oxygen and nitrogen donor atoms. The studies result in the synthesis of the heteroscorpionate titanium complexes $[\text{TiCl}_3(\kappa^3\text{-bis(3,5-dimethylpyrazol-1-yl)acetate})]$ and $[\text{TiCl}_2(\kappa^3\text{-bis(3,5-dimethylpyrazol-1-yl)acetate})\{\text{O}(\text{CH}_2)_4\text{Cl}\}]$ (Fig. 1.13.), which catalysed the polymerization of ethylene in presence of a co-catalyst like methylaluminoxane. The activity of these catalysts is comparable to that of the titanocene complex $[\text{TiCp}_2\text{Cl}_2]$ and the monocyclopentadienyl species $[\text{TiCpCl}_2(\text{L})]$ or $[\text{TiCp}^*\text{Cl}_2(\text{L})]$ (Cp = cyclopentadienyl; Cp* = 1,2,3,4,5-pentamethylcyclopentadiene)⁸⁰⁻⁸².

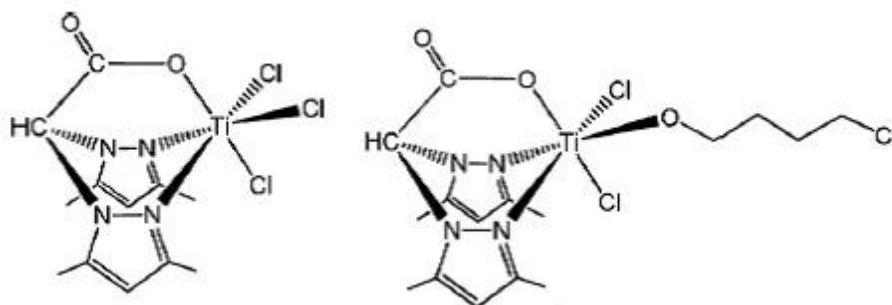


Fig. 1.13. Structure of: a) $[\text{TiCl}_3(\kappa^3\text{-bis(3,5-dimethylpyrazol-1-yl)acetate})]$; b) $[\text{TiCl}_2(\kappa^3\text{-bis(3,5-dimethylpyrazol-1-yl)acetate})\{\text{O}(\text{CH}_2)_4\text{Cl}\}]$.

Recently Burzloff and coworkers have reported the activity in the ring-closing metathesis of ruthenium carbene complexes bearing neutral carboxylate-based heteroscorpionate ligands. For example the activity of the ruthenium complexes $\{\text{RuCl}[\kappa^3\text{-bis(pyrazol-1-yl)acetate}](\text{CHPh})(\text{PCy}_3)\}$ and $\{\text{RuCl}[\kappa^3\text{-bis(3,5-dimethylpyrazol-1-yl)acetate}](\text{CHPh})(\text{PCy}_3)\}$ (Fig. 1.14.a) has been tested in the ring closing metathesis of diethyl diallylmalonate⁸³. The results are adequate in presence of CuCl as phosphine scavenger, but the activity is lower than Grubbs' catalysts under milder conditions⁸⁴.

The first ruthenium carbonyl porphyrin catalyst for alkene epoxidation was first reported in 1985⁸⁵; after that several ruthenium complexes with bis(pyrazol-1-yl) carboxylate ligands have been tested as catalysts in the epoxidation cyclohexene. Particularly ruthenium carbonyl complexes $[\text{RuCl}(\text{bis(pyrazol-1-yl)acetate})(\text{CO})_2]$ and $[\text{RuCl}(2,2\text{-bis(3,5-dimethylpyrazol-1-yl)propionate})(\text{CO})_2]$ (Fig. 1.14.b) have been tested in presence of different oxidizing agents, like hydrogen peroxide, and two nucleophilic oxidizing agents, 2,6-dichloropyridine N-oxide and iodosylbenzene. However only with the last one catalytic activity took place, even if both complexes mentioned are highly selective for the formation of cyclohexene oxide⁸⁶.

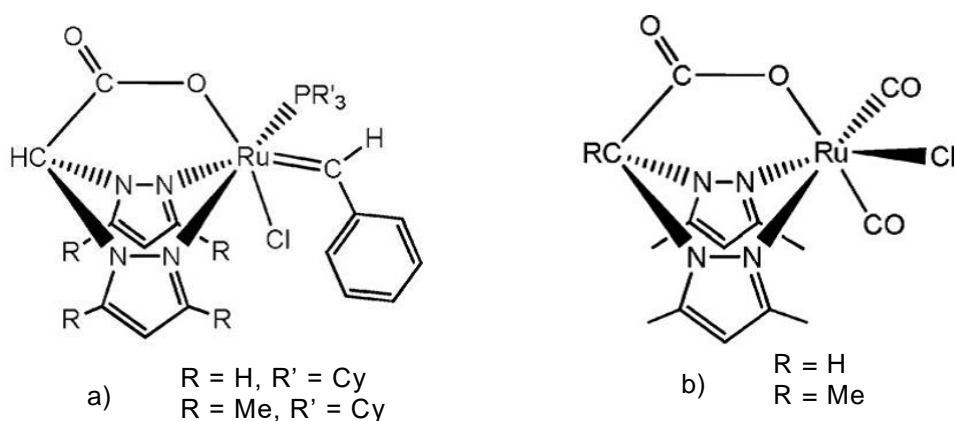


Fig. 1.14. Structure of: a) $\{RuCl[\kappa^3\text{-bis(pyrazol-1-yl)acetate}](CHPh)(PCy_3)\}$ and $\{RuCl[\kappa^3\text{-bis(3,5-dimethylpyrazol-1-yl)acetate}](CHPh)(PCy_3)\}$; b) of $[RuCl(\text{bis(pyrazol-1-yl)acetate})(CO)_2]$ and $[RuCl(2,2\text{-bis(3,5-dimethylpyrazol-1-yl)propionate})(CO)_2]$.

C-H activation/functionalization has been widely studied, especially the Shilov system regarding alkanes, which remains one of the most important catalytic processes for hydrocarbons. An alternative may be the tripodal heterosorptionate ligands with group IX metals. Rhodium and iridium complexes $Na^+\{Rh[\text{bis(3,5-dimethylpyrazol-1-yl)acetate}]Cl_3\}^-$ and $Na^+\{Ir[\text{bis(3,5-dimethylpyrazol-1-yl)acetate}]Cl_3\}^-$ are catalyst precursors for C-H activation of arenes. The catalyst activation occurs after abstraction of halides with silver salts⁸⁷. The catalytic test was executed with three deuterated solvents, methanol-d, trifluoroacetic acid-d and ethanol-d as deuterium sources, exchanging H/D with benzene. Only trifluoroacetic acid-d shows evidence of H/D exchange with benzene, with 4% of catalyst and 3 equivalents of silver trifluoroacetate at 100°C. Other chloride abstractors were examined and silver triflate is the most effective, while silver tetrafluoroborate is inactive.

NMDA receptors

NMDA receptors are cation channels with high calcium permeability involved in many aspects of the biology of higher organisms. The opening of the NMDA receptor associated cation channel is controlled by various ligands interacting with different binding sites at the receptor such as the ones for glutamate, glycine, polyamines, Zn^{2+} , Mg^{2+} , H^+ , as well as phencyclidine (PCP, Fig. 1.15.).

This last binding site is located within the cation channel and compounds interacting with the PCP site behave as non-competitive NMDA receptor antagonists by inhibiting the Ca^{2+} -ions influx through the cation channel blockade⁸⁸.

Recent findings suggest a complex relationship between NMDA and σ functions. Sigma receptors were initially classified as opioid receptor subtypes⁸⁹, and subsequently it was postulated that they were identical to the PCP binding site at the NMDA receptor channel⁹⁰.

Further studies demonstrated that they were distinct from both opioid receptors and PCP/NMDA receptor complexes.

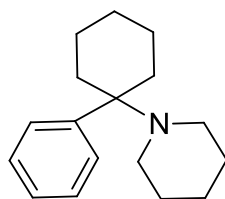


Fig. 1.15. Structure of Phencyclidine (PCP).

At present, σ receptors are considered to be a unique receptor family comprising at least two pharmacologically distinct subtypes, namely σ_1 and σ_2 receptors^{91, 92}, which are widely distributed in the central nervous system CNS as well as in some peripheral tissues such as the gastrointestinal tract, kidney, liver, lung, heart, and adrenal medulla⁹³. In addition, both σ receptor subtypes are overexpressed in many human and rodent tumour cell lines⁹⁴. Because of their widespread expression in many human tissues and their involvement in several pathophysiological processes, σ receptors have proved to be highly attractive pharmacological targets for the potential treatment of various pathologies, including neuropathic pain, depression, cocaine abuse, epilepsy, psychosis, as well as Alzheimer's and Parkinson's diseases⁹⁵. Moreover, σ_1 antagonists and σ_2 agonists may be useful as anticancer agents and radio-labelled ligands as selective tumour imaging agents⁹⁶.

On this topic 1,4-dioxane nucleus (Fig.1.16.a), differently and properly substituted in 2 and 5 or 6 positions, has already proved to be a suitable scaffold for building ligands selectively targeting different receptors⁹⁷.

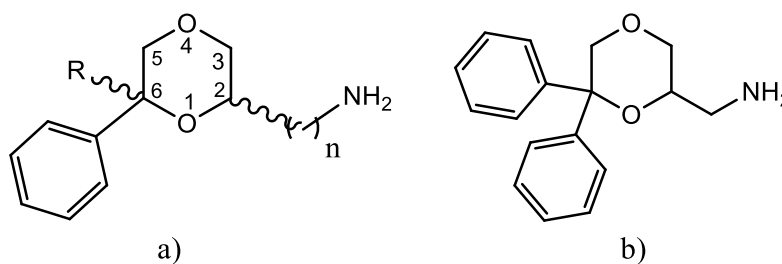


Fig. 1.16. Structure of: a) 1,4- dioxane scaffold; b) (\pm)-(6,6-Diphenyl-1,4-dioxan-2-yl)methanamine.

On the basis of these considerations the bis(pyrazolyl)acetate ligands have been functionalized through amidic bond with (\pm)-(6,6-Diphenyl-1,4-dioxan-2-yl)methanamine (Fig. 1.16.b) to give bioconjugated ligands to be coordinated to copper.

II. Experimental section

Methods and materials

All reagents were purchased from Aldrich and used without further purification. All solvents were dried, degassed and distilled prior to use. Elemental analyses (C,H,N,S) were performed in-house with a Fisons Instruments 1108 CHNS-O Elemental Analyser. Melting points were taken on an SMP3 Stuart Scientific Instrument. IR spectra were recorded from 4000 to 100 cm^{-1} with a Perkin-Elmer SPECTRUM ONE System FT-IR instrument. IR annotations used: br = broad, m = medium, s = strong, sh = shoulder, w = weak. ^1H and ^{31}P NMR spectra were recorded on an Oxford-400 Varian spectrometer (400.4 MHz for ^1H and 162.1 MHz for ^{31}P). Chemical shifts, in ppm, for ^1H NMR spectra are relative to internal Me_4Si . ^{31}P NMR chemical shifts were referenced to a 85% H_3PO_4 standard. The ^{31}P NMR spectroscopic data were accumulated with ^1H decoupling. NMR annotations used: AB q = AB quartet, br = broad, s br = broad singlet, d = doublet, dd = doublet of doublets, m = multiplet, s = singlet, v br = very broad. Electrospray ionization mass spectra (ESIMS) were obtained in positive- (ESI(+))MS or negative-ion (ESI(-))MS mode on a Series 1100 MSD detector HP spectrometer, using a methanol or acetonitrile mobile phase. The compounds were added to reagent grade methanol to give solutions of approximate concentration 0.1 mM. These solutions were injected (1 μL) into the spectrometer via a HPLC HP 1090 Series II fitted with an autosampler. The pump delivered the solutions to the mass spectrometer source at a flow rate of 300 $\mu\text{L min}^{-1}$, and nitrogen was employed both as a drying and nebulising gas. Capillary voltages were typically 4000 V and 3500 V for the positive- and negative-ion mode, respectively. Confirmation of all major species in this ESI-MS study was aided by comparison of the observed and predicted isotope distribution patterns, the latter calculated using the IsoPro 3.0 computer program.

Synthesis of the ligands

Synthesis of [HC(CO₂H)(pz)₂] (LH, **1**)

Dichloroacetic acid (4.191 g, 32.500 mmol) was dissolved in THF (100 mL), then KOH (7.294 g, 130.000 mmol) and K₂CO₃ (17.967 g, 130.000 mmol) were added and stirred for 5'. Pyrazole (pz, 4.424 g, 65.000 mmol) and tetra-*n*-butylammonium bromide (TBAB, 0.638 g, 1.980 mmol), serving as phase-transfer catalyst, were later added. The reaction mixture was heated under reflux for 12 h. The solvent was evaporated at reduced pressure, the residue dissolved in water (100 mL) and acidified to pH 7 with concentrated HCl. The solution was extracted with diethyl ether (2 x 100 mL). The water phase was further acidified with HCl concentrated to pH 1.5 and stirred for 2 h. A white precipitate was formed that was filtered off, washed by diethyl ether, and dried under reduced pressure to give ligand LH (**1**) in 48% yield. Mp. 158-162°C. ¹H NMR (acetone, 293K): δ 6.33 (t, 2H, 4-CH), 7.44 (s, 1H, CHCOO), 7.54 (d, 2H, 5-CH), 7.97 (d, 2H, 3-CH). IR (cm⁻¹): 3177w, 3149w, 3131w, 3108w, 2977w (CH); 2454br (OH); 1721s (C=O); 1518m (C=N); 1446w, 1435w, 1403m, 1391s, 1352m, 1318w, 1291s, 1258s, 1222s, 1187w, 1170s, 1092s, 1059s, 1049s, 986m, 966m, 918m, 887w, 862m, 850m, 820s, 752s, 715s, 660s. ESIMS (major positive-ions, CH₃OH), *m/z* (%): 231 (100) [LH + K]⁺. ESIMS (major negative-ions, CH₃OH), *m/z* (%): 191 (100) [L]⁻. Calcd. for C₈H₈N₄O₂: C, 50.00; H, 4.20; N, 29.15%. Found: C, 50.11; H, 4.29; N, 27.67%.

Synthesis of [HC(CO₂H)(pz^{Me2})₂] (L²H, **2**)

Dichloroacetic acid (4.191 g, 32.500 mmol) was dissolved in tetrahydrofuran (THF) (100 mL), then KOH (7.294 g, 130.000 mmol) and K₂CO₃ (17.967 g, 130.000 mmol) were added and the solution was stirred for 5'. 3,5-dimethylpyrazole (pz^{Me2}) (6.248 g, 65.000 mmol) and TBAB (0.638 g, 1.980 mmol), serving as phase-transfer catalyst, were later added. The reaction mixture was heated under reflux for 12 h. The solvent was evaporated at reduced pressure, the residue dissolved in water (100 mL) and acidified to pH 7 with concentrated HCl. The solution was extracted with diethyl ether (2 x 100 mL). The water phase was further acidified with HCl concentrated to pH 1.5 and stirred for 2 h. A white foam was formed. The residue was separated by filtration, washed by diethyl ether and dried under reduced pressure to give ligand L²H (**2**) in 41% yield. Mp. 176-179°C. ¹H NMR (CDCl₃, 293K): δ 2.20 (s, 6H, CH₃), 2.24 (s, 6H, CH₃), 5.90 (s, 2H, 4-CH), 6.91 (s, 1H, CHCOO), 8.50 (br, 1H, COOH). IR (cm⁻¹): 3130w, 3093w, 2965w, 2927w (CH); 2460br (OH); 1740s (C=O); 1560s (C=N); 1489w, 1441m, 1415s, 1378m, 1343s, 1311m, 1252s, 1219s, 1160m, 1149m, 1113w, 1048m, 1038m, 1003w, 974s, 889m, 829s, 814s, 783s, 764m, 723s, 703s, 665w. ESIMS (major positive-ions, CH₃OH), *m/z* (%): 287 (100) [L²H + K]⁺, 249 (10) [L²H + H]⁺. ESIMS (major negative-ions, CH₃OH), *m/z* (%): 247 (100) [L²]⁻. Calcd. for C₁₂H₁₆N₄O₂: C, 58.05; H, 6.50; N, 22.57%. Found: C, 58.02; H, 6.55; N, 22.00%.

Synthesis of (±)-(6,6-Diphenyl-1,4-dioxan-2-yl)methanamine (NMDA, **3**)

The syntheses of NMDA and the related bioconjugated ligands L^{NMDA} and L^{2NMDA} were performed in collaboration with Dr. Fabio Del Bello of the School of Pharmacy of the University of Camerino.

(a) 2,2-Diphenyloxirane.

Sodium hydride (60% dispersion in mineral oil, 2.195 g, 54.880 mmol) was added to a solution of benzophenone (5.000 g, 27.440 mmol) and trimethylsulfonium iodide (11.199 g, 54.880 mmol) in dimethylsulfoxide (DMSO, 30 mL) at room temperature and the reaction mixture was stirred overnight at room temperature. The mixture was poured into water and extracted with diethyl ether (Et₂O). The organic layer was concentrated under reduced pressure to give the title compound as a white solid in 89% yield. Mp. 53-55°C. ¹H NMR (CDCl₃): δ 3.28 (s, 2H, CH₂O), 7.26-7.51 (m, 10H, ArH).

(b) 2-(Allyloxy)-1,1-diphenylethanol.

2,2-Diphenyloxirane (**a**, 6.300 g, 32.104 mmol) was added dropwise to a stirred solution of freshly cut sodium (0.220 g, 9.569 mmol) in allyl alcohol (22 mL) at room temperature. After 1 h at room temperature, the reaction mixture was refluxed for 20 h. Most of the unreacted allyl alcohol was then separated by distillation at atmospheric pressure. After cooling to room temperature, 6N H₂SO₄ (0.6 mL) was added to the residual solution to neutralize the sodium alloxide, and solvent removal was continued to afford a residual oil, which was purified by column chromatography, eluting with cyclohexane/ethyl acetate (10:0.05) to give a solid in 85% yield. Mp. 29-31°C. ¹H NMR (CDCl₃): δ 3.54 (s br, 1H, OH), 4.02 (s, 2H, CH₂O), 4.15 (d, 2H, OCH₂), 5.28 (m, 2H, C=CH₂), 5.94 (m, 1H, CH=C), 7.21-7.53 (m, 10H, ArH).

(c) 2-(Oxiran-2-ylmethoxy)-1,1-diphenylethanol.

m-Chloroperbenzoic acid (50%) (11.600 g, 33.610 mmol) was added to a solution of **b** (3.000 g, 11.796 mmol) in CH₂Cl₂ (120 mL). After 20 h at room temperature under stirring the reaction mixture was washed with 10% Na₂SO₃, 5% Na₂CO₃, and H₂O. Removal of dried solvents afforded a solid in 90% yield. Mp. 83-84°C. ¹H NMR (CDCl₃): δ 1.60 (s br, 1H, OH), 2.55 and 2.80 (two dd, 2H, CH₂O oxiran), 3.16 (m, 1H, CHO oxiran), 3.52 and 3.90 (two dd, 2H, OCH₂), 4.10 (dd, 2H, CH₂O), 7.18-7.52 (m, 10H, ArH).

(d) (6,6-Diphenyl-1,4-dioxan-2-yl)methanol.

A solution of **c** (29.400 g, 108.760 mmol) and (1S)-(+)-10-camphorsulfonic acid (3.300 g, 14.206 mmol) in CH₂Cl₂ (500 mL) was refluxed for 8 h. The reaction mixture was then washed with NaHCO₃ saturated solution and dried over Na₂SO₄. Removal of the solvent gave a residue, which was purified by column chromatography eluting with cyclohexane/ethyl acetate (9:1) to afford a solid in 60% yield. Mp. 114-115°C. ¹H NMR

(CDCl₃): δ 1.84 (s br, 1H, OH), 3.53-3.83 (m, 5H, dioxan and CH₂), 3.64 and 4.61 (two d, 2H, dioxan), 7.20-7.58 (m, 10H, ArH).

(e) (6,6-Diphenyl-1,4-dioxan-2-yl)methyl 4-Methylbenzenesulfonate.

Tosyl chloride (0.400 g, 2.098 mmol) was added to a stirred solution of **d** (0.400 g, 1.480 mmol) in pyridine (5 mL) at 0°C for 30 min. After 3 h at 0°C, the mixture was left for 20 h at 4°C in the freezer. Then it was poured into ice and concentrated HCl (5 mL) and extracted with CHCl₃. The organic layers were washed with 2N HCl (15 mL), NaHCO₃ saturated solution (15 mL), and H₂O (15 mL) and then dried over Na₂SO₄. The evaporation of the solvent afforded **e** as a solid in 69% yield. Mp. 130-131°C. ¹H NMR (CDCl₃): δ 2.41 (s, 3H, CH₃), 3.41 (m, 2H, CH₂O), 3.70 (m, 2H, dioxan), 4.01 (m, 2H, dioxan), 4.48 (d, 1H, dioxan), 7.08-7.78 (m, 14H, ArH).

(f) 6-(Azidomethyl)-2,2-diphenyl-1,4-dioxane.

NaN₃ (0.300 g, 4.615 mmol) was added to a solution of **e** (0.960 g, 2.261 mmol) in dimethylformamide (DMF, 5 mL). The mixture was stirred at 100°C for 3 h and then poured into H₂O and extracted with Et₂O. The organic layer was washed with brine, dried over Na₂SO₄ and concentrated in vacuo to give 0.85 g of azide **f**, which was employed in the next step without further purification.

(NMDA, **3**) (\pm)-(6,6-Diphenyl-1,4-dioxan-2-yl)methanamine.

A solution of **f** (0.250 g, 0.846 mmol) in Et₂O (10 mL) was added dropwise, at 0°C, to a suspension of LiAlH₄ (0.360 g, 9.486 mmol) in Et₂O (10 mL). The mixture was stirred at room temperature for 4 h. The reaction was quenched with saturated Na₂SO₄ solution and filtered. After evaporation of the filtrate, the residue was purified by column chromatography eluting with CHCl₃/MeOH (95:5) to obtain an oil in 79% yield. ¹H NMR (CDCl₃): δ 1.96 (s br, 2H, NH₂), 2.78 (m, 2H, CH₂N), 3.40-3.80 (m, 4H, dioxan), 4.60 (d, 1H, dioxan), 7.18-7.57 (m, 10H, ArH). The free base was transformed into the oxalate salt that was crystallized from ethanol (EtOH). Mp. 211-212°C. Calcd. for C₁₇H₁₉NO₂·H₂C₂O₄: C, 63.50; H, 5.89; N, 3.90%. Found: C, 63.42; H, 5.89; N, 3.90%.

Synthesis of L^{NMDA} (**4**)

Carbonyldiimidazole (CDI, 0.302 g, 1.860 mmol) was added to a solution of LH (**1**) (0.357 g, 1.860 mmol) in THF. The reaction mixture was stirred at reflux for 2 h. Then it was cooled to 0°C, NMDA was added (0.501 g, 1.860 mmol) and the solution was stirred at room temperature for 3 h. Then it was dried under reduced pressure, and the oil formed dissolved in CHCl₃ and washed with NaHCO₃ saturated solution and HCl 2N. The CHCl₃ phase was dried with Na₂SO₄, filtered and dried under reduced pressure to give a solid, which was purified by column chromatography, eluting first with cyclohexane, and then with cyclohexane/ethyl acetate (5:5), obtained in 47% yield. Mp. 172-173°C. ¹H NMR (CDCl₃, 293K): δ 3.37-3.76 (m, 6H, dioxan and CH₂N), 4.58 (d, 1H, dioxan), 6.35 (m, 2H, 4-CH),

7.10 (s, 1H, CH), 7.18–7.39 (m, 14H, ArH, 3-CH and 5-CH), 7.83 (s br, 1H, NH). IR (cm⁻¹): 3287br (NH); 3121w, 3103w, 3052w, 3026w, 2978w, 2935w, 2915w, 2860w (CH); 1682s (C=O); 1560m (C=N); 1516w, 1495m, 1451m, 1432m, 1388m, 1350w, 1312m, 1293m, 1271m, 1244m, 1211w, 1188w, 1163w, 1122s, 1088s, 1065s, 1050s, 1026m, 1000m, 991s, 958m, 916s, 886w, 858m, 844m, 809s, 766s, 750s, 729s, 705s, 694s, 661m. ESIMS (major positive-ions, CH₃CN), *m/z* (%): 444 (100) [L^{NMDA} + H]⁺. ESIMS (major negative-ions, CH₃CN), *m/z* (%): 442 (100) [L^{NMDA} - H]⁻. Calcd. for C₂₂H₂₅N₅O₃: C, 67.70; H, 5.68; N, 15.79%. Found: C, 67.08; H, 5.76; N, 14.50%.

Synthesis of L^{2NMDA} (**5**)

Carbonyldiimidazole (CDI, 0.180 g, 1.110 mmol) was added to a solution of L²H (**2**) (0.275 g, 1.110 mmol) in THF. The reaction mixture was stirred for 2 h. Then it was cooled to 0°C, NMDA was added (0.299 g, 1.110 mmol) and the solution was stirred at room temperature (r.t.) for 3 h. Then it was dried under reduced pressure, and the oil formed dissolved in CHCl₃ and washed by NaHCO₃ saturated solution and HCl 2N. The CHCl₃ phase was dried with Na₂SO₄, filtered and dried under reduced pressure to give a solid, which was purified by column chromatography, eluting first with cyclohexane/ethyl acetate (EtOAc) (7:3), and then with cyclohexane/EtOAc (5:5), obtained in 54% yield. Mp. 171-172°C. ¹H NMR (CDCl₃, 293K): δ 2.10 (s, 3H, CH₃), 2.13 (s, 3H, CH₃), 2.38 (s, 3H, CH₃), 2.39 (s, 3H, CH₃), 3.30-3.79 (m, 6H, dioxan and CH₂N), 4.61 (d, 1H, dioxan), 5.84 (s, 1H, 4-CH), 5.85 (s, 1H, 4-CH), 6.77 (s, 1H, CH), 7.18–7.39 (m, 10H, ArH), 8.10 (s br, 1H, NH). IR (cm⁻¹): 3423w (NH); 3090w, 3062w, 2985w, 2961w, 2926w, 2907w, 2869w (CH); 1702s (C=O); 1568m (C=N); 1520s, 1465m, 1446s, 1415m, 1372m, 1364m, 1335w, 1316m, 1295m, 1260m, 1240m, 1221w, 1128m, 1102s, 1064s, 1028m, 998m, 985m, 940m, 919m, 874m, 835m, 814m, 799m, 773s, 757s, 739s, 722m, 707s, 698s, 663m. ESIMS (major positive-ions, CH₃OH), *m/z* (%): 1022 (100) [2L^{2NMDA} + Na]⁺; 522 (20) [L^{2NMDA} + Na]⁺. ESIMS (major negative-ions, CH₃OH), *m/z* (%): 498 (100) [L^{2NMDA} - H]⁻. Calcd. for C₂₉H₃₃N₅O₃: C, 69.72; H, 6.66; N, 14.02%. Found: C, 69.93; H, 6.85; N, 13.01%.

Synthesis of the complexes

Synthesis of [(L^{OMe})CuCl₂] (**6**)

To a methanol suspension (50 mL) of LH (**1**, 0.192 g, 1.000 mmol) CuCl₂·2H₂O was added (0.170 g, 1.000 mmol). The reaction mixture was stirred at room temperature for 3 h to obtain a green precipitate, which was filtered off and dried at reduced pressure to give a light green complex [(L^{OMe})CuCl₂] (**6**) in 81% yield. Mp. 214-216°C. IR (cm⁻¹): 3139w, 3118w, 2990w, 2959w (CH); 1747s (C=O); 1518w (C=N); 1454m, 1431m, 1402s, 1355w, 1285s, 1255m, 1229s, 1198m, 1177m, 1148w, 1105w, 1093m, 1072s, 1059s, 1003w, 989m, 973s, 924w, 911w, 854w, 805m, 767s, 664m. ESIMS (major positive-ions, CH₃OH),

m/z (%): 304 (100) $[(L^{OMe})CuCl]^+$; 255 (30) $[(L)Cu]^+$. ESIMS (major negative-ions, CH_3OH), m/z (%): 170 (100) $[CuCl_3]^-$. Calcd. for $C_9H_{10}Cl_2CuN_4O_2$: C, 31.73; H, 2.96; N, 16.45%. Found: C, 31.28; H, 2.93; N, 16.08%.

This synthesis has been also performed starting from a 1:2 stoichiometric ratio between metal and ligand, and the same product resulted from this synthesis.

Synthesis of $[(L^{2OMe})CuCl_2]$ (**7**)

To a methanol solution (50 mL) of L^2H (**2**, 0.248 g, 1.000 mmol) $CuCl_2 \cdot 2H_2O$ was added (0.170 g, 1.000 mmol). The reaction mixture was stirred at room temperature for 3 h, filtered, and dried at reduced pressure to give the green complex $[(L^{2OMe})CuCl_2]$ (**7**) in 90% yield. Mp. 212-217°C. IR (cm^{-1}): 3136w, 3101w, 2953w, 2919w (CH); 1757s (C=O); 1638m; 1559s (C=N); 1469s, 1420s, 1385s, 1318s, 1297s, 1234s, 1272s, 1163m, 1135w, 1119m, 1059m, 1038s, 990s, 916w, 896s, 868s, 833m, 804s, 780s, 711s, 662m. ESIMS (major positive-ions, CH_3OH), m/z (%): 622 (100) $[(L^{2OMe})_2CuCl]^+$; 572 (55) $[(L^2)(L^{2OMe})Cu]^+$; 360 (50) $[(L^{2OMe})CuCl]^+$. ESIMS (major negative-ions, CH_3OH), m/z (%): 170 (100) $[CuCl_3]^-$. Calcd. for $C_{13}H_{18}Cl_2CuN_4O_2$: C, 39.35; H, 4.57; N, 14.12%. Found: C, 41.29; H, 5.06; N, 14.03%.

By dissolving the crude complex **7** in methanol solution and by slow evaporation of the solution, single blue crystals suitable for X-ray diffraction analysis were obtained. The crystal were characterized by IR analyses (cm^{-1}): 3364br; 3100w, 2925w (CH); 1630s (C=O); 1560s (C=N); 1464m, 1420m, 1390m, 1378m, 1361s, 1341m, 1316s, 1244m, 1130w, 1053w, 991w, 937w, 913w, 886w, 834w, 810m, 792m, 773w, 756s, 708s. The X-ray diffraction study revealed that the structure of the crystals corresponds to the $[(L^2)_2Cu]$. This synthesis has been also performed starting from a 1:2 stoichiometric ratio between metal and ligand, and the same product resulted from this synthesis.

Synthesis of $[(L^{NMDA})CuCl_2]$ (**8**)

To a methanol suspension (25 mL) of L^{NMDA} (**4**, 0.015 g, 0.338 mmol) $CuCl_2 \cdot 2H_2O$ was added (0.006 g, 0.338 mmol). The reaction mixture was stirred at room temperature for 12 h to obtain a light blue precipitate, which was filtered off and dried at reduced pressure to give the cyan complex $[(L^{NMDA})CuCl_2]$ (**8**) in 61% yield. Mp. 232-235°C. IR (cm^{-1}): 3274w (NH); 3112w, 3053w, 2979w, 2957w, 2916w, 2859w (CH); 1678s (C=O); 1567m (C=N); 1509w, 1492w, 1452m, 1427w, 1401m, 1366w, 1325w, 1307w, 1283m, 1239m, 1202w, 1127m, 1093m, 1065s, 1051m, 1026w, 1001w, 985m, 936m, 915w, 899w, 889w, 865w, 845m, 830m, 747s, 726m, 706s, 694m, 662m. ESIMS (major positive-ions, $CH_3OH/DMSO$ (10:1)), m/z (%): 984 (50) $[(L^{NMDA})_2CuCl]^+$. ESIMS (major negative-ions, CH_3OH), m/z (%): 170 (100) $[CuCl_3]^-$, 478 (70) $[L^{NMDA} + Cl]^-$. Calcd. for $C_{25}H_{25}Cl_2CuN_5O_3$: C, 51.95; H, 4.36; N, 12.12%. Found: C, 52.00; H, 4.40; N, 12.45%.

Synthesis of $[(L^{2NMDA})CuCl_2] \cdot H_2O$ (**9**)

To a methanol solution (25 mL) of L^{2NMDA} (**5**, 0.015 g, 0.300 mmol) $CuCl_2 \cdot 2H_2O$ (0.005 g, 0.300 mmol) was added. The reaction mixture was stirred at room temperature for 12 h to obtain a light blue solution, which was evaporated at reduced pressure to give the brown complex $[(L^{2NMDA})CuCl_2] \cdot H_2O$ (**9**) in 65% yield. Mp. 194°C dec. IR (cm^{-1}): 3432br (OH); 3198br, 3058w, 3024w, 2968br, 2904br (CH); 1667s (C=O); 1562s (C=N); 1490w, 1460m, 1448m, 1418m, 1395m, 1351w, 1311m, 1247m, 1226m, 1126m, 1106m, 1062m, 1050m, 1026m, 989m, 935w, 900m, 874m, 859w, 796w, 767m, 753m, 729m, 700s, 665m. ESIMS (major positive-ions, CH_3OH), m/z (%): 531 (100) $[(L^{2NMDA})_2Cu]^{++}$. ESIMS (major negative-ions, CH_3OH), m/z (%): 170 (100) $[CuCl_3]^-$, 247 (25) $[L^2]^-$. Calcd. for $C_{29}H_{35}Cl_2CuN_5O_4$: C, 53.42; H, 5.41; N, 10.74%. Found: C, 52.72; H, 5.20; N, 10.77%.

Synthesis of $[(LH)Cu(PPh_3)_2]PF_6$ (**10**)

To an acetonitrile suspension (50 mL) of triphenylphosphine (PPh_3 , 0.524 g, 2.000 mmol), $Cu(MeCN)_4PF_6$ was added (0.373 g, 1.000 mmol). The reaction mixture was stirred at room temperature for 3 h, then LH (**1**) was added (0.192 g, 1.000 mmol) and the suspension stirred overnight. The reaction mixture was filtered, and dried at reduced pressure; the solid was washed by Et_2O to remove the excess of PPh_3 and dried at reduced pressure to give the white complex $[(LH)Cu(PPh_3)_2]PF_6$ (**10**) in 40% yield. Mp. 92°C dec. 1H NMR (DMSO, 293K): δ 6.36 (s, 2H, 4-CH), 7.26-7.61 (m, 33H, C_5H_6 , $CHCOO$ and 5-CH), 8.02 (s, 2H, 3-CH). $^{31}P\{^1H\}$ NMR (DMSO, 293K): δ -143.10 (septet, $J(F-P) = 711$ Hz, PF_6), -3.09 (s br), 26.64 (s). IR (cm^{-1}): 3138w, 3056w 3004w, 2987w (CH); 1751m (C=O); 1586w (C=N); 1522w, 1481m, 1435m, 1403m, 1298m, 1224w, 1207w, 1184w, 1159w, 1095m, 1058w, 1027w, 999w, 986w, 918w, 833s, 741s, 692s. ESIMS (major positive-ions, CH_3OH), m/z (%): 587 (100) $[Cu(PPh_3)_2]^+$; 517 (60) $[(LH)CuPPh_3]^+$. ESIMS (major negative-ions, CH_3OH), m/z (%): 145 (100) $[PF_6]^-$. Calcd. for $C_{44}H_{38}CuF_6N_4O_2P_3$: C, 57.12; H, 4.14; N, 6.06%. Found: C, 57.95; H, 4.26; N, 4.95%.

Synthesis of $[(L^2H)Cu(PPh_3)_2]PF_6$ (**11**)

To an acetonitrile suspension (50 mL) of PPh_3 (0.524 g, 2.000 mmol), $Cu(MeCN)_4PF_6$ was added (0.373 g, 1.000 mmol). The reaction mixture was stirred at room temperature for 3 h, then L^2H (**2**) was added (0.248 g, 1.000 mmol) and the suspension stirred overnight. The reaction mixture was filtered and dried at reduced pressure; the solid was washed by Et_2O to remove the excess of PPh_3 and dried at reduced pressure to give complex $[(L^2H)Cu(PPh_3)_2]PF_6$ (**11**) in 62% yield. Mp. 50°C dec. 1H NMR ($CDCl_3$, 293K): δ 2.01 (s, 6H, CH_3), 2.47 (s, 6H, CH_3), 6.01 (s, 2H, 4-CH), 6.81 (br, 1H, $CHCOO$), 7.26-7.41 (m, 30H, C_5H_6). $^{31}P\{^1H\}$ NMR ($CDCl_3$, 293K): -143.31 (septet, $J(F-P) = 713$ Hz, PF_6), -2.85 (sbr), 8.03 (sbr), 34.26 (s). $^{31}P\{^1H\}$ NMR ($CDCl_3$, 243K): δ -144.48 (septet, $J(F-P) = 713$ Hz, PF_6),

-4.60 (s), 6.63 (s), 34.82 (s). IR (cm⁻¹): 3144br, 3056w, 3001w, 2990w, 2932br (CH); 1752m (C=O); 1563m (C=N); 1481m, 1436s, 1393w, 1315m, 1223w, 1160w, 1095m, 1028w, 999w, 833s, 743s, 723s, 693s. ESIMS (major positive-ions, CH₃OH), *m/z* (%): 573 (100) [(L²H)CuPPh₃]⁺. ESIMS (major negative-ions, CH₃OH), *m/z* (%): 145 (100) [PF₆]⁻. Calcd. for C₄₈H₄₆CuF₆N₄O₂P₃: C, 58.75; H, 4.72; N, 5.71%. Found: C, 55.05; H, 5.04; N, 5.64%.

Synthesis of [(LH)Cu(PTA)₂]PF₆ (**12**)

To an acetonitrile suspension (50 mL) of PTA (0.236 g, 1.500 mmol), Cu(MeCN)₄PF₆ was added (0.280 g, 0.750 mmol). The reaction mixture was stirred at room temperature for 3 h, then a methanol suspension of LH (**1**) was added (0.144 g, 0.750 mmol) and the suspension was stirred overnight. The reaction mixture was filtered and dried at reduced pressure to give complex [(LH)Cu(PTA)₂]PF₆·MeCN (**12**) in 63% yield. Mp. 50°C dec. ¹H NMR (DMSO, 293K): δ 4.10 (br, 12H, CH₂P), 4.52 (m, J(H-H) = 12.4 Hz, 12H, NCH₂N), 6.40 (s, 2H, CH), 7.29 (s, 1H, CHN), 7.66 (s, 2H, CH), 8.03 (s, 2H, CH). ³¹P{¹H} NMR (D₂O, 293K): δ -143.95 (septet, J(F-P) = 708 Hz, PF₆), -85.54 (br). ³¹P{¹H} NMR (CD₃CN, 293K): δ -143.47 (septet, J(F-P) = 707 Hz, PF₆), -87.21 (br). ³¹P{¹H} NMR (CD₃CN, 238K): δ -144.62 (septet, J(F-P) = 708 Hz, PF₆), -85.50 (br). IR (cm⁻¹): 3130br, 2943br (CH); 1646s (C=O); 1515w (C=N); 1450w, 1405m, 1358w, 1292s, 1242m, 1119w, 1100m, 1060w, 1016s, 972s, 950s, 830s, 747s, 657m. ESIMS (major positive-ions, CH₃CN), *m/z* (%): 412 (100) [(LH)CuPTA]⁺. ESIMS (major negative-ions, CH₃CN), *m/z* (%): 145 (100) [PF₆]⁻; 191 (10) [L]⁻. Calcd. for C₂₀H₃₂CuF₆N₁₀O₂P₃: C, 33.60; H, 4.51; N, 19.59%. Found: C, 36.02; H, 5.11; N, 18.71%.

Synthesis of [(L²H)Cu(PTA)₂]PF₆ (**13**)

To an acetonitrile suspension (50 mL) of PTA (0.236 g, 1.500 mmol), Cu(MeCN)₄PF₆ was added (0.280 g, 0.750 mmol). The reaction mixture was stirred at room temperature for 3 h, then a methanol suspension of L²H (**2**) was added (0.186 g, 0.750 mmol) and the suspension stirred overnight. The reaction mixture was filtered and dried at reduced pressure to give complex [(L²H)Cu(PTA)₂]PF₆ (**13**) in 50% yield. Mp. 55°C dec. ¹H NMR (DMSO, 293K): δ 2.17 (s, 9H, CH₃), 2.34 (s, 9H, CH₃), 4.15 (s br, 12H, CH₂P), 4.48-4.67 (AB q, J(H-H) = 12.4 Hz, 12H, NCH₂N), 6.03 (s, 2H, 4-CH), 6.42 (br, 1H, CHCOO). ³¹P{¹H} NMR (D₂O, 293K): δ -144.03 (septet, J(F-P) = 709 Hz, PF₆), -85.87 (br). ³¹P{¹H} NMR (CD₃CN, 293K): δ -144.53 (septet, J(F-P) = 706 Hz, PF₆), -90.70 (br). ³¹P{¹H} NMR (CD₃CN, 238K): δ -144.68 (septet, J(F-P) = 706 Hz, PF₆), -89.93 (br). IR (cm⁻¹): 2923br (CH); 1639s (C=O); 1560m (C=N); 1484w, 1420m, 1358w, 1292s, 1242m, 1119w, 1100m, 1060w, 1016s, 972s, 950s, 830s, 747s. ESIMS (major positive-ions, CH₃CN), *m/z* (%): 468 (100) [(L²H)CuPTA]⁺. ESIMS (major negative-ions, CH₃CN), *m/z* (%): 145 (100) [PF₆]⁻.

Calcd. for $C_{24}H_{40}CuF_6N_{10}O_2P_3$: C, 37.38; H, 5.23; N, 18.16%. Found: C, 34.32; H, 4.88; N, 15.71%.

Synthesis of $[(L^{NMDA})Cu(PTA)_2]PF_6$ (**14**)

To an acetonitrile suspension (50 mL) of PTA (0.094 g, 0.600 mmol) $Cu(MeCN)_4PF_6$ was added (0.112 g, 0.300 mmol). The reaction mixture was stirred at room temperature for 3 h, then a methanol suspension of L^{NMDA} (**4**) was added (0.133 g, 0.300 mmol) and the suspension stirred overnight. The reaction mixture was filtered, and dried at reduced pressure to give complex $[(L^{NMDA})Cu(PTA)_2]PF_6$ (**14**) in 62% yield. Mp. 110°C dec. 1H NMR ($CDCl_3$, 293K): δ 3.32-3.67 (m, 6H, dioxan and CH_2N), 4.04 (s br, 12H, CH_2P), 4.38-4.81 (m, 13H, dioxan and NCH_2N), 6.43 (m, 2H, 4-*CH*), 7.18-8.04 (m, 14H, *ArH*, 3-*CH* and 5-*CH*), 8.53 (s br, 1H, *NH*). ^{31}P NMR (CD_3CN , 293K): δ -143.52 (septet, $J(F-P) = 706$ Hz, PF_6), -91.63 (br). IR (cm^{-1}): 2925br (CH); 1738sh, 1696br (C=O); 1520br (C=N); 1449w, 1403w, 1366w, 1292m, 1242m, 1127w, 1100m, 1061w, 1044w, 1015s, 970s, 948s, 917w, 893w, 831s, 757s, 742s, 729m, 700s, 664m. ESIMS (major positive-ions, CH_3CN), m/z (%): 506 (100) $[(L^{2NMDA})Cu]^+$, 663 (70) $[(L^{2NMDA})CuPTA]^+$. ESIMS (major negative-ions, CH_3CN), m/z (%): 145 (100) $[PF_6]^-$. Calcd. for $C_{37}H_{49}CuF_6N_{11}O_3P_3$: C, 45.99; H, 5.11; N, 15.94%. Found: C, 44.57; H, 5.06; N, 15.10%.

Synthesis of $[(L^{2NMDA})Cu(PTA)_2]PF_6$ (**15**)

To an acetonitrile suspension (50 mL) of PTA (0.094 g, 0.600 mmol) $Cu(MeCN)_4PF_6$ was added (0.112 g, 0.300 mmol). The reaction mixture was stirred at room temperature for 3 h, then a methanol suspension of L^{2NMDA} (**5**) was added (0.150 g, 0.300 mmol) and the suspension stirred overnight. The reaction mixture was filtered, and dried at reduced pressure to give complex $[(L^{2NMDA})Cu(PTA)_2]PF_6$ (**15**) in 59% yield. Mp. 120°C dec. 1H NMR ($CDCl_3$, 293K): δ 2.06-2.17 (m, 12H, CH_3), 3.24-3.63 (m, 6H, dioxan and CH_2N), 4.02 (s br, 12H, CH_2P), 4.20-4.62 (m, 13H, dioxan and NCH_2N), 6.19 (s, 1H, 4-*CH*), 6.21 (s, 1H, 4-*CH*), 6.98 (s, 1H, *CH*), 7.22-7.46 (m, 10H, *ArH*), 9.01 (s br, 1H, *NH*). ^{31}P NMR (CD_3CN , 293K): δ -143.52 (septet, $J(F-P) = 706$ Hz, PF_6), -89.53 (v br). IR (cm^{-1}): 2921br (CH); 1699br (C=O); 1563w (C=N); 1519br, 1449m, 1416m, 1315w, 1293m, 1242s, 1127w, 1102m, 1062w, 1045w, 1014s, 959s, 947s, 893w, 873w, 830s, 800s, 741s, 731s, 700s, 664m. ESIMS (major positive-ions, CH_3CN), m/z (%): 719 (100) $[(L^{2NMDA})CuPTA]^+$. ESIMS (major negative-ions, CH_3CN), m/z (%): 145 (100) $[PF_6]^-$. Calcd. for $C_{41}H_{57}CuF_6N_{11}O_3P_3$: C, 48.16; H, 5.62; N, 15.07%. Found: C, 46.47; H, 5.56; N, 14.32%.

Synthesis of [(LH)Cu(L)ClO₄] (**16**)

To a methanol suspension (25 mL) of LH (**1**) (0.384 g, 2.000 mmol) a water solution (25 mL) of Cu(ClO₄)₂·6H₂O was added (0.371g, 1.000 mmol). The suspension was stirred at room temperature for 3 h. The precipitate was filtered off and dried at reduced pressure to give the blue complex [(LH)Cu(L)ClO₄] (**16**) in 69% yield Mp. 223-224°C. By dissolving the crude complex **16** in DMSO solution and by slow evaporation of the solution, single blue crystals suitable for X-ray diffraction analysis (Table 3.1. and Table 3.2.) were obtained. The X-ray diffraction study revealed that the structure of the crystals corresponds to the [(L)₂Cu] (Fig. 3.7.). The same crystals were obtained by dissolving the crude complex **16** in DMSO/CH₃OH (2:1) solution and by slow evaporation of the solution. IR (cm⁻¹): 3592br; 3491br; 3114br, 3147w, 3114w, 3013w (CH); 1722br, 1621sh, (C=O); 1510w (C=N); 1454w, 1407s, 1372w, 1286s, 1259m, 1235br, 1190m, 1107s, 1064s, 1031s, 994s, 929s, 859s, 847m, 770s, 715s, 670s. ESIMS (major positive-ions, H₂O), m/z (%): 446 (100) [(LH)(L)Cu]⁺. ESIMS (major negative-ions, H₂O), m/z (%): 99 (100) [ClO₄]⁻, 191 (95) [L]⁻. Calcd. for C₁₆H₁₅ClCuN₈O₈: C, 35.17; H, 2.77; N, 20.51%. Found: C, 34.70; H, 3.01; N, 19.82%.

III. Results and discussion

The topic of my work was the design and the synthesis of bis(pyrazolyl)acetates ligands and of bioconjugated ones, to be used in the synthesis of Cu(I) and Cu(II) complexes. All the ligands and the complexes were characterized using IR spectroscopy, NMR spectroscopy (^1H , ^{31}P), electrospray ionization mass (ESIMS) and elemental analysis. The evaluation of the biological activity as anticancer agents of the products as well as of the free ligands is in progress. My work follows the topics of the research group, which is focused on: (a) development of new boron- and carbon-centred scorpionate ligands with mixed C-, N-, O- and S-donor set; (b) evaluation of their coordination capabilities with main group and late transition metal ions; (c) applications in bioinorganic and medicinal chemistry (d) development of copper radiopharmaceuticals.

In the last years, the research group efforts involve the synthesis of group 11 metal complexes and the evaluation of their biological activity as potential anticancer compounds. Some water soluble Cu(I) complexes have been successfully tested as new metal-based anti-cancer agents able to circumvent the cisplatin resistance. At present, the research group is interested in the design, synthesis, study of the structural properties of innovative water soluble copper(I/II) complexes, their biological evaluation as anticancer agents and in particular in the synthesis of new heteroscorpionate ligands bearing pyrazole, triazole, 2-mercaptopyridine or 2-mercaptoimidazole rings, and the development of bioconjugated ligands. In particular I have synthesised the ligands $[\text{HC}(\text{CO}_2\text{H})(\text{pz}^{\text{Me}_2})_2]$ and $[\text{HC}(\text{CO}_2\text{H})(\text{pz})_2]$ that have also been functionalized by the research group of the School of Pharmacy of the University of Camerino with the potent NMDA receptor antagonist (6,6-diphenyl-1,4-dioxan-2-yl)methanamine, which showed a significant cytotoxic activity on MCF7 human breast cancer cell lines, highly expressing NMDA receptors.

Synthesis and characterization of the ligands

Starting from dichloroacetic acid and pyrazole (pz) for LH (**1**), 3,5-dimethylpyrazole (pz^{Me_2}) for L^2H (**2**), with an excess of potassium carbonate and potassium hydroxide in THF solvent, with a small quantity of tetra-*n*-butylammonium bromide as phase-transfer catalyst, I have synthesized, in a reasonable yield bis(pyrazol-1-yl)acetic acid $[\text{HC}(\text{CO}_2\text{H})(\text{pz})_2]$ (**1**) and bis(3,5-dimethylpyrazol-1-yl)acetic acid $[\text{HC}(\text{CO}_2\text{H})(\text{pz}^{\text{Me}_2})_2]$ (**2**), following the one-step synthesis design by Burzlaff *et al.* (Fig. 3.1.). The elemental analysis confirmed the stoichiometries of the two ligands and showed a good purity of the products, confirmed also by the narrow melting points. LH is soluble in acetone, methanol, THF and DMSO and insoluble in water, acetonitrile, chloroform, *n*-hexane and diethyl ether, while L^2H is soluble in water, methanol, ethanol, DMSO ethyl acetate and THF and insoluble in acetone, acetonitrile, chloroform, *n*-hexane and diethyl ether.

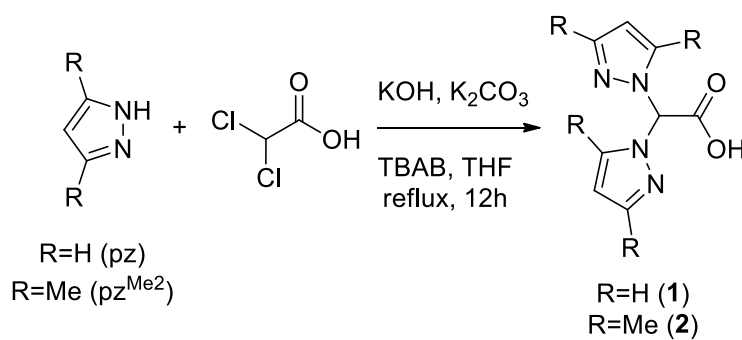


Fig. 3.1. Reaction scheme of the synthesis of **1** and **2**.

The infrared spectra carried out on solid samples of **1** and **2** showed all the expected bands for the ligands: weak absorptions in the range $2927\text{--}3177\text{ cm}^{-1}$ due to the pyrazole rings, broad peaks at 2454 and 2429 cm^{-1} for **1** and **2** respectively, attributable to the stretching of the OH of the carboxylic groups. The asymmetric stretchings of C=O of **1** and **2** are detected respectively at 1720 and 1740 cm^{-1} as strong peaks.

The ^1H NMR spectra of **1** and **2**, recorded in acetone and CDCl_3 solution, respectively, showed a single set of resonances for pyrazole rings, indicating that the pyrazoles are equivalent. The signals at δ 7.41 and 6.91 ppm, for **1** and **2** respectively, are attributable to the bridging carbons and are diagnostic for the effective substitution of the chlorides on the acetic acid with the pyrazoles. In the spectrum of **2** the chemical shifts of the methyls appear at δ 2.20 and 2.24 ppm, and the protons in the four position of the pyrazole rings are present at δ 5.90 ppm. In the spectrum of **1** the pyrazoles' hydrogens 3-CH, 4-CH, 5-CH are detectable at δ 7.97, 6.33, 7.54 ppm, respectively.

The ESIMS study was conducted by dissolving the ligands **1** and **2** in MeOH and recording the spectra in positive- and negative-ion mode. The molecular structures of the **1** and **2** are confirmed by the presence in the negative-ions spectra of the molecular peak at m/z 191 and 247 respectively attributable to the $[\text{L}]^-$ and $[\text{L}^2]^-$ species.

The synthesis of NMDA (**3**) was performed in 7 steps (Fig. 3.2.), in collaboration with Dr. Fabio Del Bello of the School of Pharmacy of the University of Camerino.

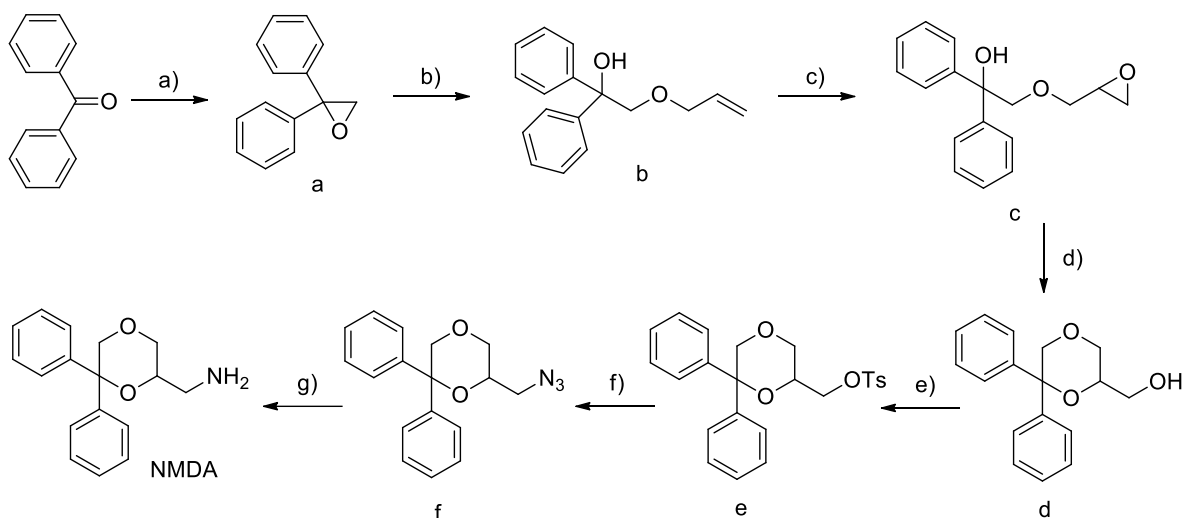


Fig. 3.2. Reaction scheme of the synthesis of **3**: (a) NaH, $(\text{CH}_3)_3\text{Si}$, DMSO (b) Na, $\text{CH}_2=\text{CHCH}_2\text{OH}$; (c) *m*-CPBA, CH_2Cl_2 ; (d) (1*S*)-(+)-CSA, CH_2Cl_2 ; (e) *p*-TsCl, pyridine; (f) NaN_3 , DMF; (g) LiAlH_4 , Et_2O .

The successive syntheses of L^{NMDA} (**4**) and $\text{L}^{2\text{NMDA}}$ (**5**) were performed in collaboration with Dr. Fabio Del Bello of the School of Pharmacy of the University of Camerino. To a solution of LH (**1**) and L^2H (**2**) respectively, CDI was added to promote amide bond formation between ligands and NMDA (**3**), later added at 0°C . After separation and purification by column chromatography L^{NMDA} and $\text{L}^{2\text{NMDA}}$ were formed in a reasonable yield and purity (Mp. $172\text{--}173^\circ\text{C}$ (**4**), $171\text{--}172^\circ\text{C}$ (**5**)) (Fig. 3.3.). The ligand **4** is soluble in acetonitrile, chloroform and DMSO, while **5** is soluble in methanol, acetonitrile, chloroform and DMSO.

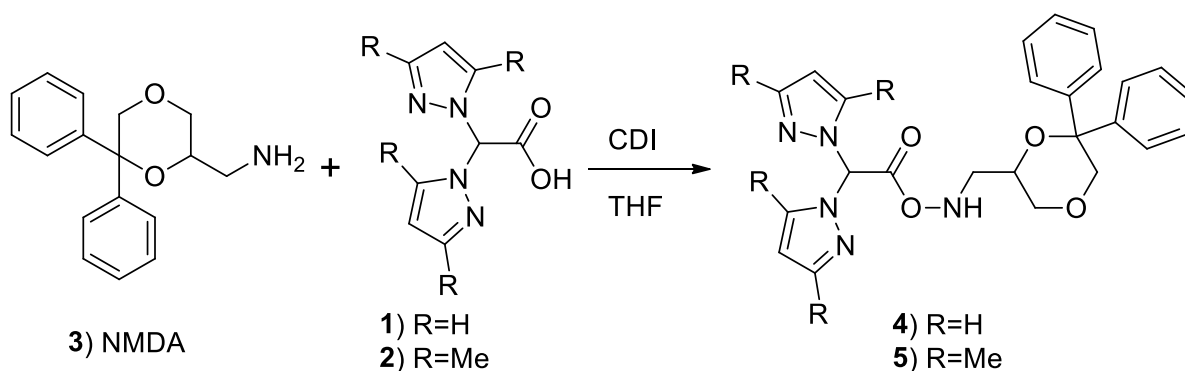


Fig. 3.3. Reaction scheme of the synthesis of **4** and **5**.

The infrared spectra carried out on solid samples of L^{NMDA} (**4**) and $\text{L}^{2\text{NMDA}}$ (**5**) showed all the expected bands for the ligands: in particular, weak absorptions due to the CH stretchings have been observed in the range $2860\text{--}3157\text{ cm}^{-1}$, while peaks attributable to the amide stretchings are present at 3287 cm^{-1} and 3423 cm^{-1} , respectively for L^{NMDA} and $\text{L}^{2\text{NMDA}}$. The asymmetric stretchings of the C=O groups are detected as strong peaks at 1681 and 1702 cm^{-1} , respectively, in the typical range for the amide groups.

The ^1H NMR spectra of L^{NMDA} (**4**) and $\text{L}^{2\text{NMDA}}$ (**5**), recorded in CDCl_3 solution, showed all the expected signals for the bioconjugated ligands. Interestingly, a double set of resonances appears for the pyrazole rings, indicating that the pyrazoles are not equivalents.

The ESIMS study was conducted by dissolving the ligands **4** and **5** in acetonitrile and methanol, respectively, and recording the spectra in positive- and negative-ion mode. The molecular structures of the **4** and **5** are confirmed by the presence in the negative-ions spectra of the molecular peak at m/z 442 and 498, attributable to the $[\text{L}^{\text{NMDA}} - \text{H}]^-$ and $[\text{L}^{2\text{NMDA}} - \text{H}]^-$ species, respectively. The positive-ions spectrum of **4** also shows the molecular peak $[\text{L}^{\text{NMDA}} + \text{H}]^+$ at m/z 444, while in the spectrum of **5** are observable the peaks at m/z 1022 and 522, relative to the species $[(\text{L}^{2\text{NMDA}})_2 + \text{Na}]^+$ and $[\text{L}^{2\text{NMDA}} + \text{Na}]^+$, respectively.

To confirm the stoichiometry the elemental analysis gives a positive matching between the calculated and the measured values for C, H and N.

Synthesis and characterization of the complexes

The copper complexes $[(\text{L}^{\text{OMe}})\text{CuCl}_2]$ (**6**, light green) and $[(\text{L}^{2\text{OMe}})\text{CuCl}_2]$ (**7**, green) have been prepared from the reaction of $\text{CuCl}_2 \cdot 2\text{H}_2\text{O}$ with LH (**1**) and L^2H (**2**) respectively, in methanol solution at room temperature (Fig. 3.4.). The compounds are soluble in water and DMSO, and **7** is also soluble in methanol.

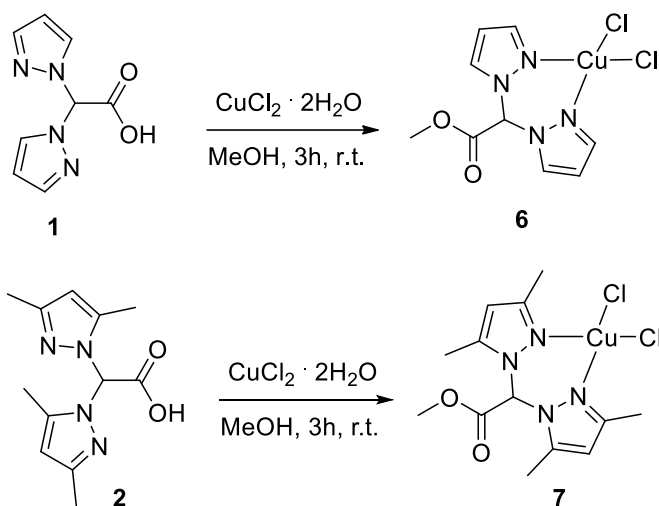


Fig. 3.4. Reaction scheme of the syntheses of **6** and **7**.

Interestingly, based on the spectroscopic analysis (*vide* Experimental Section) we observed the metal-catalysed esterification of the carboxylic group with methanol used as solvent in the synthesis. The exact mechanism of such a process has not been yet clarified but it is in accordance with a similar behaviour observed for the same ligands in the presence of Re(V) acceptors⁹⁸.

The infrared spectra carried out on the solid samples for **6** and **7** showed the absence of the OH stretchings of the carboxylic groups (present at 2450 and 2460 cm^{-1} in the free ligands, respectively), and the appearance of strong absorptions of C=O at 1748 and 1757 cm^{-1} , respectively, in a range typical for non-coordinating esters groups. In fact, I had synthesized the ester of the ligand L^2H and in the infrared spectra the stretching of the C=O group is observable as a strong peak at 1760 cm^{-1} . The weak absorption in the range 2919-3139 cm^{-1} is due to the pyrazole rings.

The ESIMS study was conducted by dissolving the compound **6** and **7** in acetonitrile and methanol respectively and recording the spectra in positive- and negative-ion mode. The formation of the complexes **6** and **7** are confirmed by the presence in the positive-ions spectra of the peaks at m/z 304 and 360 respectively attributable to the $[(\text{L}^{\text{OMe}})\text{CuCl}]^+$ and $[(\text{L}^{2\text{OMe}})\text{CuCl}]^+$ species. For **7** in positive-ion collection is also possible to individuate the major peak at m/z 622 for $[(\text{L}^{2\text{OMe}})_2\text{CuCl}]^+$ species, and at m/z 572 the fragment $[(\text{L}^2)(\text{L}^{2\text{OMe}})\text{Cu}]^+$. The elemental analyses confirm the stoichiometry and the purity of the products. Both the syntheses have been performed also in presence of an excess of ligand (up to 1:2 metal:ligand ratio) obtaining products with the same stoichiometry, to confirm that the initial stoichiometric ratio does not influence the final product.

By dissolving the crude complex $[(\text{L}^{2\text{OMe}})\text{CuCl}_2]$ (**7**) in methanol solution and by slow evaporation of the solution, single blue crystals suitable for X-ray diffraction analysis were obtained and the analysis gives the molecular structure (Fig. 3.5.) in which the metal centre is hexacoordinated by two anionic ligands in the typical “scorpionate” fashion. The X-ray diffraction analysis was performed by Prof. Luciano Marchiò of the Department of Chemistry of the University of Parma.

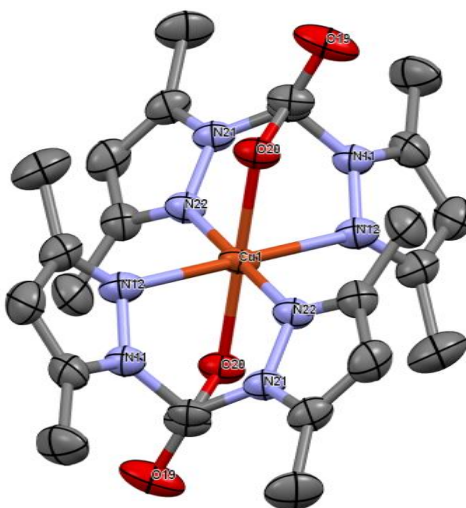


Fig. 3.5. Crystal structure of $[(\text{L}^2)_2\text{Cu}]$.

Studying more in detail the reactivity of **7**, I observed that if the drying process is continued after the formation of the green solid product, an orange powder appears in a small percentage with respect to the total residue (< 5%). It's possible to separate this new product by dissolving the mixture in methanol; obtaining a green solution (because compound **7** is soluble in methanol) and filtering off the orange product, which resulted to

be diamagnetic by recording ^1H and ^{13}C NMR spectra. Further investigations on the behaviour of the compound in solution and in the solid state, and on the possibility to obtain it performing the reaction in different solvents are in progress.

The copper complexes $[(\text{L}^{\text{NMDA}})\text{CuCl}_2]$ (**8**) and $[(\text{L}^{2\text{NMDA}})\text{CuCl}_2]\cdot\text{H}_2\text{O}$ (**9**), cyan and brown solids, have been prepared from the reaction of $\text{CuCl}_2\cdot 2\text{H}_2\text{O}$ with L^{NMDA} (**4**) and $\text{L}^{2\text{NMDA}}$ (**5**) respectively, in methanol solution for **8** and in methanol suspension for **9**, at room temperature (Fig. 3.6.). The compounds are soluble in DMSO, and **9** is also soluble in methanol, ethanol and chloroform.

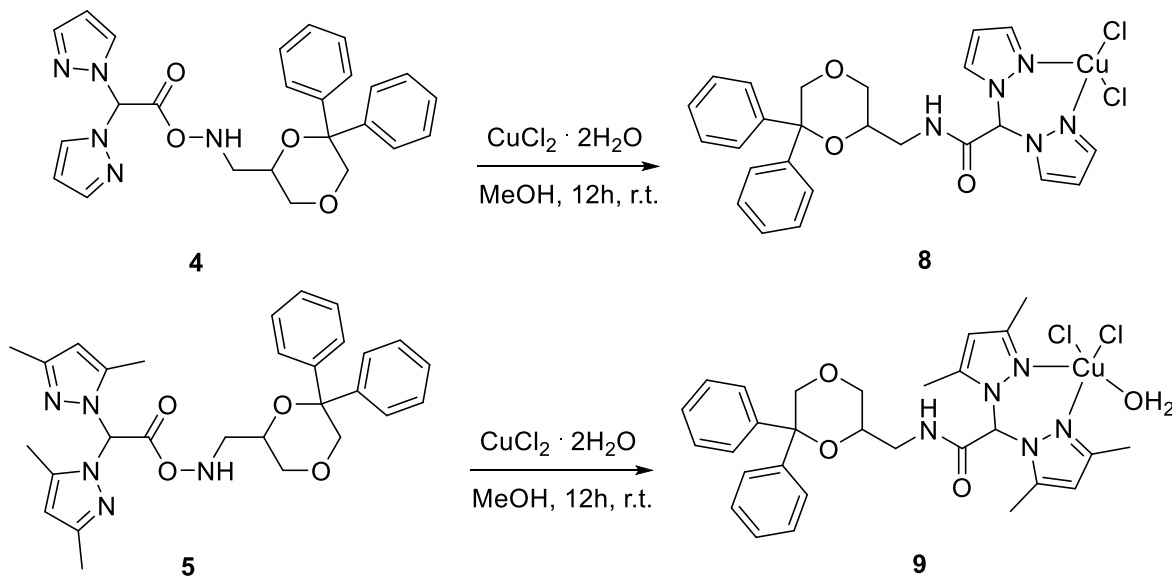


Fig. 3.6. Reaction scheme of the syntheses of **8** and **9**.

The infrared spectra carried out on solid samples **8** and **9** showed all the expected bands for the complexes reported: NH stretching is detected without a significant variation with a weak absorption peak at 3274 cm^{-1} for **8** and very broad absorption peak at 3432 cm^{-1} for **9** indicating the presence of a molecule of water; weak absorptions are observed in the range $2859\text{--}3198\text{ cm}^{-1}$ due to the pyrazoles rings. The strong absorption at 1667 and 1678 cm^{-1} for **9** and **8** respectively, without a significant variation with respect to the absorptions detectable in the free ligands, indicate that the carbonyl groups are not involved in the coordination of the metal. The copper centre results in a tetracoordinated environment with the ligand chelating in a bidentate fashion, and the other two positions occupied by the chlorides.

The ESIMS study was conducted by dissolving compounds **8** and **9** in methanol/DMSO and methanol respectively, and recording the spectra in positive- and negative-ion mode. In the positive ion spectrum of **9** it's possible to detect a major peak, at m/z 531, attributable to the $[(\text{L}^{2\text{NMDA}})_2\text{Cu}]^{++}$ species, confirming the complex formation, while in the spectrum of **8** a peak at m/z 984 is attributable to the $[(\text{L}^{\text{NMDA}})_2\text{CuCl}]^+$ species. The negative-ion mode spectra of **8** and **9** showed two peaks at m/z 478 and 247, attributable to the species $[\text{L}^{\text{NMDA}} + \text{Cl}]^-$ and $[\text{L}^2]^-$, respectively, confirming the presence of the ligands in

the complexes. The elemental analyses confirm the stoichiometry of the complexes and the presence of a molecule of water for compound **9**.

The blue copper complex $[(LH)Cu(L)ClO_4]$ (**16**) has been prepared from the reaction of $CuClO_4 \cdot 6H_2O$ with LH (**1**) in a water/methanol suspension at room temperature. The compound is water soluble.

By dissolving the crude complex **16** in DMSO solution and by slow evaporation of the solution, single blue crystals suitable for X-ray diffraction analysis were obtained and the analysis results in the molecular structure (Fig. 3.7.) in which the metal centre is hexacoordinated by two anionic ligands in the typical “scorpionate” fashion. The X-ray diffraction analysis was performed by Prof. Luciano Marchiò of the Department of Chemistry of the University of Parma.

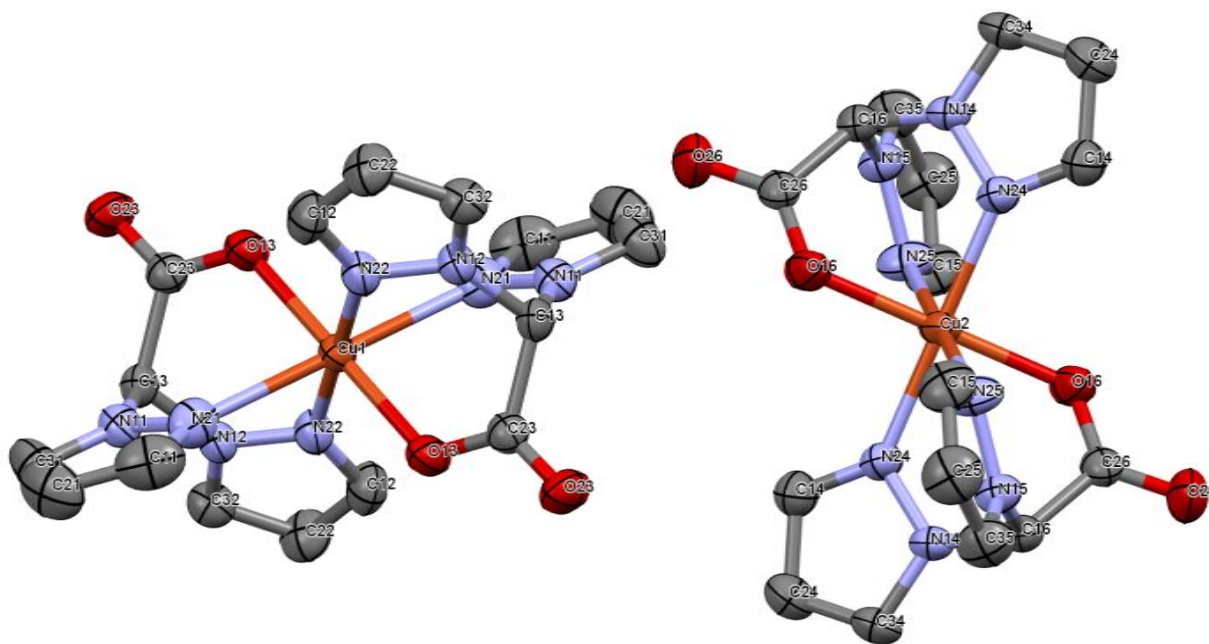


Fig. 3.7. Crystal structure of $[(L)_2Cu]$.

The crystallographic data have been summarized in the following tables (Table 3.1. and Table 3.2.).

Identification code	shelx
Empirical formula	$C_{16}H_{14}CuN_8O_4$
Formula weight	445.89
Temperature	296K
Wavelength	0.71073 Å
Crystal system	Monoclinic
Space group	P 21/n
Unit cell dimensions	$a = 9.5260(10)$ Å; $\alpha = 90^\circ$. $b = 15.731(2)$ Å; $\beta = 104.566(3)^\circ$.

	$c = 12.396(2) \text{ \AA}; \gamma = 90^\circ$.
Volume	1797.9 \AA^3
Z	4
Density (calculated)	1.647 Mg/m^3
Absorption coefficient	1.259 mm^{-1}
F(000)	908
Crystal size	$0.22 \times 0.20 \times 0.15 \text{ mm}^3$
Theta range for data collection	$2.135 \text{ to } 27.218^\circ$.
Index ranges	$-12 \leq h \leq 12, -20 \leq k \leq 20, -15 \leq l \leq 15$
Reflections collected	22775
Independent reflections	4012 [R(int) = 0.0568]
Completeness to theta = 25.242°	100.0 %
Absorption correction	Semi-empirical from equivalents
Max. and min. transmission	0.746 and 0.639
Refinement method	Full-matrix least-squares on F^2
Data / restraints / parameters	4012 / 0 / 265
Goodness-of-fit on F^2	1.007
Final R indices [$I > 2\sigma(I)$]	R1 = 0.0378, wR2 = 0.0927
R indices (all data)	R1 = 0.0696, wR2 = 0.1113
Extinction coefficient	n/a
Largest diff. peak and hole	0.262 and $-0.539 \text{ e.\AA}^{-3}$

Table 3.1. Crystal data and structure refinement for $[(L)_2Cu]$.

atom	x	y	z	U(eq)
Cu(1)	5000	0	5000	30(1)
Cu(2)	0	0	10000	37(1)
N(14)	-495(2)	1814(1)	9829(2)	31(1)
N(11)	4075(2)	669(1)	7055(2)	35(1)
O(16)	-114(2)	395(1)	8482(2)	47(1)
O(23)	2826(2)	-1325(1)	6867(2)	52(1)
N(12)	2209(2)	504(1)	5372(2)	31(1)
N(24)	-813(2)	1096(1)	10315(2)	36(1)
C(23)	3349(3)	-787(2)	6381(2)	34(1)
N(25)	2358(3)	865(2)	10353(2)	47(1)

C(34)	-1084(3)	2494(2)	10205(2)	39(1)
C(32)	917(3)	888(2)	5002(2)	37(1)
N(15)	2015(2)	1656(1)	9924(2)	36(1)
N(22)	2919(2)	441(1)	4555(2)	37(1)
N(21)	5257(3)	746(2)	6635(2)	45(1)
C(13)	2857(3)	151(2)	6470(2)	33(1)
C(24)	-1850(3)	2204(2)	10922(3)	45(1)
C(16)	596(3)	1804(2)	9190(2)	32(1)
C(14)	-1645(3)	1334(2)	10969(2)	42(1)
C(12)	2038(3)	781(2)	3662(2)	46(1)
C(26)	288(3)	1127(2)	8254(2)	36(1)
C(35)	3058(3)	2225(2)	10373(3)	51(1)
O(26)	481(3)	1345(1)	7361(2)	62(1)
C(25)	4123(4)	1794(2)	11112(3)	57(1)
C(15)	3639(3)	966(2)	11061(3)	55(1)
C(22)	770(3)	1075(2)	3902(2)	48(1)
C(31)	4255(4)	1098(2)	8018(3)	53(1)
C(11)	6163(4)	1233(2)	7374(3)	60(1)
C(21)	5589(4)	1463(2)	8247(3)	67(1)
O(13)	4270(2)	-922(1)	5813(2)	44(1)

Table 3.2. Atomic coordinates ($\times 10^4$) and equivalent isotropic displacement parameters ($\text{\AA}^2 \times 10^3$) for $[(L)_2Cu]$. $U(eq)$ is defined as one third of the trace of the orthogonalized U^{ij} tensor.

The copper(I) complexes $[(LH)Cu(PPh_3)_2]PF_6$ (**10**) and $[(L^2H)Cu(PPh_3)_2]PF_6$ (**11**) have been prepared from the reaction of triphenylphosphine and $Cu(MeCN)_4PF_6$, in the presence of the ligands **1** and **2**, respectively (Fig. 3.8.). The mixture was filtered and dried at reduced pressure, and the residues washed by diethyl ether to obtain the complexes as white solids. The compounds are soluble in methanol, chloroform and DMSO, and complex **11** is also soluble in acetone. The acetonitrile solution stabilizes the copper in the oxidation state +1 and with this solvent the esterification was not observed. The infrared spectra carried out on the solid samples of **10** and **11** showed all the expected bands for the heteroscorpionate ligands and triphenylphosphine coligands: the strong absorptions due to the C=O stretchings are detectable at 1752 and 1751 cm^{-1} , respectively, with no significant variations with respect to the same absorptions detectable in the spectra of the free ligands; the weak absorptions in the range $2932\text{--}3144\text{ cm}^{-1}$ are due to the CH stretchings.

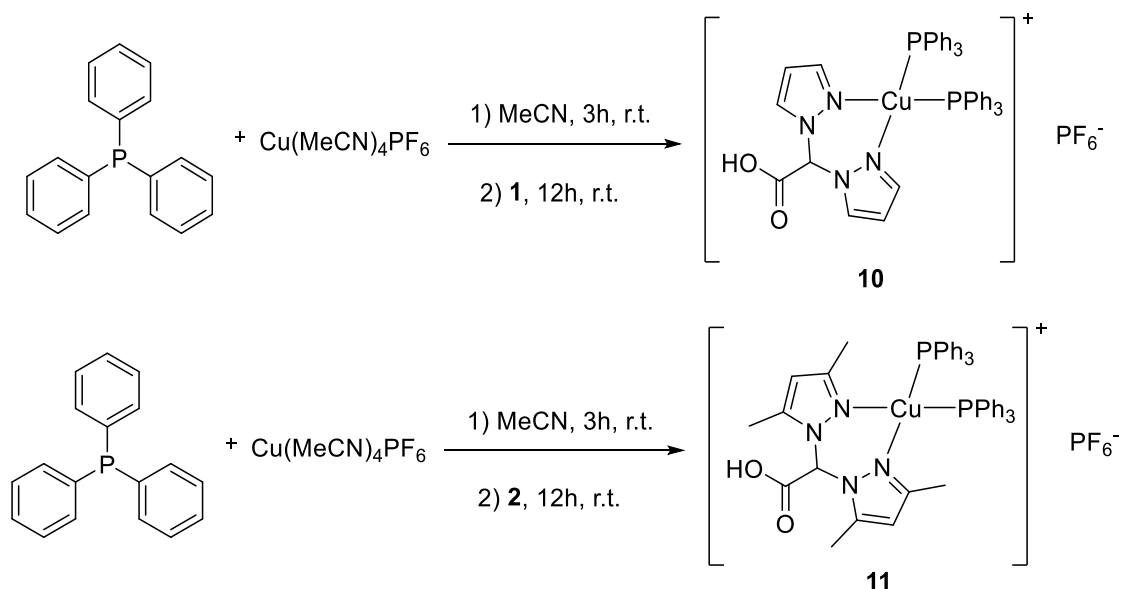


Fig. 3.8. Reaction scheme of the syntheses of complexes **10** and **11**.

The ^1H NMR spectra of **10** and **11**, recorded in DMSO and CDCl_3 solution, respectively, showed a single set of resonances for the pz rings, indicating that the pyrazoles are equivalent. The triphenylphosphine coligands showed a characteristic series of resonances in the aromatic region at δ 7.21-7.61 ppm, with an integration of the peaks, with respect to the ligand resonances, that confirms the 1:2 stoichiometric ratio between the ligand and the PPh_3 .

The r.t. $^{31}\text{P}\{^1\text{H}\}$ NMR spectrum of $[(\text{LH})\text{Cu}(\text{PPh}_3)_2]\text{PF}_6$ (**10**) in DMSO solution, gave a singlet centred at δ -3.10 ppm, along with the characteristic septet centred at about δ -143.10 ppm due to the PF_6^- counteranion. The $^{31}\text{P}\{^1\text{H}\}$ NMR spectrum of $[(\text{L}^2\text{H})\text{Cu}(\text{PPh}_3)_2]\text{PF}_6$ (**11**), recorded at room temperature in CDCl_3 solution, gave a singlet centred at δ -2.85 ppm, along with a minor peak at δ 8.03 ppm; the characteristic septet due to the PF_6^- counteranion is detectable at δ -143.31 ppm. On lowering the temperature to 243K, the $^{31}\text{P}\{^1\text{H}\}$ NMR spectrum of **11** showed two singlets centred at δ -4.60 and 6.63 ppm.

The ESIMS study was conducted by dissolving compounds **10** and **11** in methanol and recording the spectra in positive- and negative-ion mode. The formation of the complexes **10** and **11** is confirmed by the presence in the positive-ions spectra of the peaks at m/z 517 and 573, respectively attributable to the $[(\text{LH})\text{CuPPh}_3]^+$ and $[(\text{L}^2\text{H})\text{CuPPh}_3]^+$ species. In the positive-ion spectrum of **10** it's also possible to individuate the major peak at m/z 587 attributable to the $[\text{Cu}(\text{PPh}_3)_2]^+$ species. In the negative ion spectra the $[\text{PF}_6]^-$ ion is observed as the major peak for both the complexes at m/z 145. The elemental analyses confirm the stoichiometry of the products in the solid state.

The water soluble phosphine PTA was used in the reaction with $\text{Cu}(\text{MeCN})_4\text{PF}_6$ and the ligands **1** and **2** to synthesize the Cu(I) complexes $[(\text{LH})\text{Cu}(\text{PTA})_2]\text{PF}_6$ (**12**) and $[(\text{L}^2\text{H})\text{Cu}(\text{PTA})_2]\text{PF}_6$ (**13**) (Fig. 3.9.). The white compounds as expected are water soluble, and also soluble in MeCN and DMSO.

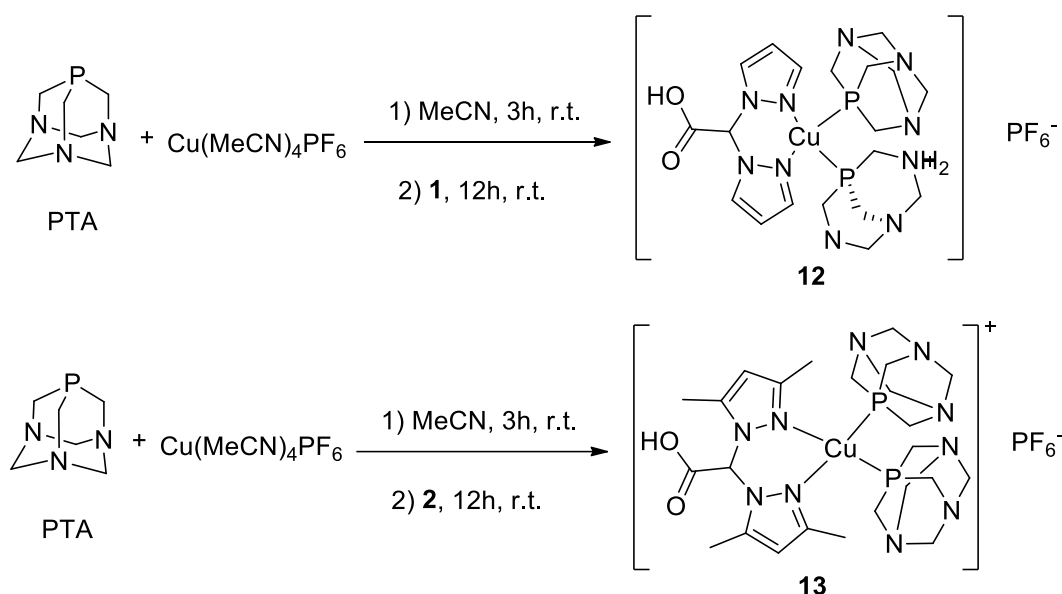


Fig. 3.9. Reaction scheme of the syntheses of **12** and **13**.

The infrared spectra carried out on the solid samples of **12** and **13** showed all the expected bands for the heteroscorpionate ligands and the PTA coligands: the absorptions due to the C=O stretchings are detectable at 1646 and 1639 cm^{-1} , respectively, slightly shifted at lower frequency, due to a possible interaction between the carbonyl of the ligands and the nitrogen atoms of the PTA; the weak absorptions in the range 2923-3130 cm^{-1} are due to the CH stretchings.

The ^1H NMR spectra of **12** and **13**, recorded in DMSO solution, showed a single set of resonances for the pz rings, indicating that the pyrazoles are equivalent. The PTA coligands showed a characteristic series of resonances in the region at δ 4.10-4.67 ppm, with an integration of the peaks, with respect to the ligand resonances, that confirms the 1:2 stoichiometric ratio between the ligand and the PTA. The methylene protons of the PTA upper rim fall at δ 4.10 and 4.15 ppm (broad singlets) in the spectra of **12** and **13**, respectively. The magnetically unequivalent methylene protons of the PTA lower rim appear as a doublet of doublets (AB quartet) in the range 4.48-4.67 ppm in **12** complex, and they appear as a multiplet around δ 4.52 ppm for **13**.

The $^{31}\text{P}\{^1\text{H}\}$ NMR spectrum of $[(\text{LH})\text{Cu}(\text{PTA})_2]\text{PF}_6$ (**12**), recorded at room temperature in D_2O solution, gave a broad singlet centred at δ -85.54 ppm, along with the characteristic septet centred at about δ -143.95 ppm due to the PF_6^- counteranion, with the $J(\text{H}-\text{H}) = 12.4$ Hz, in accordance with the literature for analogues phosphine complexes⁴⁸. The signal at δ -85.54 ppm is downfield shifted with respect to the signal exhibited by the uncoordinated PTA ligand (δ -97.70 ppm in D_2O solution) confirming the formation and the stoichiometry of the complex. The r.t. $^{31}\text{P}\{^1\text{H}\}$ NMR spectrum of **12**, recorded in CD_3CN solution, gave a broad singlet centred at δ -87.21 ppm, along with the characteristic septet due to the PF_6^- counteranion at δ -143.47 ppm. On lowering the temperature to 243K, the $^{31}\text{P}\{^1\text{H}\}$ NMR spectrum of **12** showed a similar broad singlet centred at δ -87,21. The $^{31}\text{P}\{^1\text{H}\}$ NMR

spectrum of $[(L^2H)Cu(PTA)_2]PF_6$ (**13**), recorded at room temperature in D_2O solution, gave a singlet centred at δ -85.87 ppm, downfield shifted compared to the signal of the PTA in the D_2O spectrum, along with the characteristic septet centred at about δ -144.03 ppm due to the PF_6 counteranion. The r.t. $^{31}P\{^1H\}$ NMR spectrum of **13**, recorded at room temperature in CD_3CN solution, gave a singlet centred at δ -90.70 ppm, along with the characteristic septet due to the PF_6 counteranion at δ -144.53 ppm. On lowering the temperature to 243K, the $^{31}P\{^1H\}$ NMR spectrum of **13** showed the singlet centred at δ -89,93, without a significant shifting in the frequency, in agreement with the coordination of two phosphines around the metal.

The ESIMS study was conducted by dissolving compounds **12** and **13** in acetonitrile and recording the spectra in positive- and negative-ion mode. The formation of the complexes **12** and **13** is confirmed by the presence in the positive-ions spectra of the peaks at m/z 412 and 468 respectively, as major peaks, attributable to the $[(LH)CuPTA]^+$ and $[(L^2H)CuPTA]^+$ species. In the negative ion spectra the $[PF_6]^-$ ion is observed as the major peak for both the complexes at m/z 145. The elemental analyses confirm the stoichiometry and the purity of the products.

In analogy with the reactions for the formation of the complexes **12** and **13** two syntheses were performed with the functionalized ligands L^{NMDA} (**4**) and L^{2NMDA} (**5**) obtaining the complexes $[(L^{NMDA})Cu(PTA)_2]PF_6$ (**14**) and $[(L^{2NMDA})Cu(PTA)_2]PF_6$ (**15**). The coligand PTA was used in the reaction with $Cu(MeCN)_4PF_6$ and the ligands **4** and **5** (Fig. 3.10.). The white compounds are soluble in MeCN and DMSO.

The infrared spectra carried out on the solid samples of **14** and **15** showed all the expected bands for the bioconjugated ligands and PTA coligands: the absorptions due to the C=O stretchings are detectable at 1696 and 1698 cm^{-1} , respectively, with no significant variations with respect to the same absorptions detectable in the spectra of the free ligands; the broad absorption at about 2925 cm^{-1} are due to the CH stretchings.

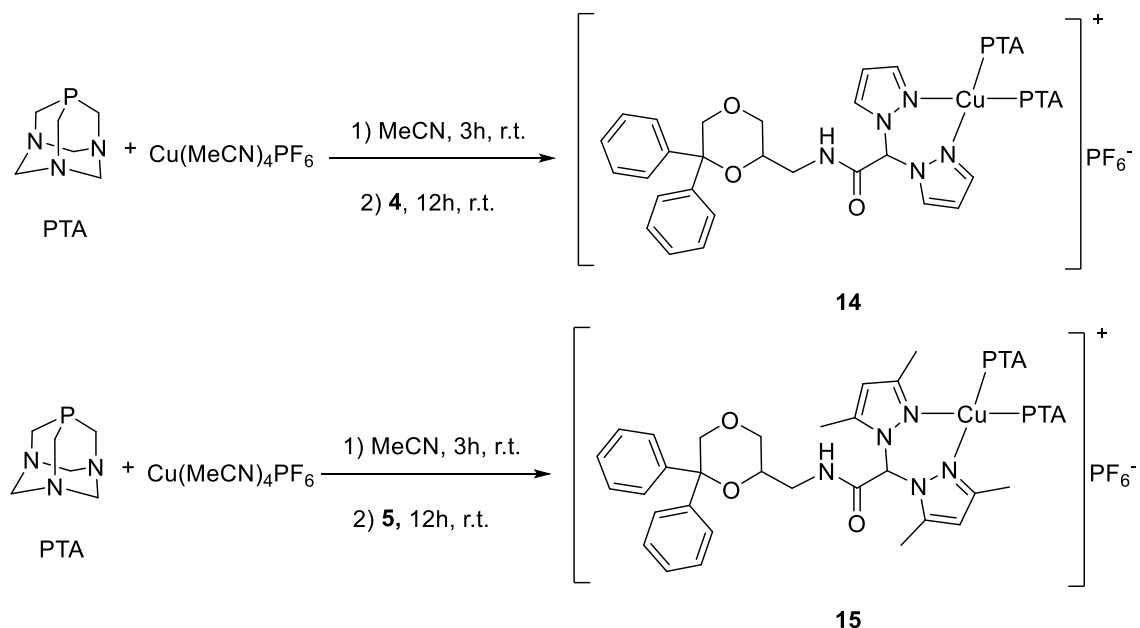


Fig. 3.10. Reaction scheme of the syntheses of **14** and **15**.

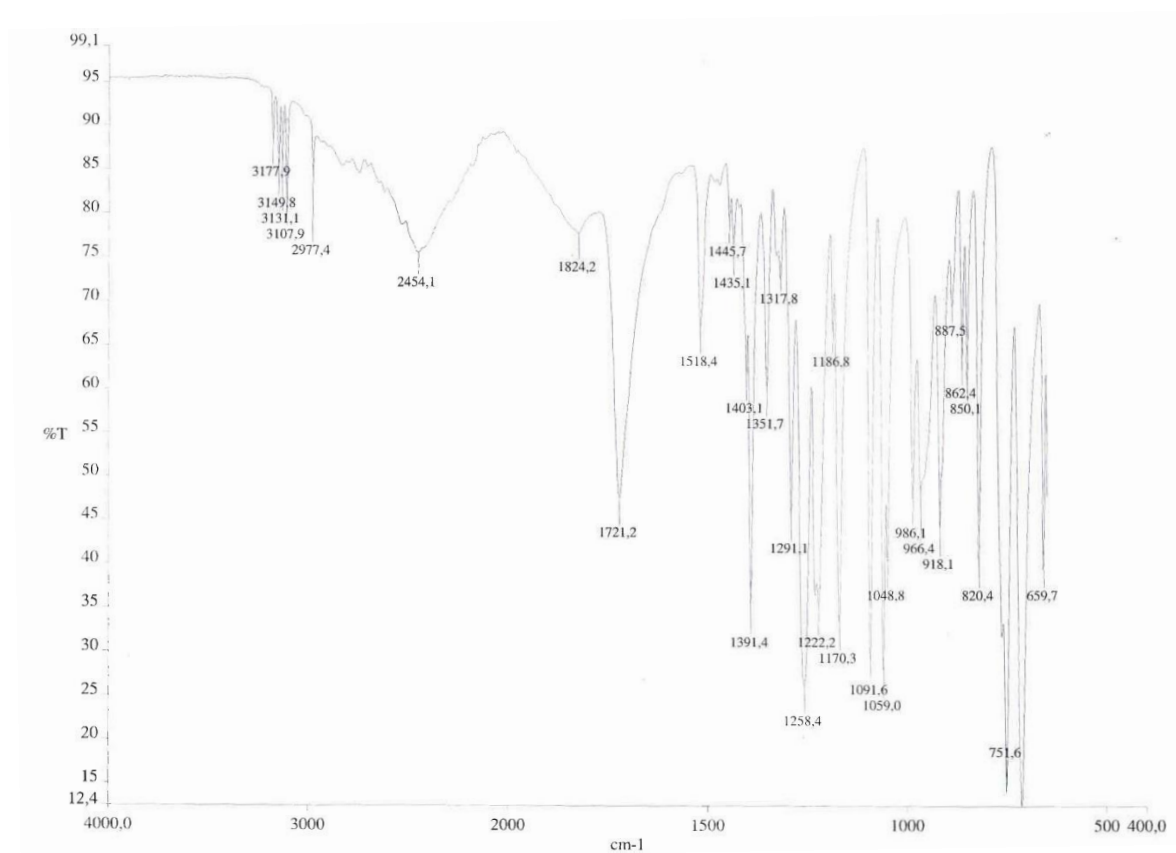
The ^1H NMR spectra of **14** and **15**, recorded in DMSO solution, showed all the signals attributable to the ligands **4** and **5** and the PTA coligands with similar patterns and small shifts observed upon complex formation.

The $^{31}\text{P}\{^1\text{H}\}$ NMR spectra of **14** and **15**, recorded at room temperature in CD_3CN solution, gave broad singlets centred at δ -91.63 and -89.53 ppm, respectively, along with the characteristic septet centred at about δ -143.52 ppm due to the PF_6 counteranion, in agreement with the coordination of two phosphines around the metal

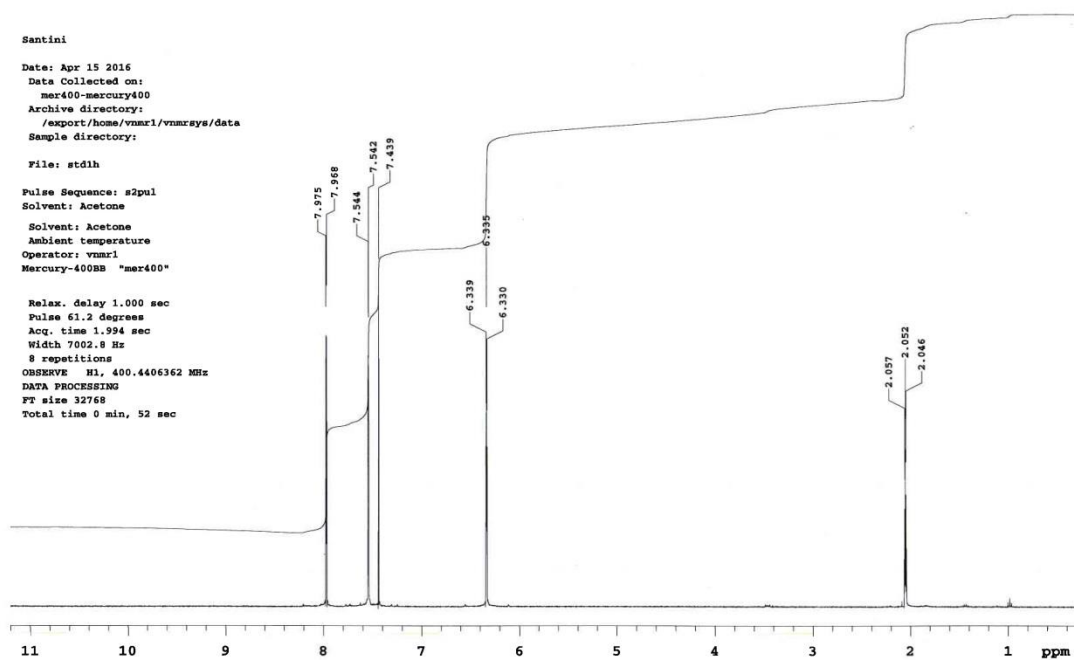
The ESIMS study was conducted by dissolving compounds **14** and **15** in acetonitrile and recording the spectra in positive- and negative-ion mode. The formation of the complexes **14** and **15** is confirmed by the presence in the positive-ion spectra of the peaks at m/z 663 and 719, attributable to the $[(\text{L}^{\text{NMDA}})\text{CuPTA}]^+$ and $[(\text{L}^{2\text{NMDA}})\text{CuPTA}]^+$ species, respectively. In the negative ion spectra the $[\text{PF}_6]^-$ ion is observed as the major peak for both the complexes at m/z 145. The elemental analyses confirm the stoichiometry and the purity of the products.

IV Appendix

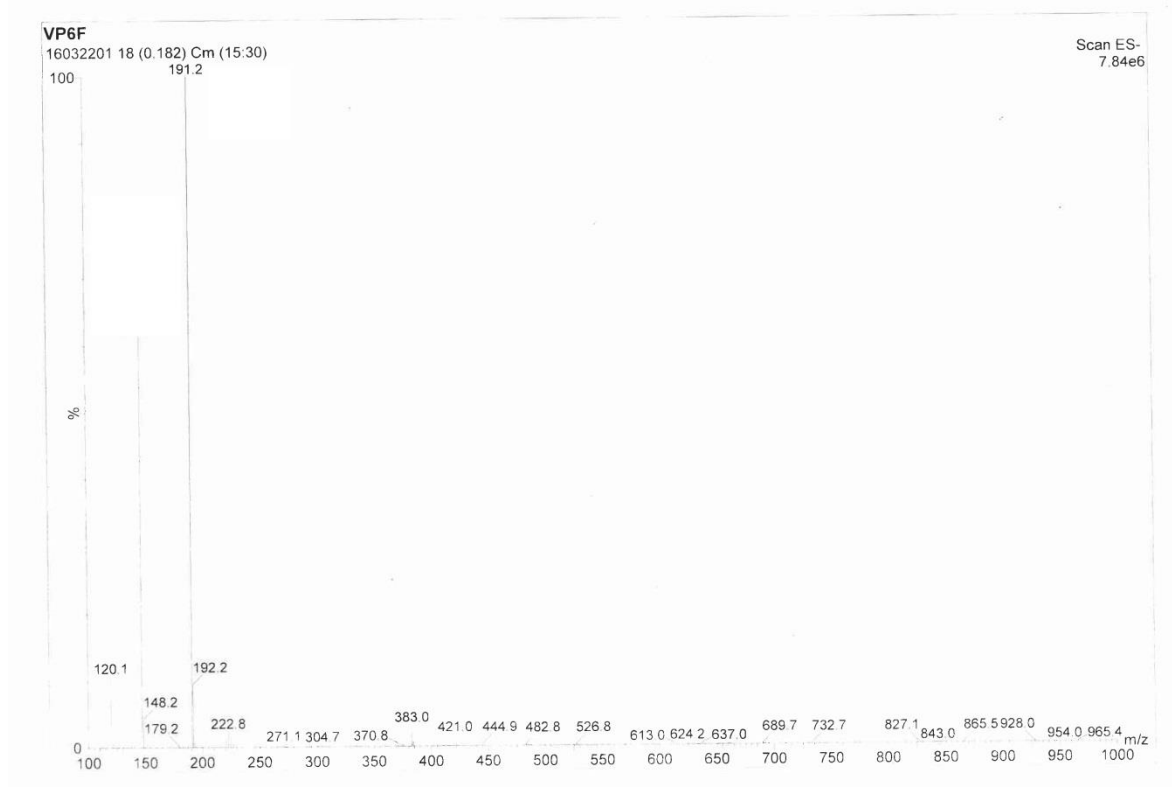
IR spectrum of LH (1)



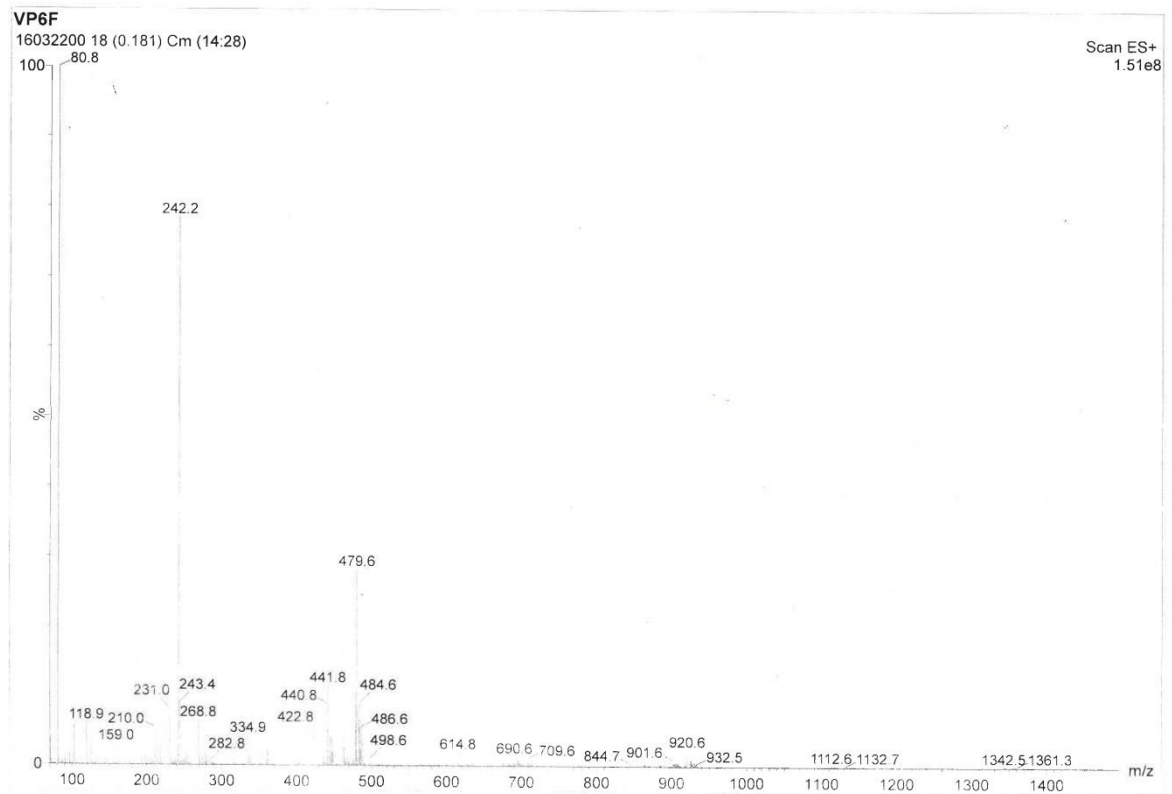
¹H NMR spectrum of LH (1) in acetone.



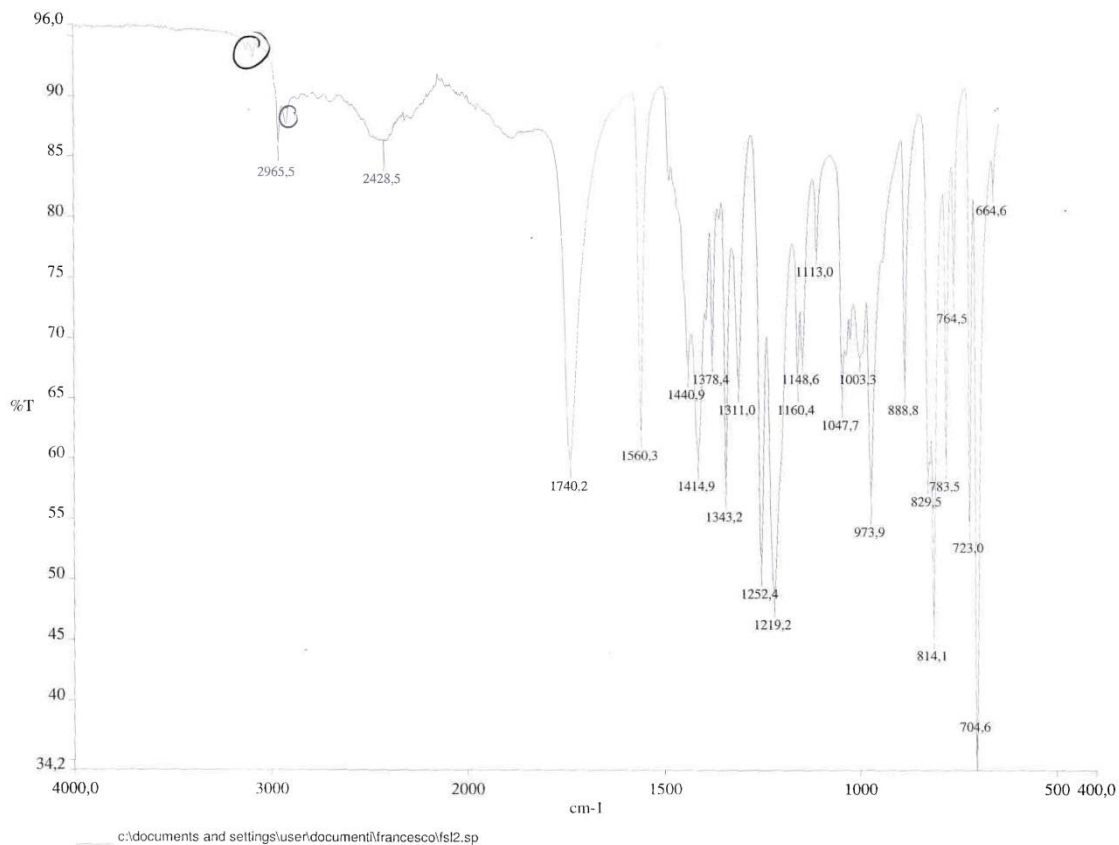
ESIMS (major negative-ions, CH₃OH) spectrum of LH (1).



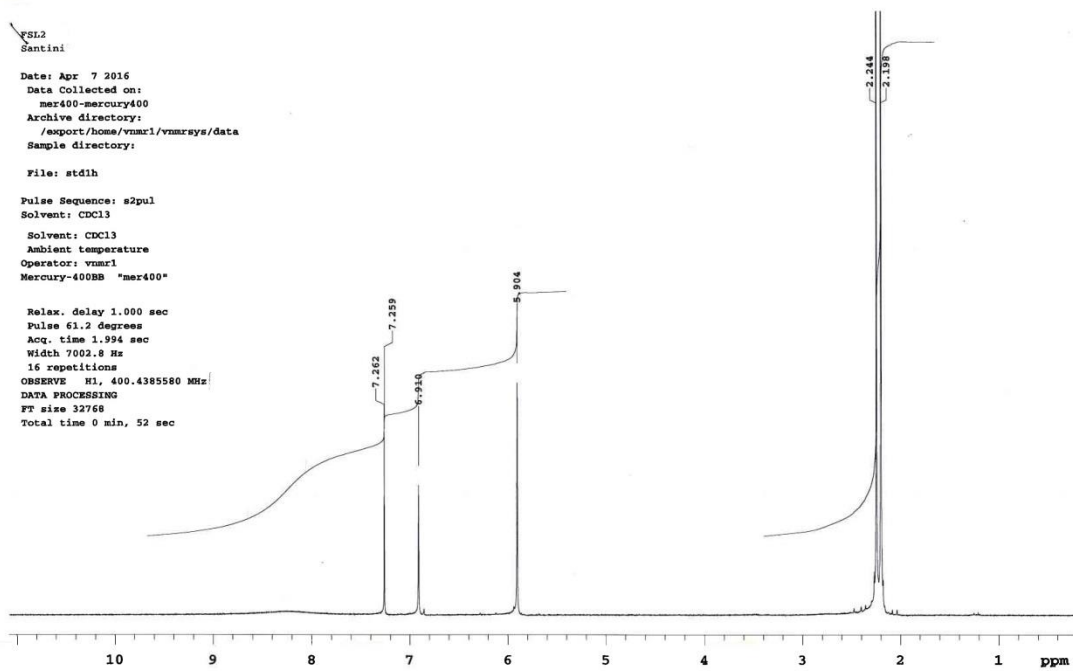
ESIMS (major positive-ions, CH₃OH) spectrum of LH (1).



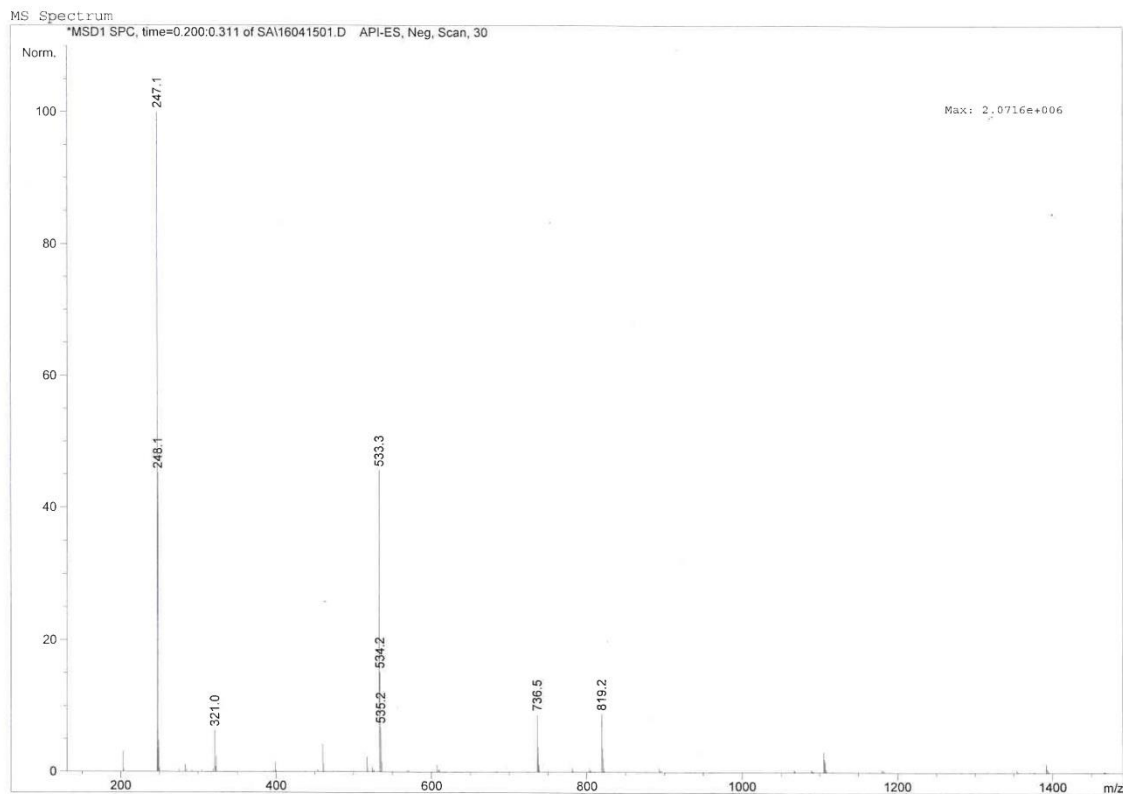
IR spectrum of L²H (2).



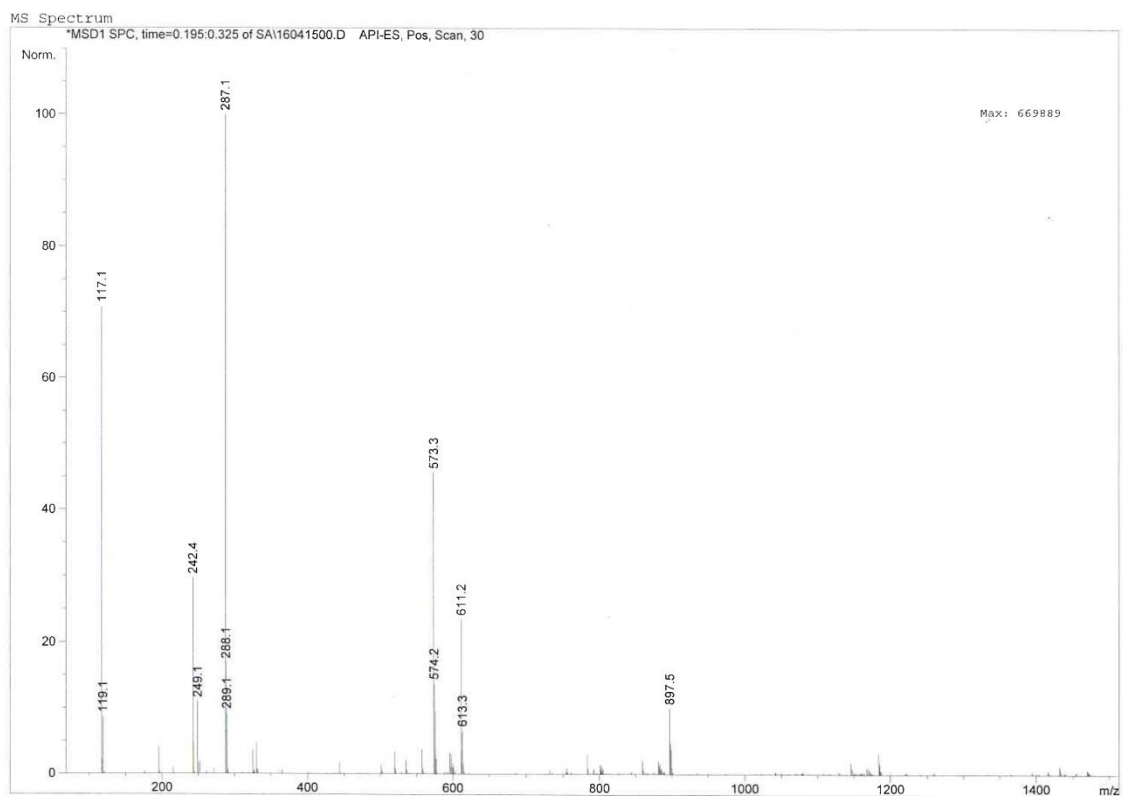
¹H NMR spectrum of L²H (2) in CDCl₃.



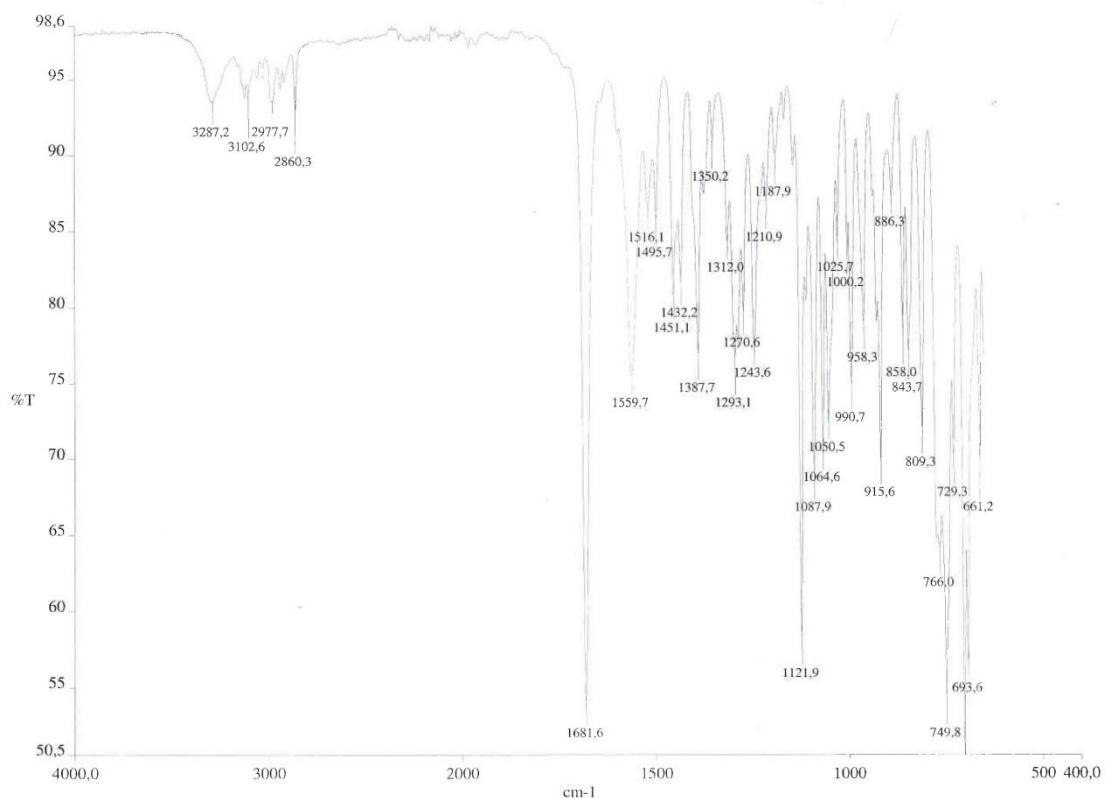
ESIMS (major negative-ions, CH₃OH) spectrum of L²H (2).



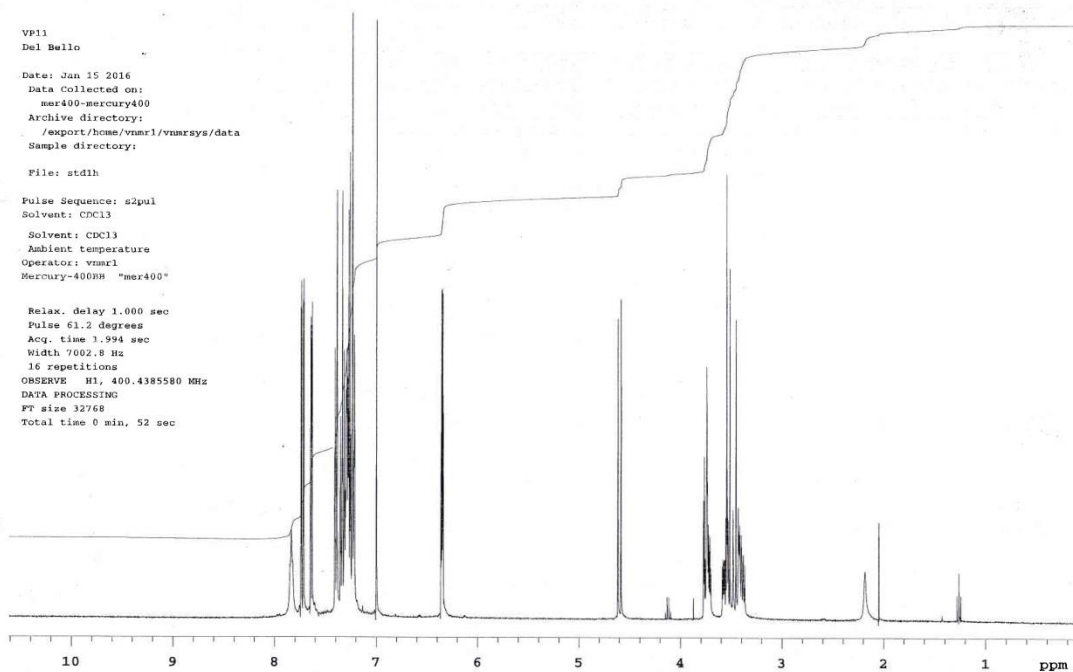
ESIMS (major positive-ions, CH₃OH) spectrum of L²H (2).



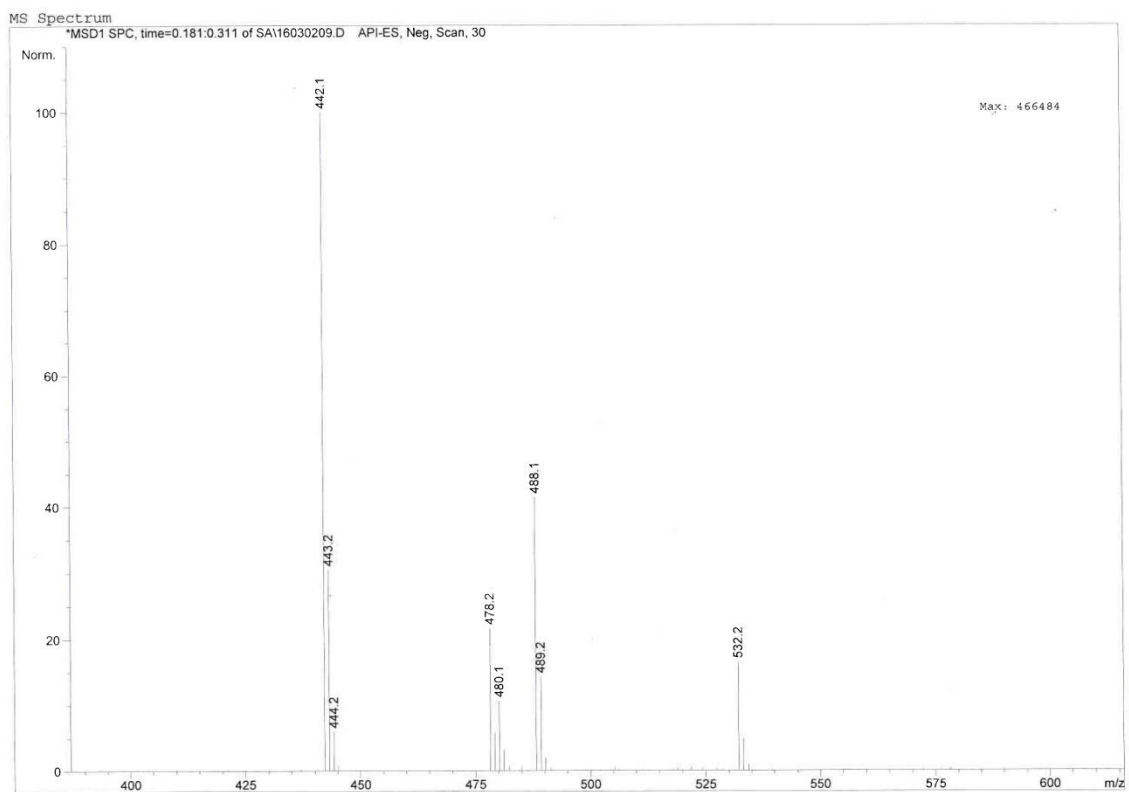
IR spectrum of L^{NMDA} (4)



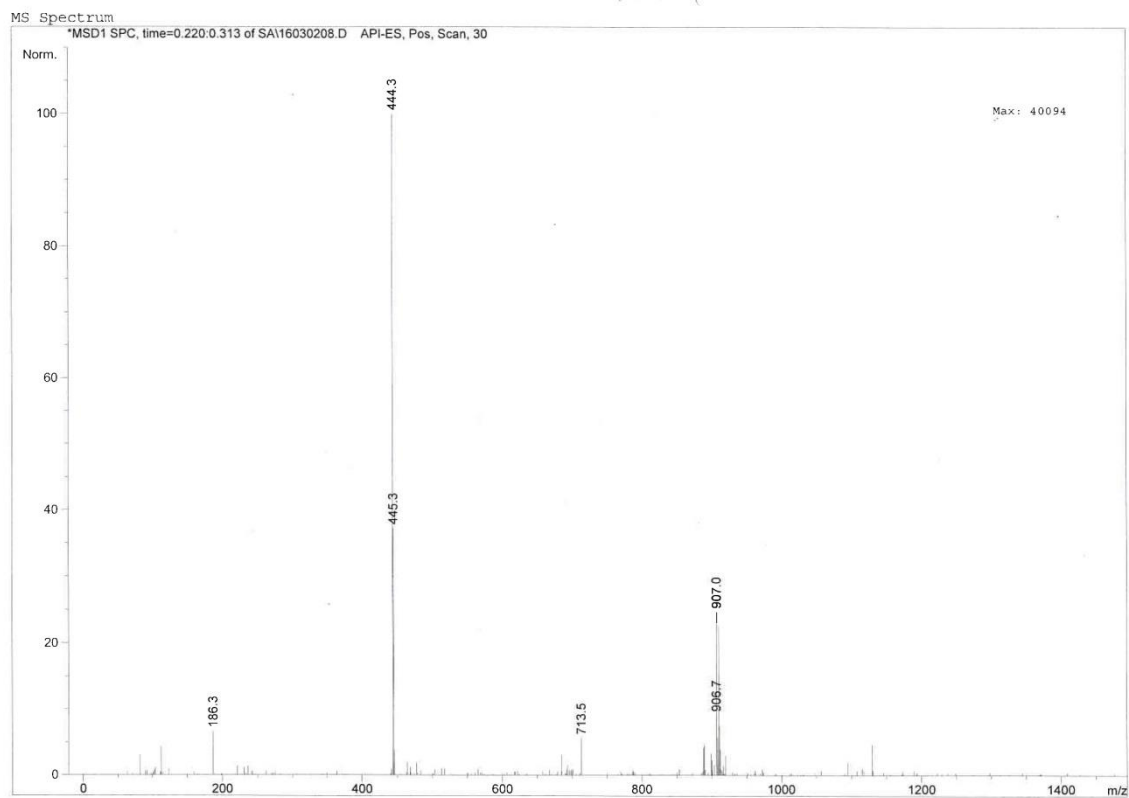
¹H NMR spectrum of L^{NMDA} (4) in CDCl₃



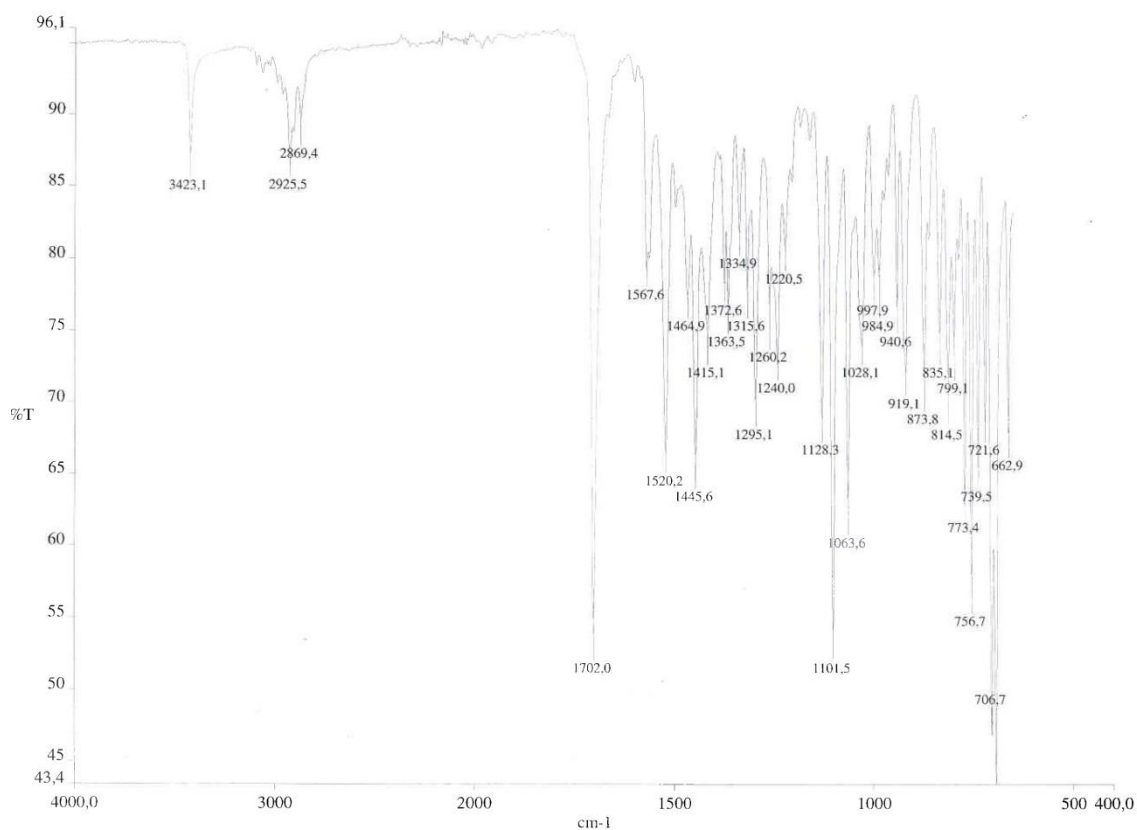
ESIMS (major negative-ions, CH₃CN) spectrum of L^{NMDA} (4).



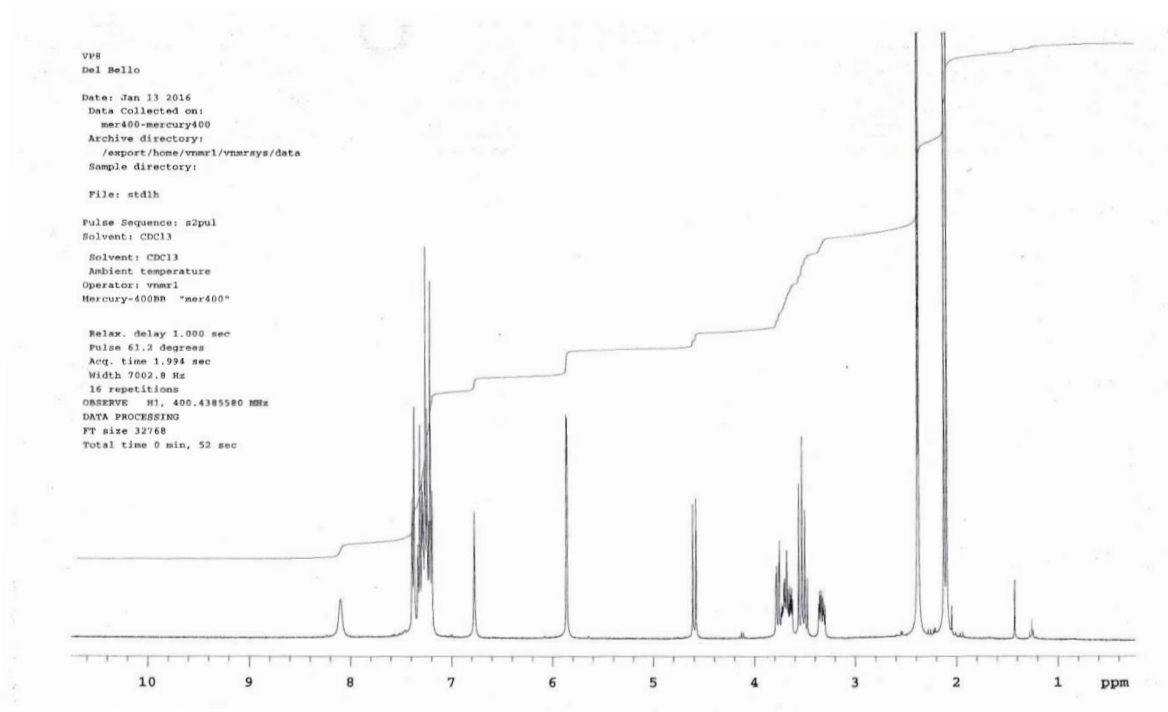
ESIMS (major positive-ions, CH₃CN) spectrum of L^{NMDA} (4)



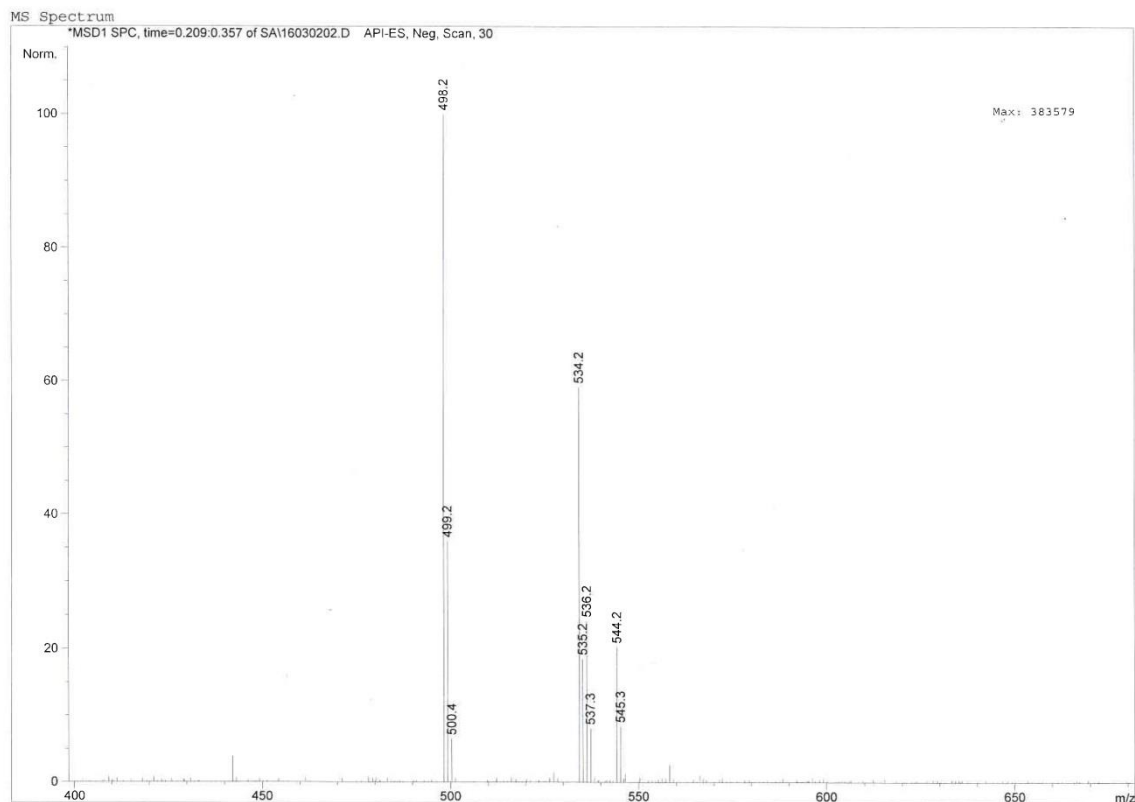
IR spectrum of L^{2NMDA} (5)



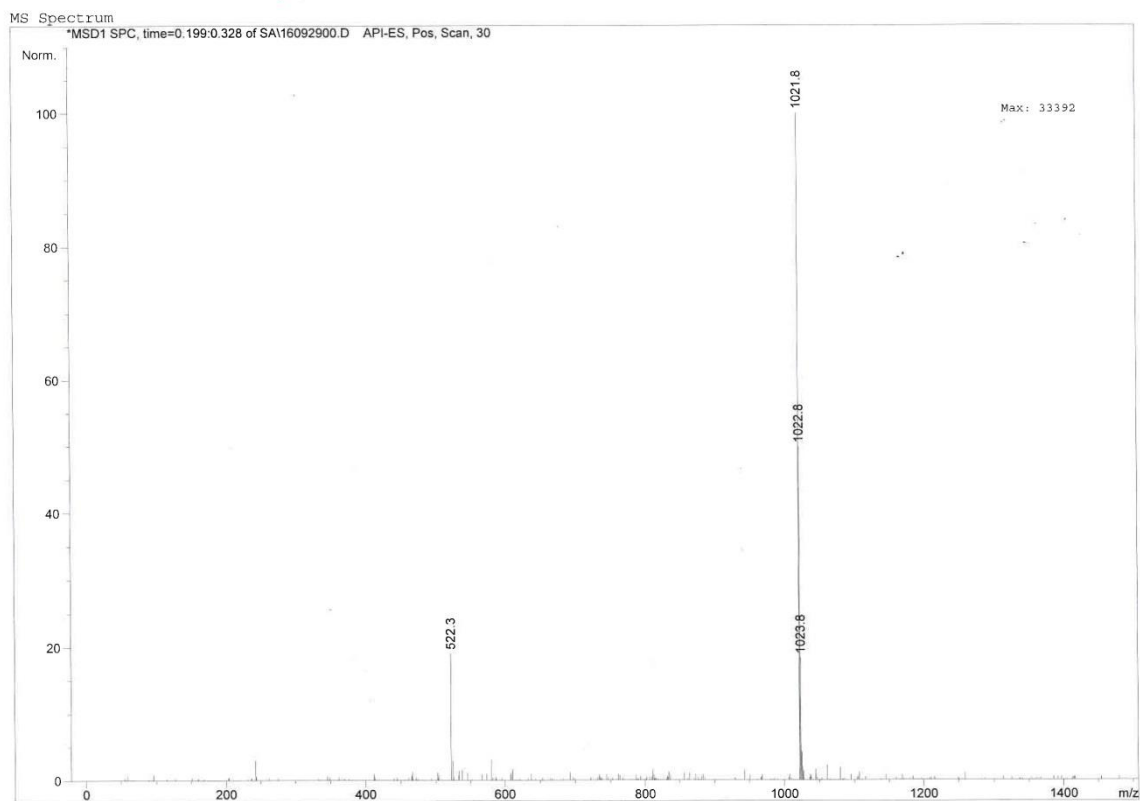
¹H NMR spectrum of L^{2NMDA} (5) in CDCl₃.



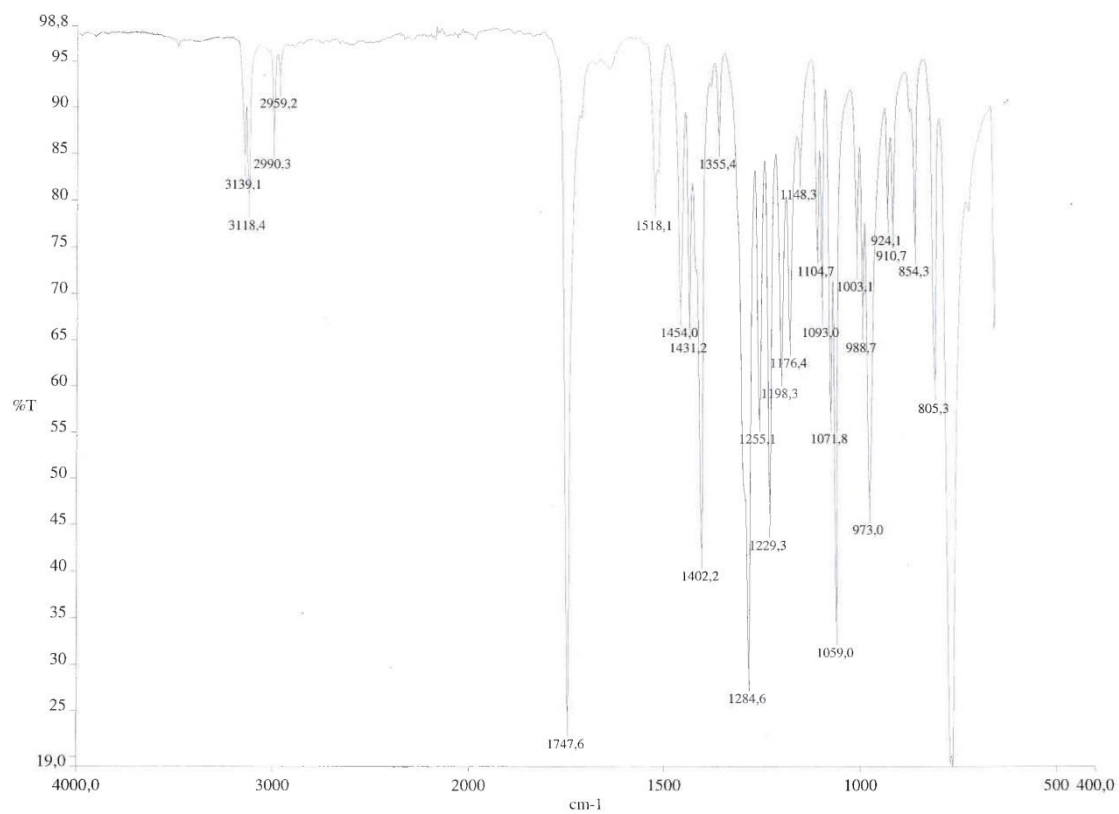
ESIMS (major negative-ions, CH₃OH) spectrum of L^{2NMDA} (5).



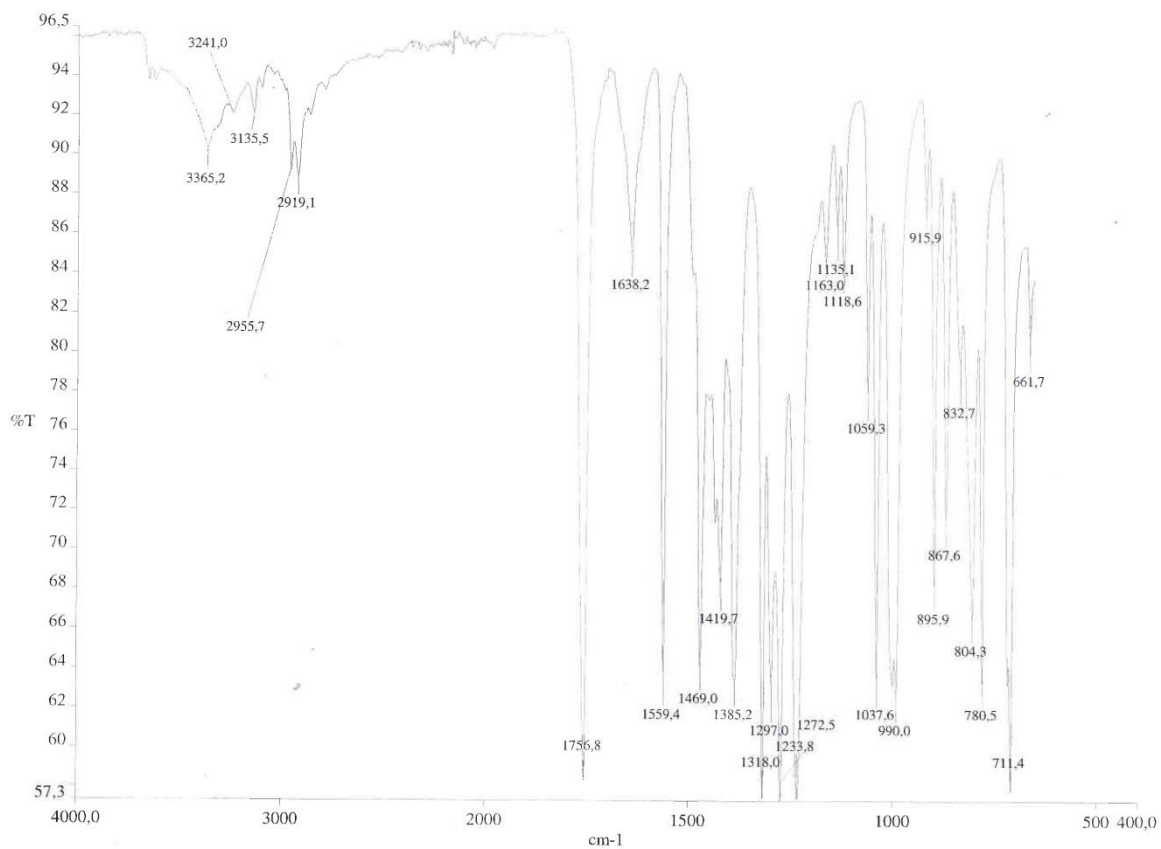
ESIMS (major positive-ions, CH₃OH) spectrum of L^{2NMDA} (5).



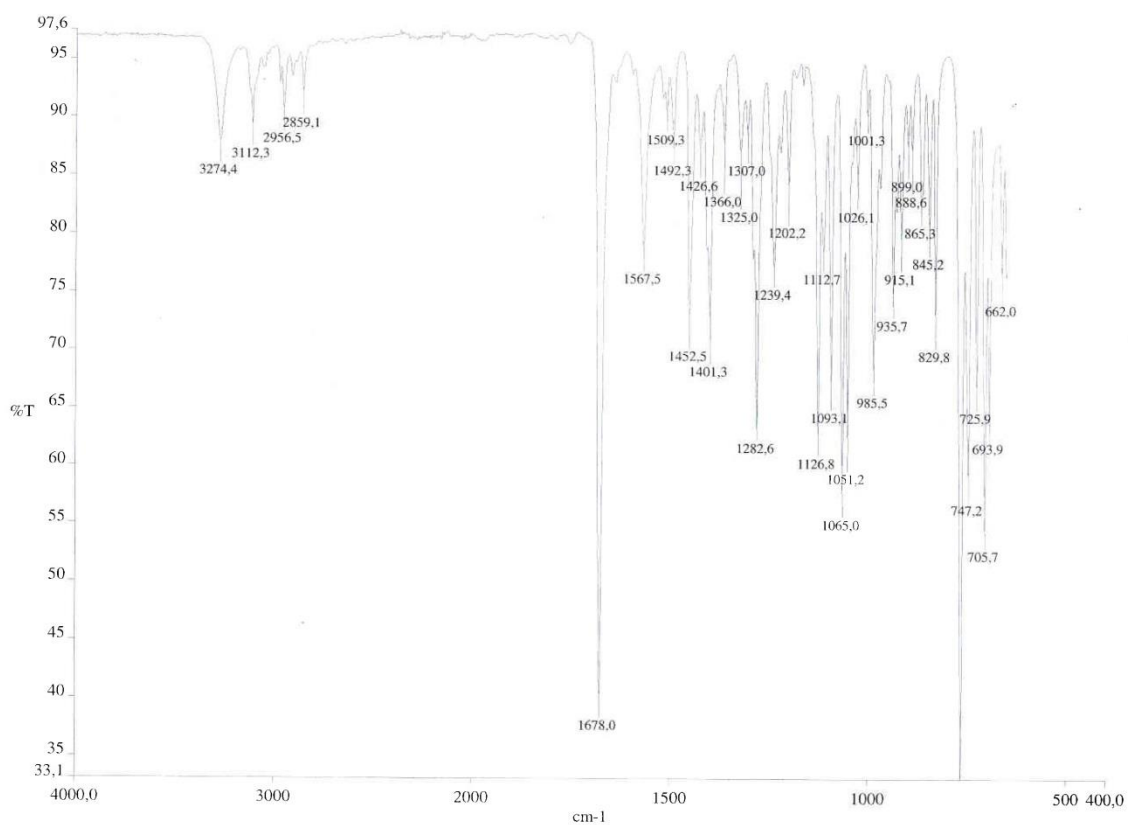
IR spectrum of $[(L^{OMe})CuCl_2]$ (6).



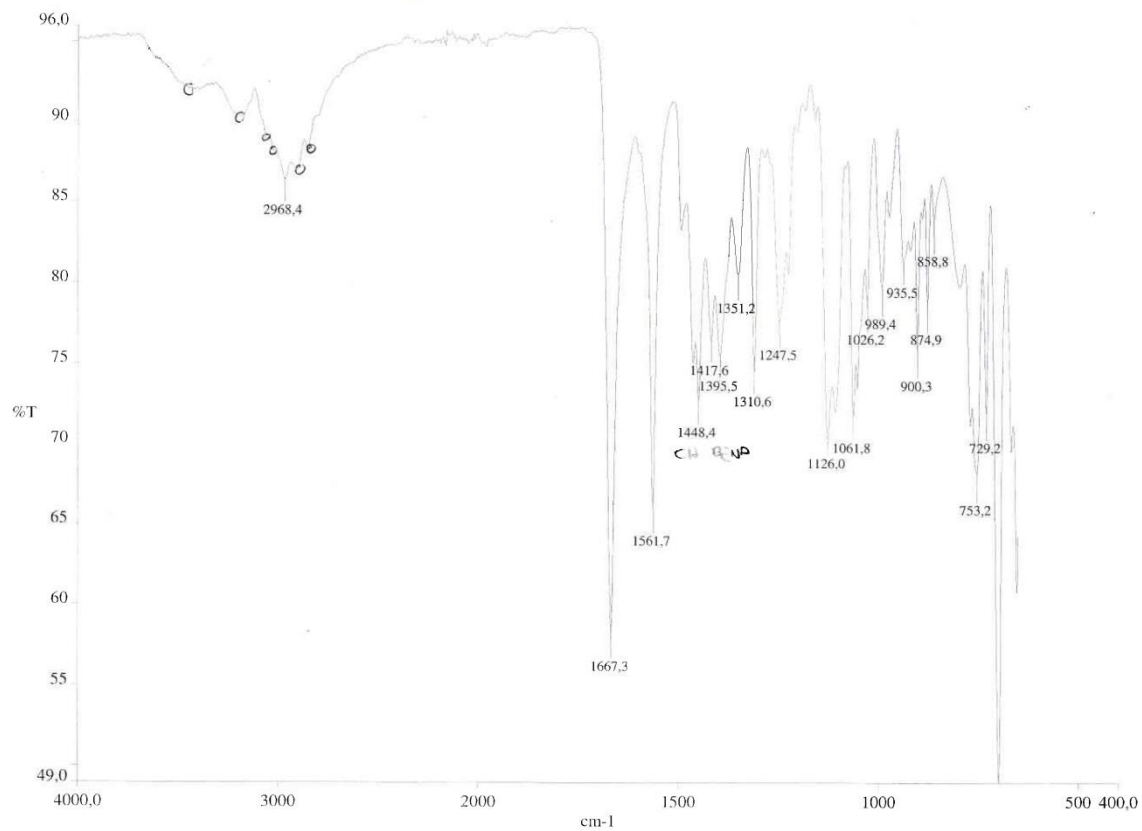
IR spectrum of $[(L^{2OMe})CuCl_2]$ (7).



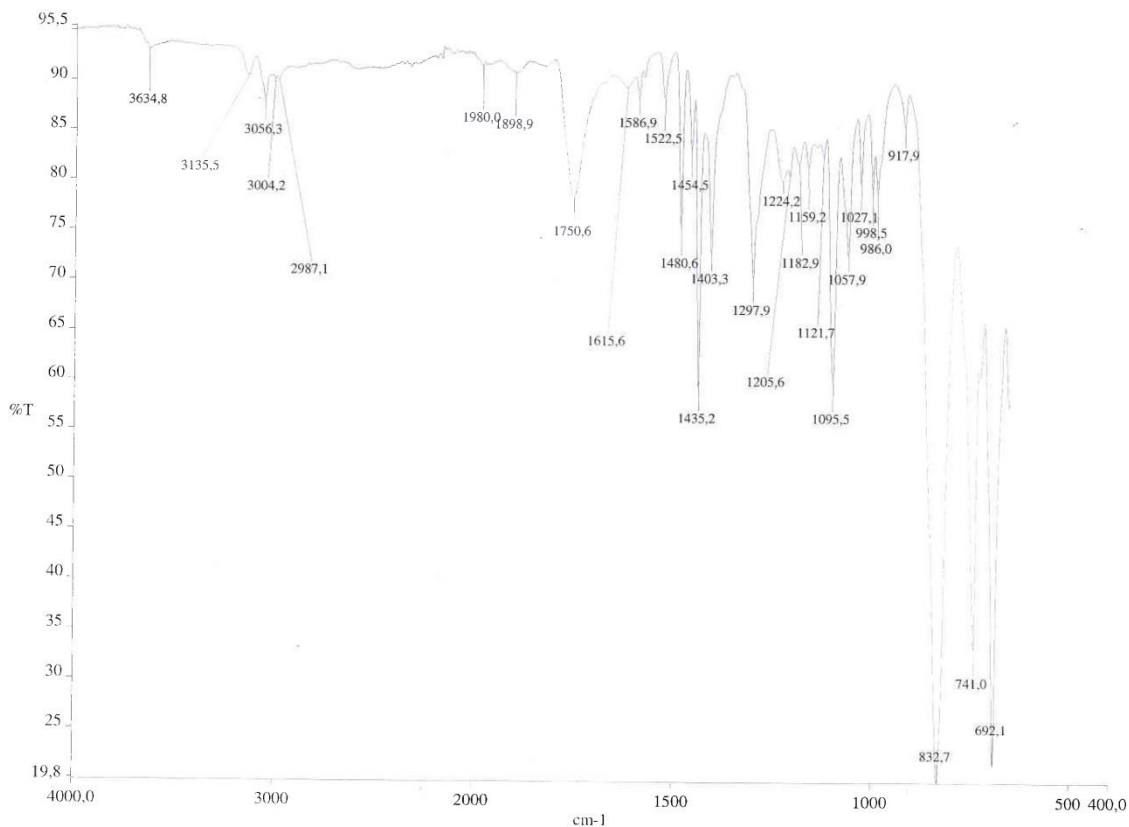
IR spectrum of $[(L^{NMDA}CuCl_2)]$ (**8**).



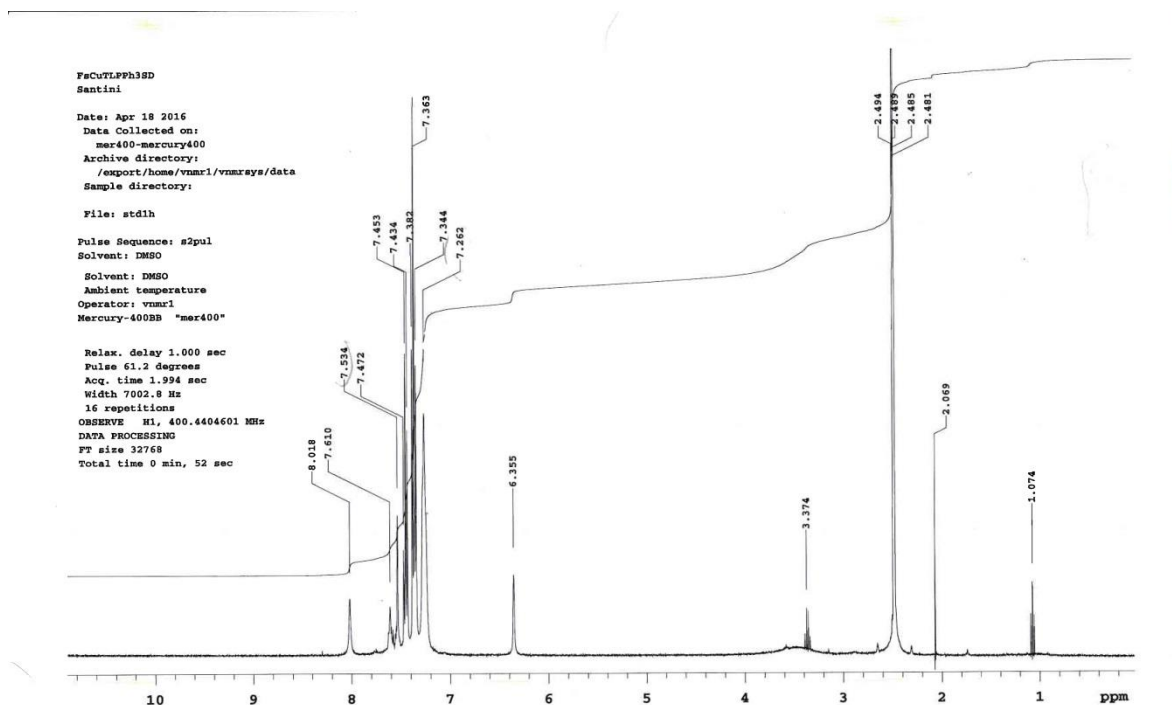
IR spectrum of $[(L^{2NMDA}CuCl_2) \cdot H_2O]$ (**9**).



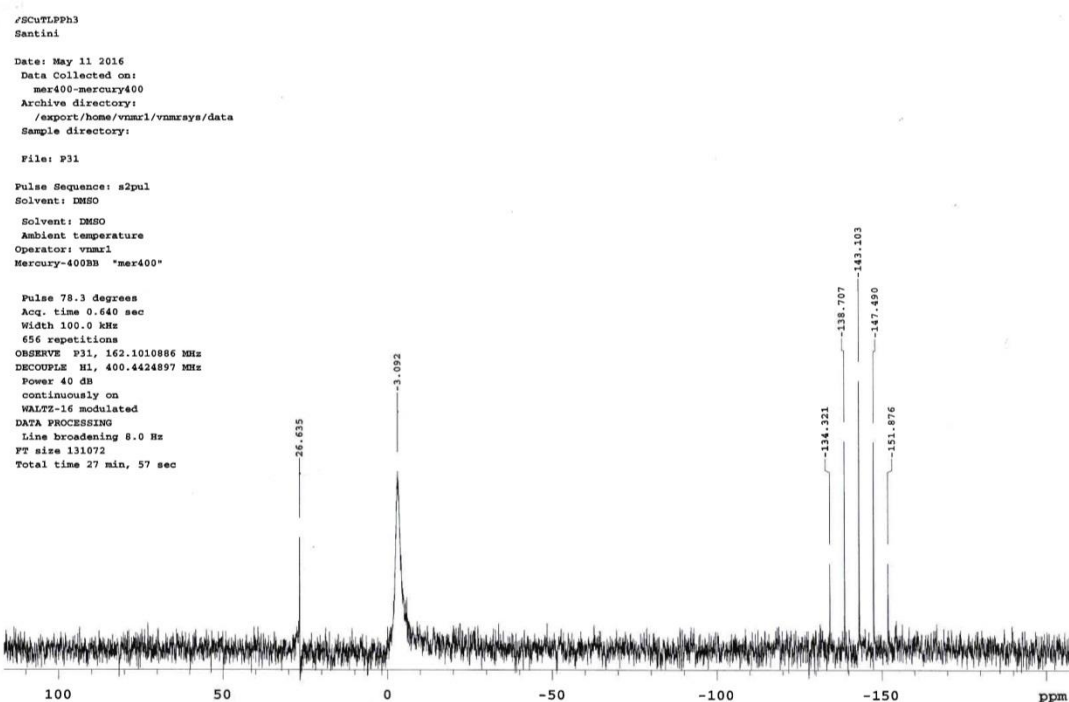
IR spectrum of $[(\text{LH})\text{Cu}(\text{PPh}_3)_2]\text{PF}_6$ (**10**).



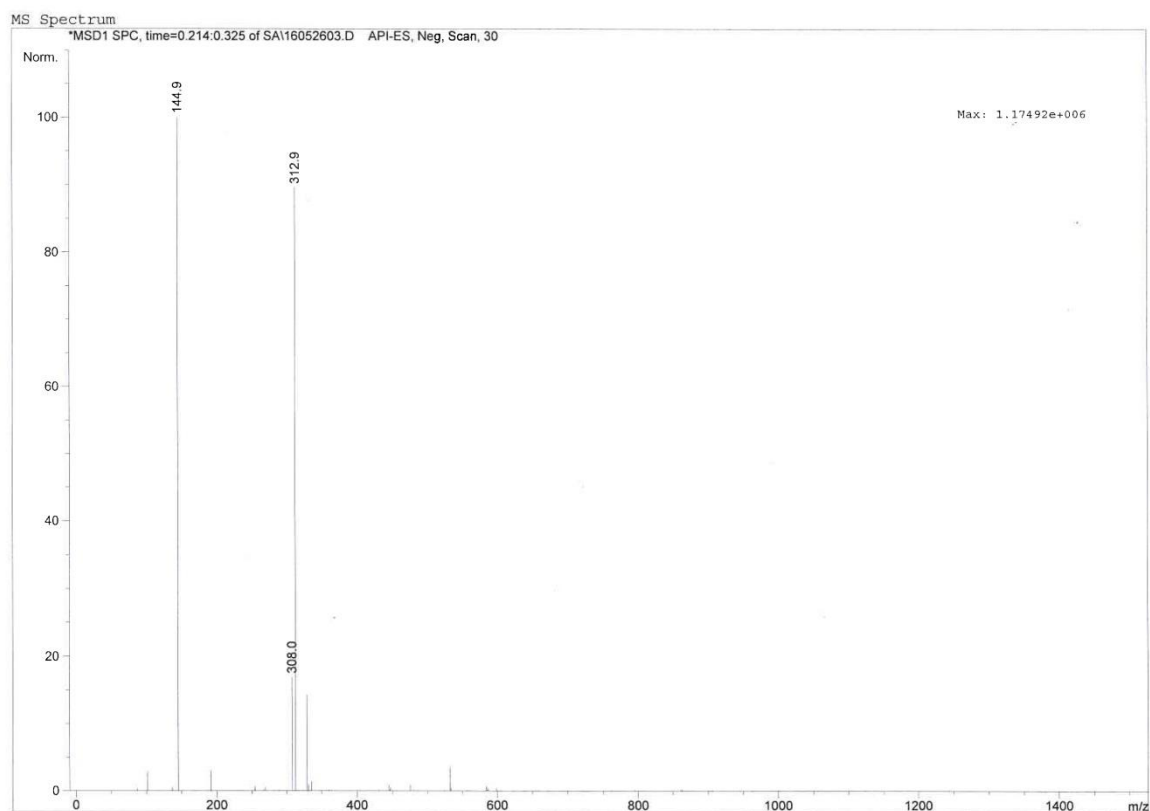
^1H NMR spectrum of $[(\text{LH})\text{Cu}(\text{PPh}_3)_2]\text{PF}_6$ (**10**) in DMSO.



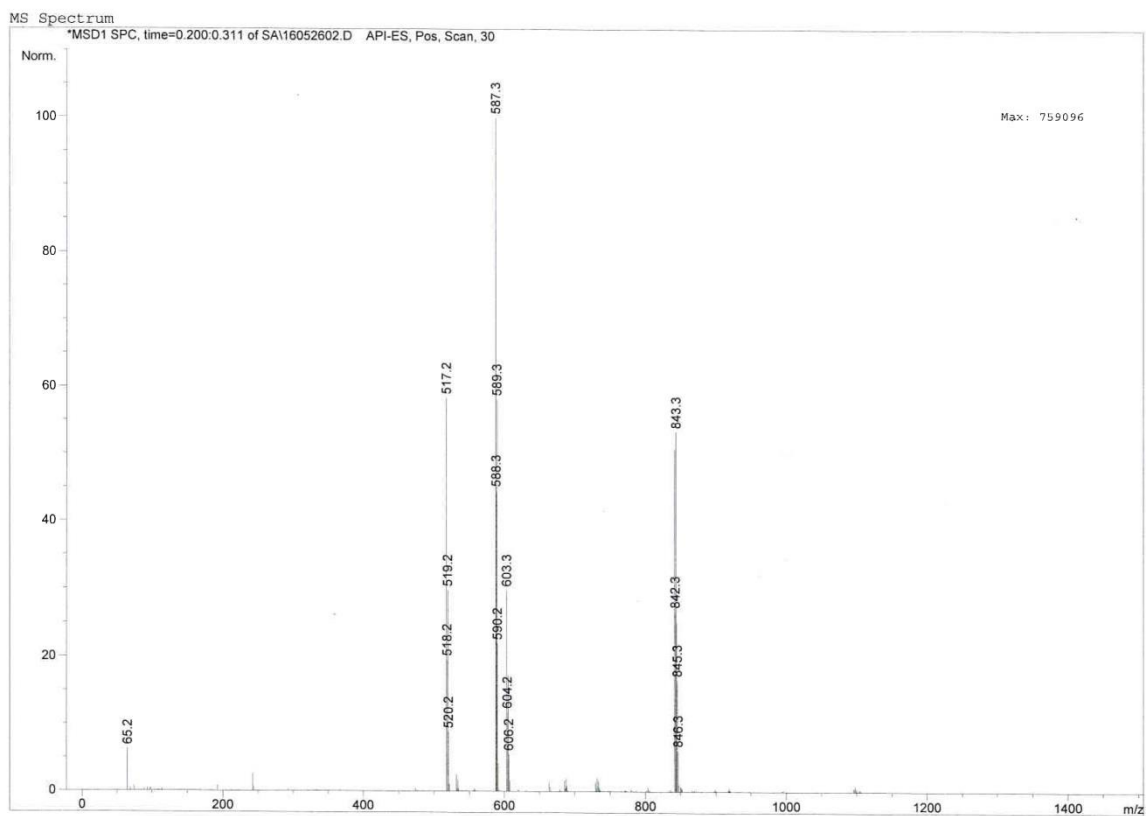
^{31}P NMR spectrum of $[(\text{LH})\text{Cu}(\text{PPh}_3)_2]\text{PF}_6$ (**10**) in DMSO at 293K.



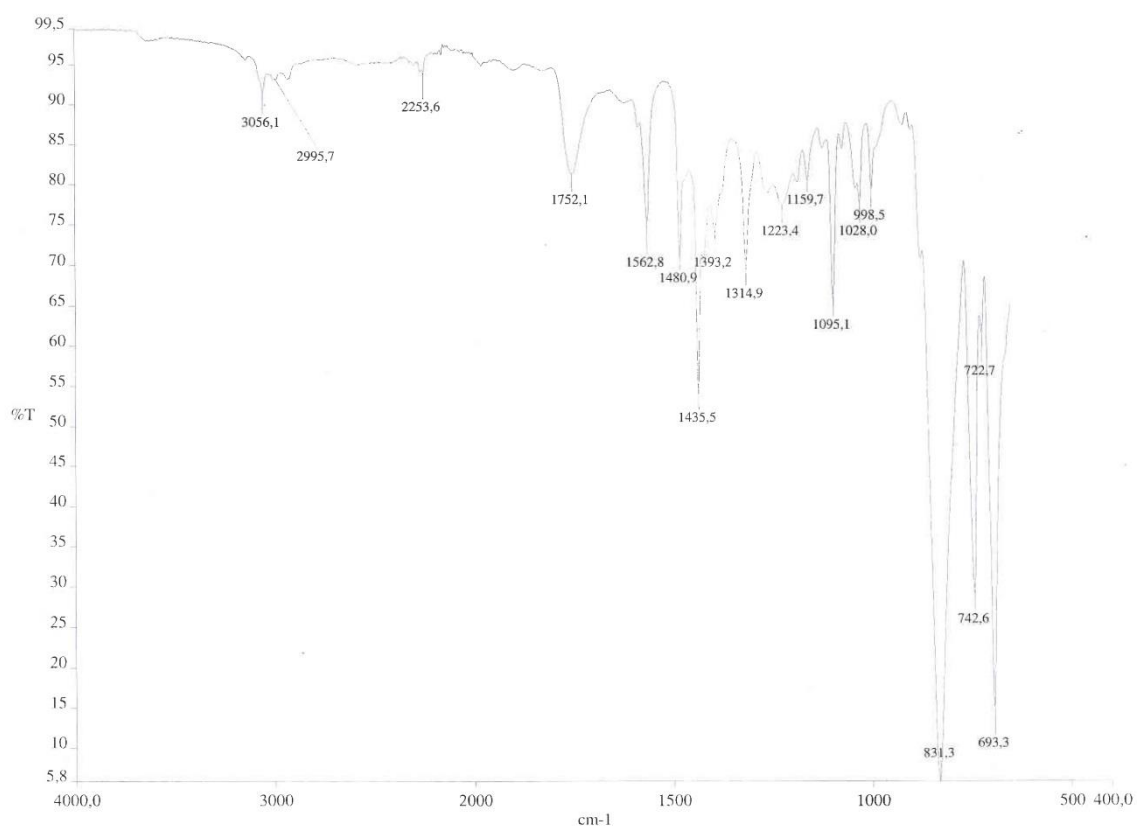
ESIMS (major negative-ions, CH_3OH) spectrum of $[(\text{LH})\text{Cu}(\text{PPh}_3)_2]\text{PF}_6$ (**10**).



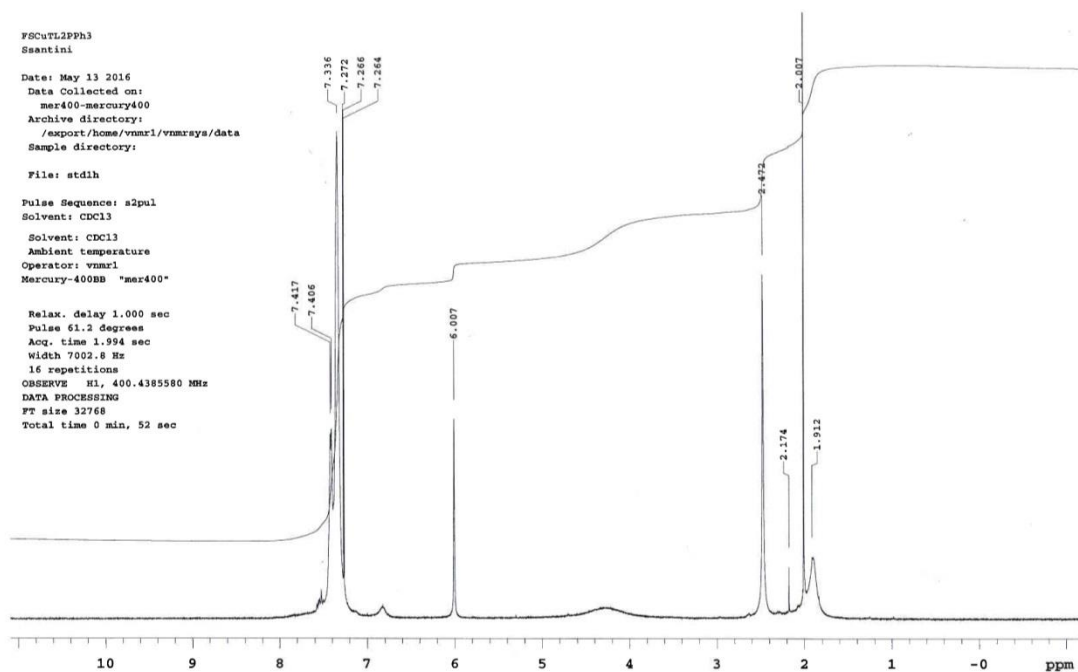
ESIMS (major positive-ions, CH₃OH) spectrum of [(LH)Cu(PPh₃)₂]PF₆ (**10**).



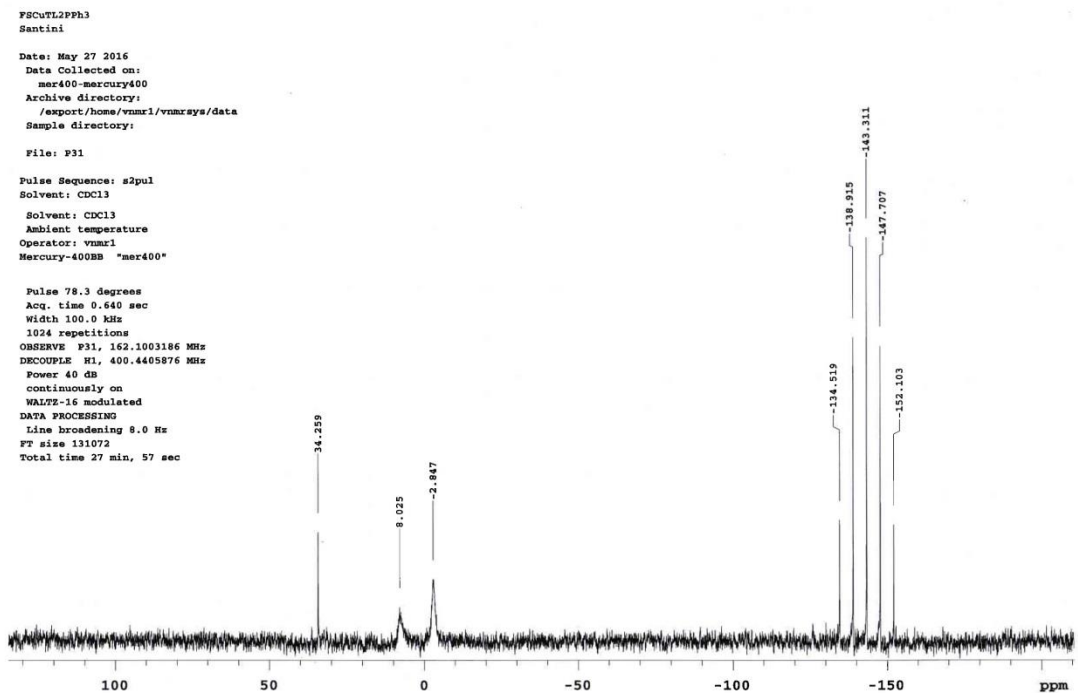
IR spectrum of [(L²H)Cu(PPh₃)₂]PF₆ (**11**).



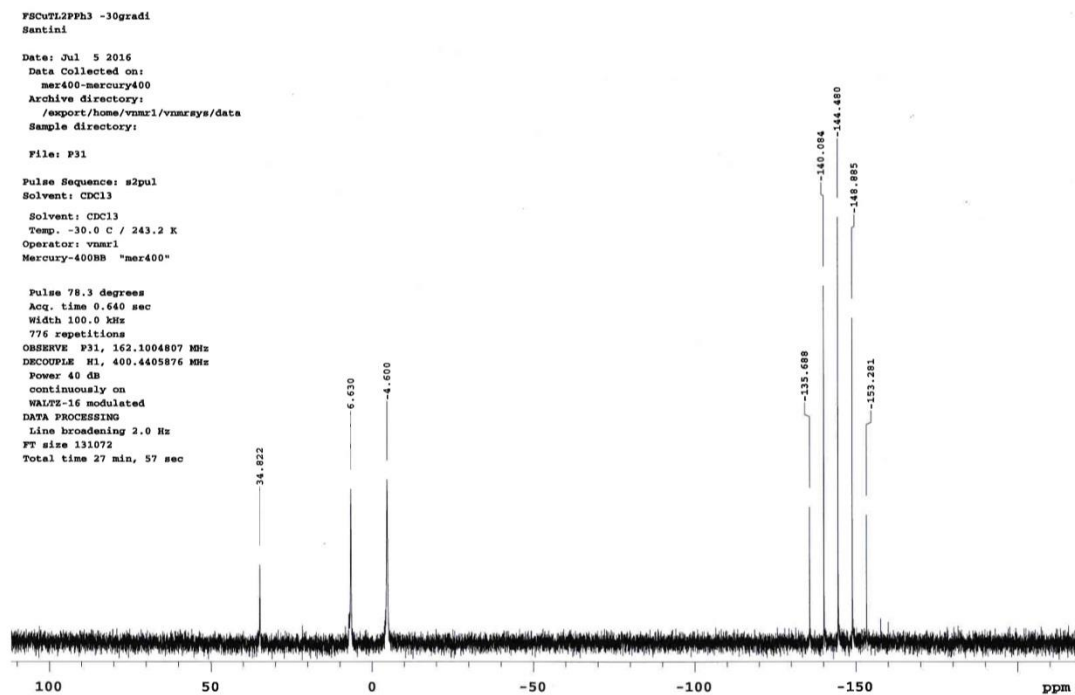
^1H NMR spectrum of $[(\text{L}^2\text{H})\text{Cu}(\text{PPh}_3)_2]\text{PF}_6$ (**11**) in CDCl_3 .



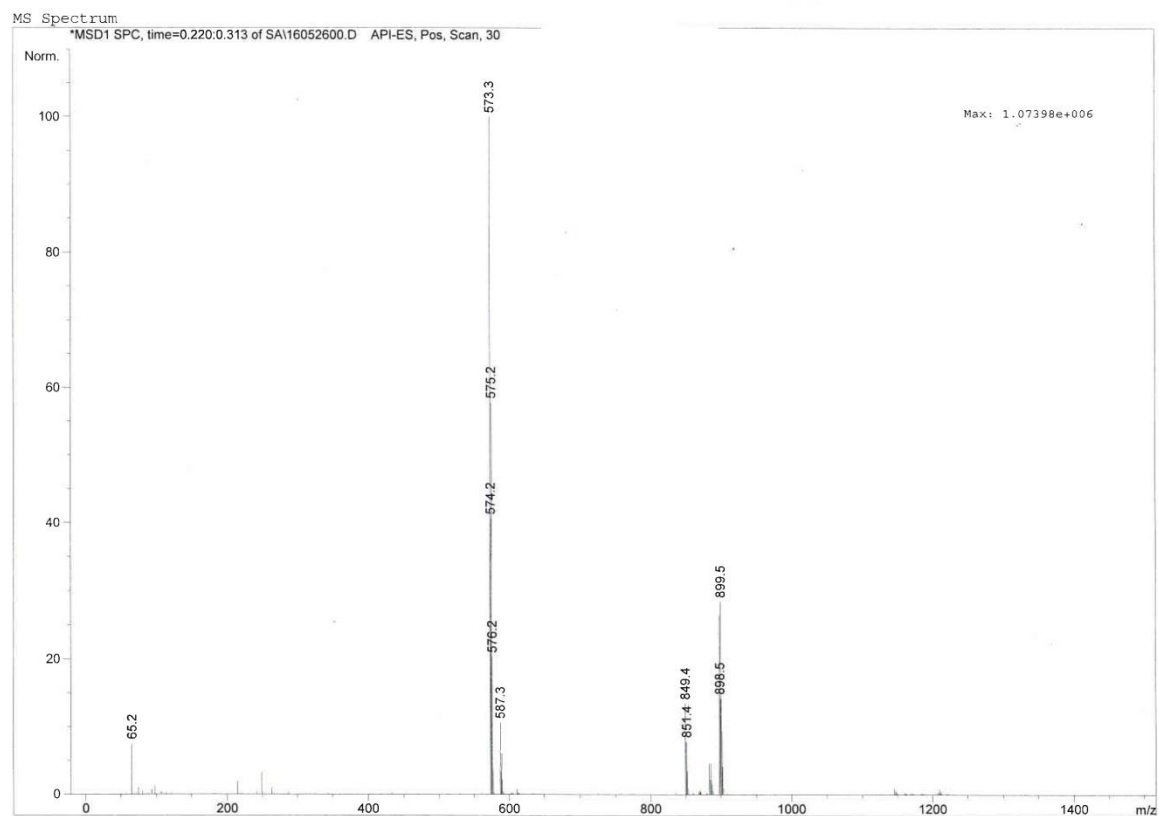
^{31}P NMR spectrum of $[(\text{L}^2\text{H})\text{Cu}(\text{PPh}_3)_2]\text{PF}_6$ (**11**) in CDCl_3 at 293K.



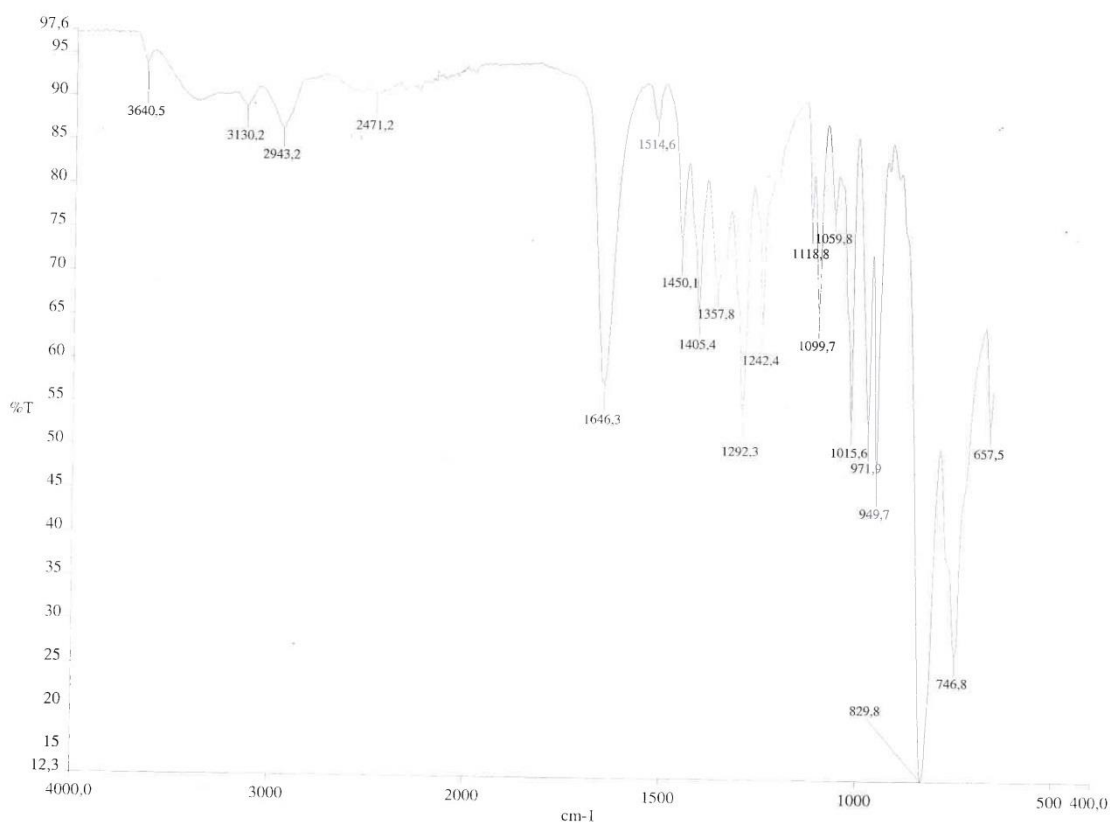
^{31}P NMR spectrum of $[(\text{L}^2\text{H})\text{Cu}(\text{PPh}_3)_2]\text{PF}_6$ (**11**) in CDCl_3 at 243K.



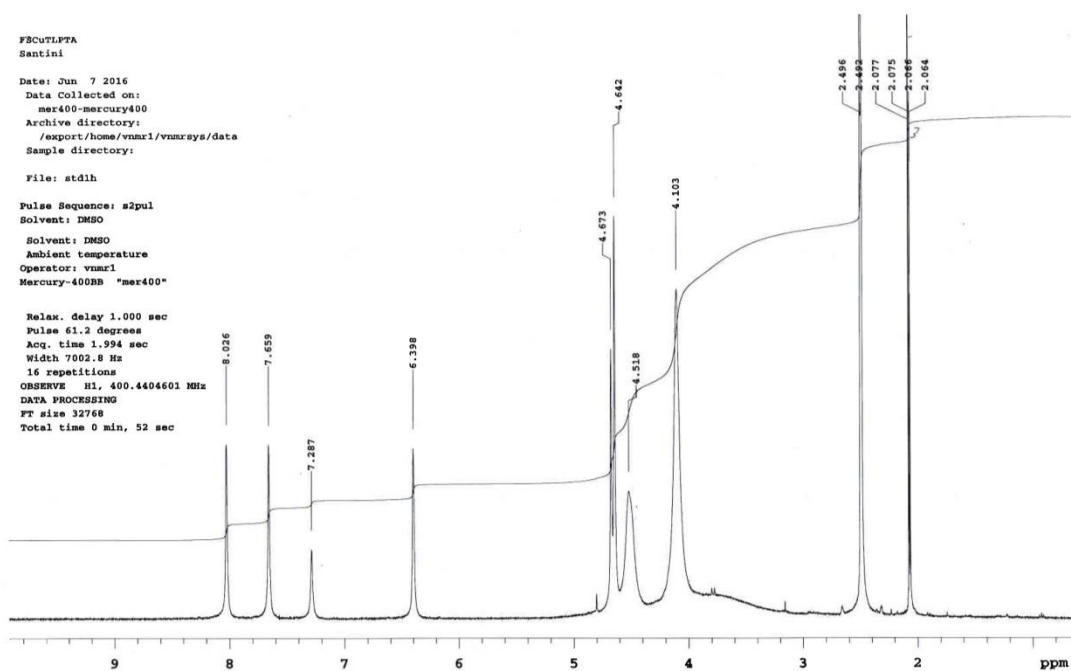
ESIMS (major positive-ions, CH_3OH) spectrum of $[(\text{LH})\text{Cu}(\text{PPh}_3)_2]\text{PF}_6$ (**11**).



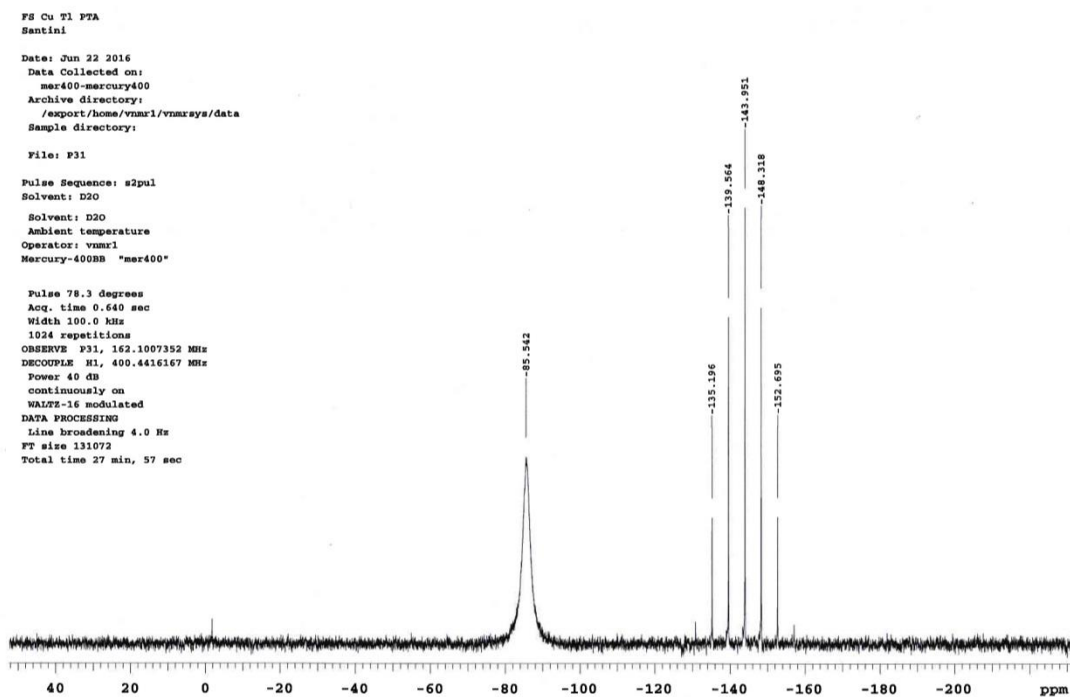
IR spectrum of $[(\text{LH})\text{Cu}(\text{PTA})_2]\text{PF}_6$ (**12**).



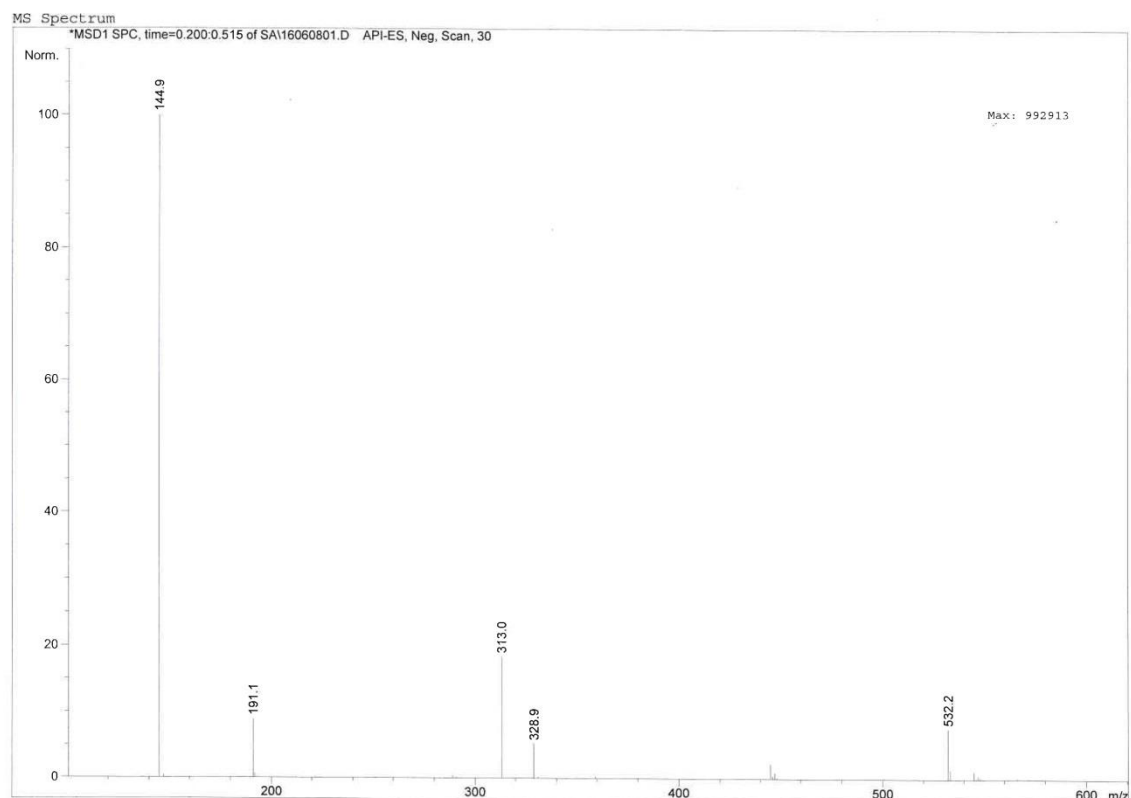
¹H NMR spectrum of $[(\text{LH})\text{Cu}(\text{PTA})_2]\text{PF}_6$ (**12**) in DMSO.



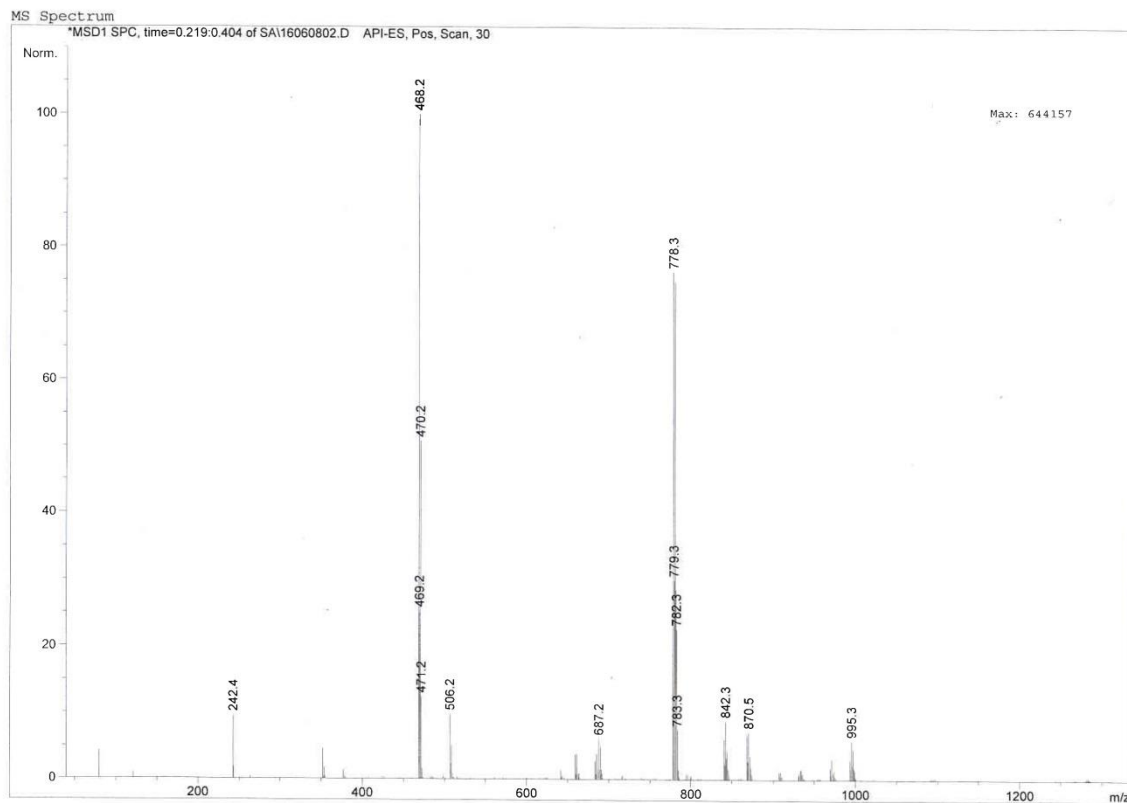
^{31}P NMR spectrum of $[(\text{LH})\text{Cu}(\text{PTA})_2]\text{PF}_6$ (**12**) in D_2O at 293K.



ESIMS (major negative-ions, CH_3CN) spectrum of $[(\text{LH})\text{Cu}(\text{PTA})_2]\text{PF}_6$ (**12**).



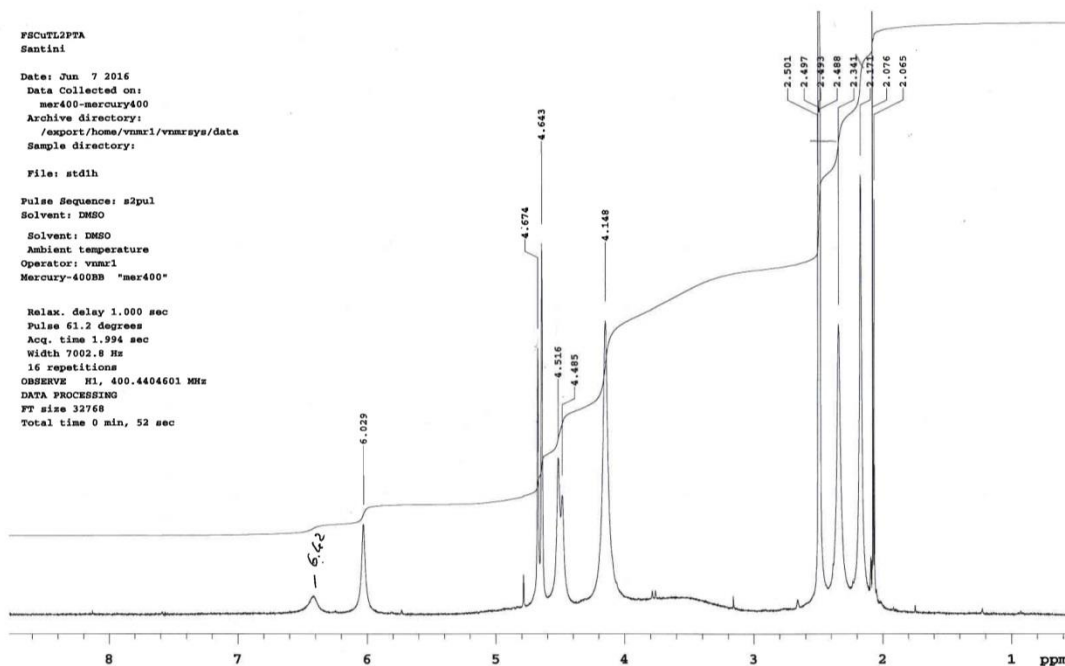
ESIMS (major positive-ions, CH₃CN) spectrum of [(LH)Cu(PTA)₂]PF₆ (**12**).



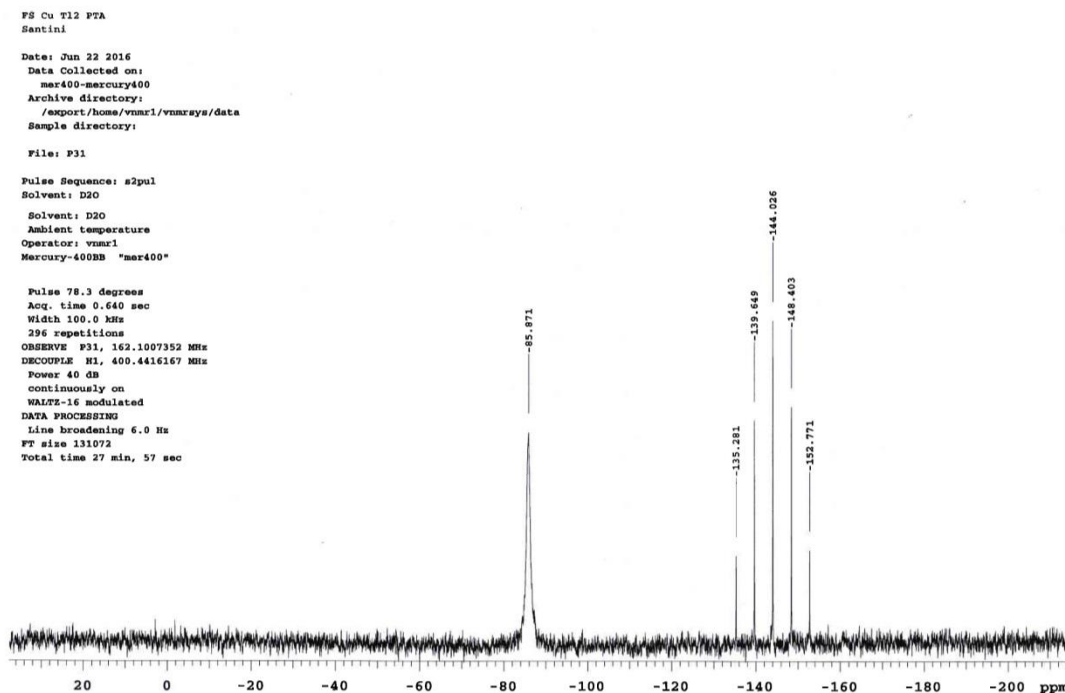
IR spectrum of [(L²H)Cu(PTA)₂]PF₆ (**13**).



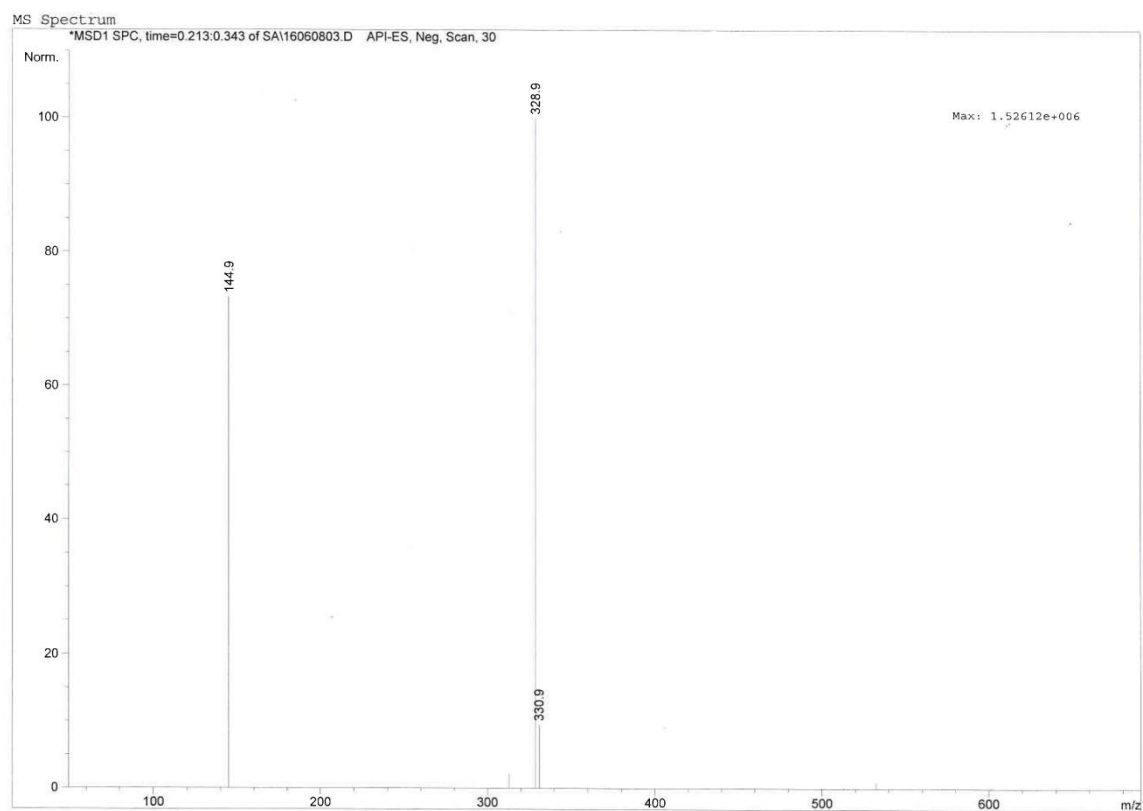
^1H NMR spectrum of $[(\text{L}^2\text{H})\text{Cu}(\text{PTA})_2]\text{PF}_6$ (**13**) in DMSO.



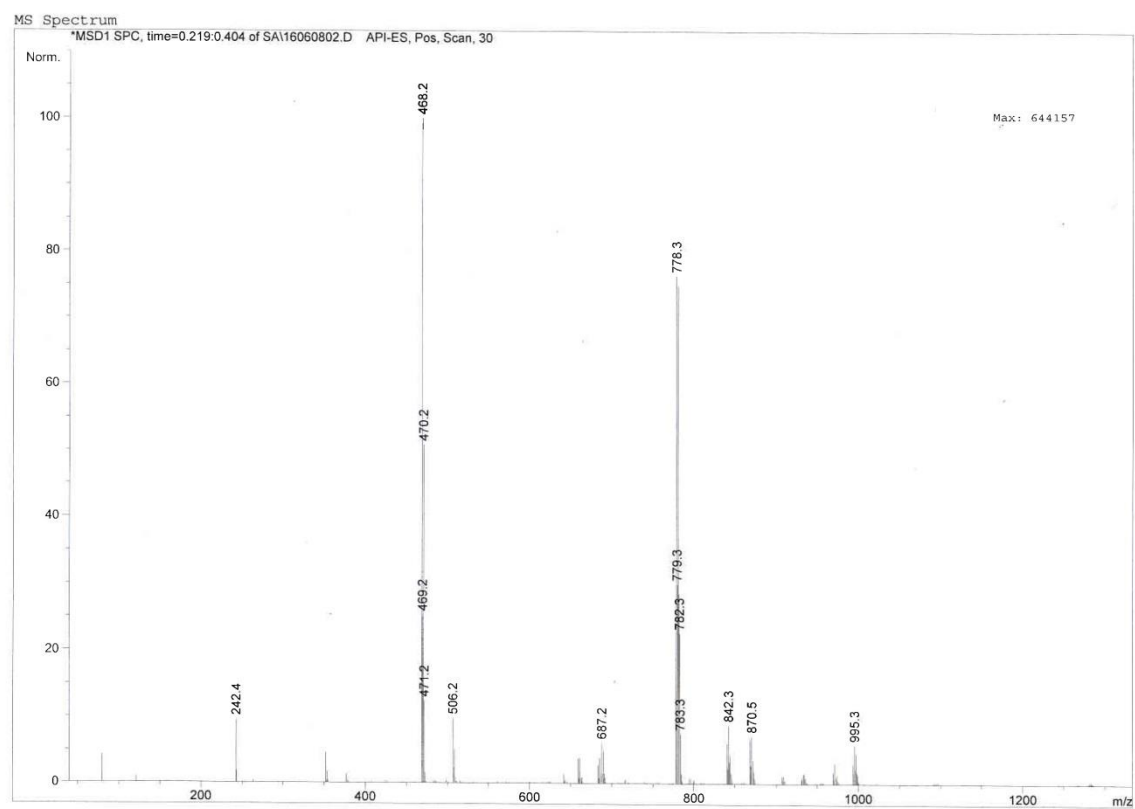
^{31}P NMR spectrum of $[(\text{L}^2\text{H})\text{Cu}(\text{PTA})_2]\text{PF}_6$ (**13**) in D_2O at 293K.



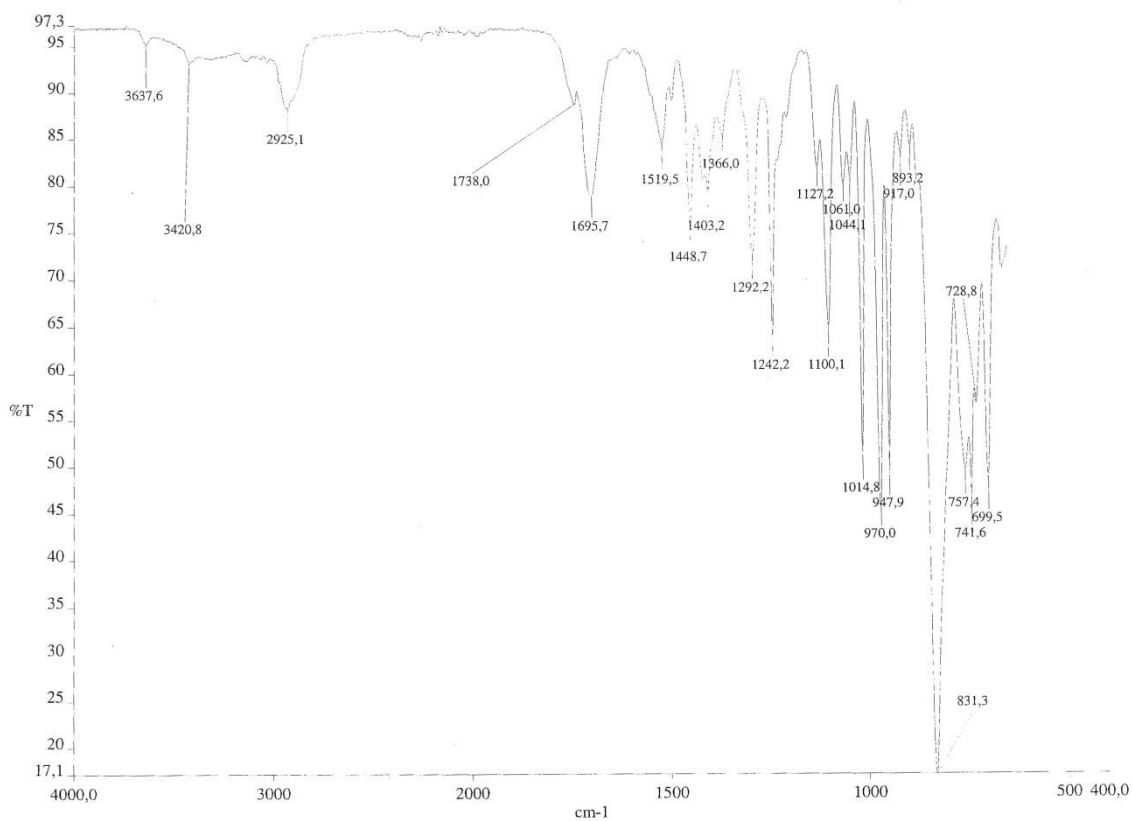
ESIMS (major negative-ions, CH₃CN) spectrum of [(L²H)Cu(PTA)₂]PF₆ (**13**).



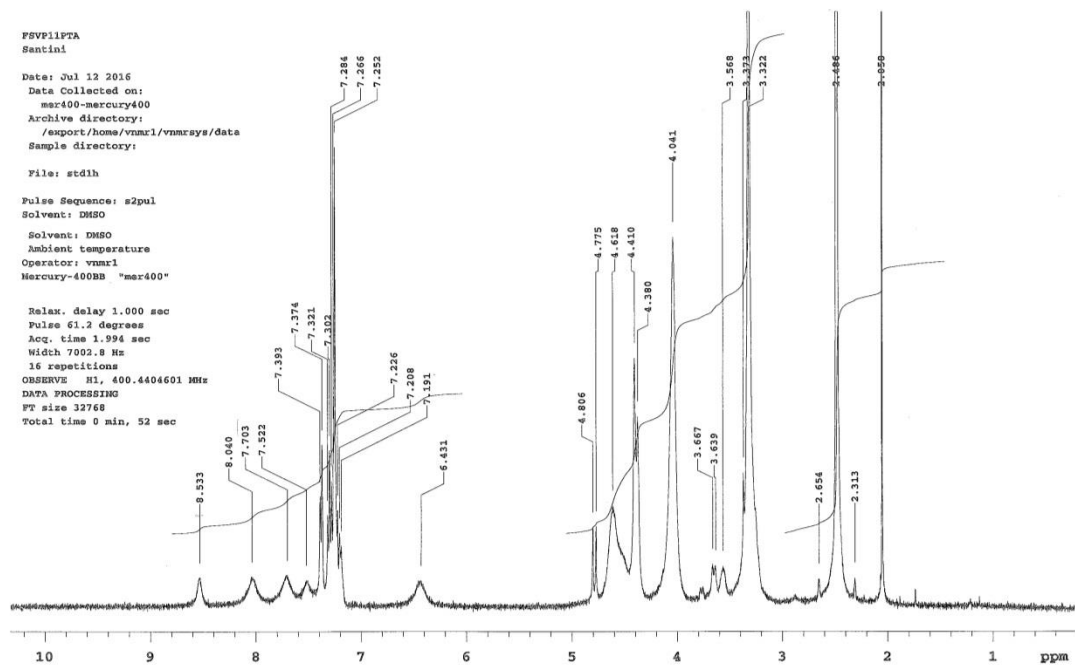
ESIMS (major positive-ions, CH₃CN) spectrum of [(L²H)Cu(PTA)₂]PF₆ (**13**).



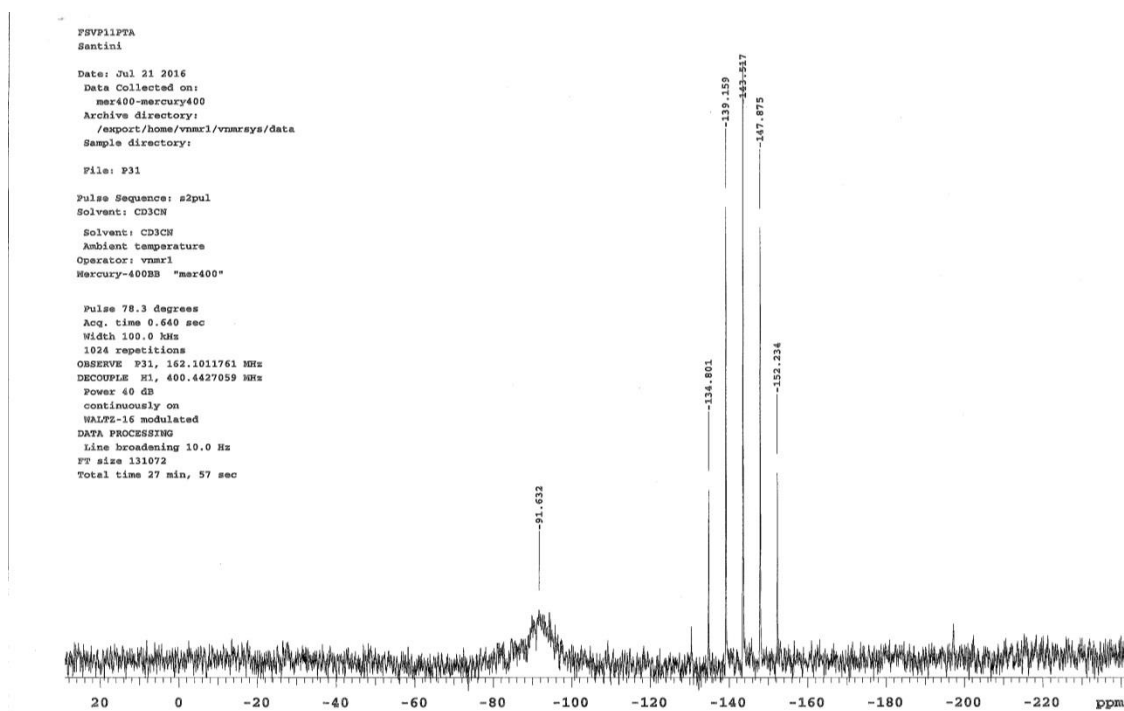
IR spectrum of $[(L^{NMDA})Cu(PTA)_2]PF_6$ (**14**).



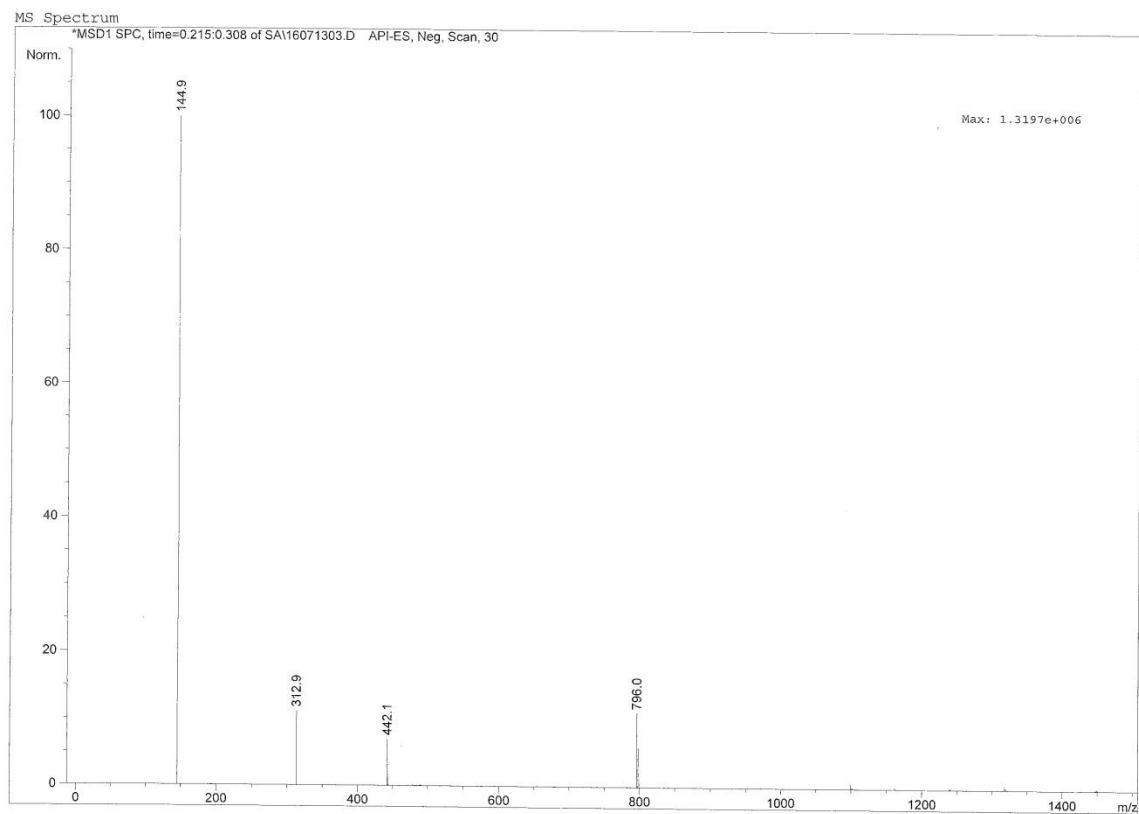
1H NMR spectrum of $[(L^{NMDA})Cu(PTA)_2]PF_6$ (**14**) in DMSO.



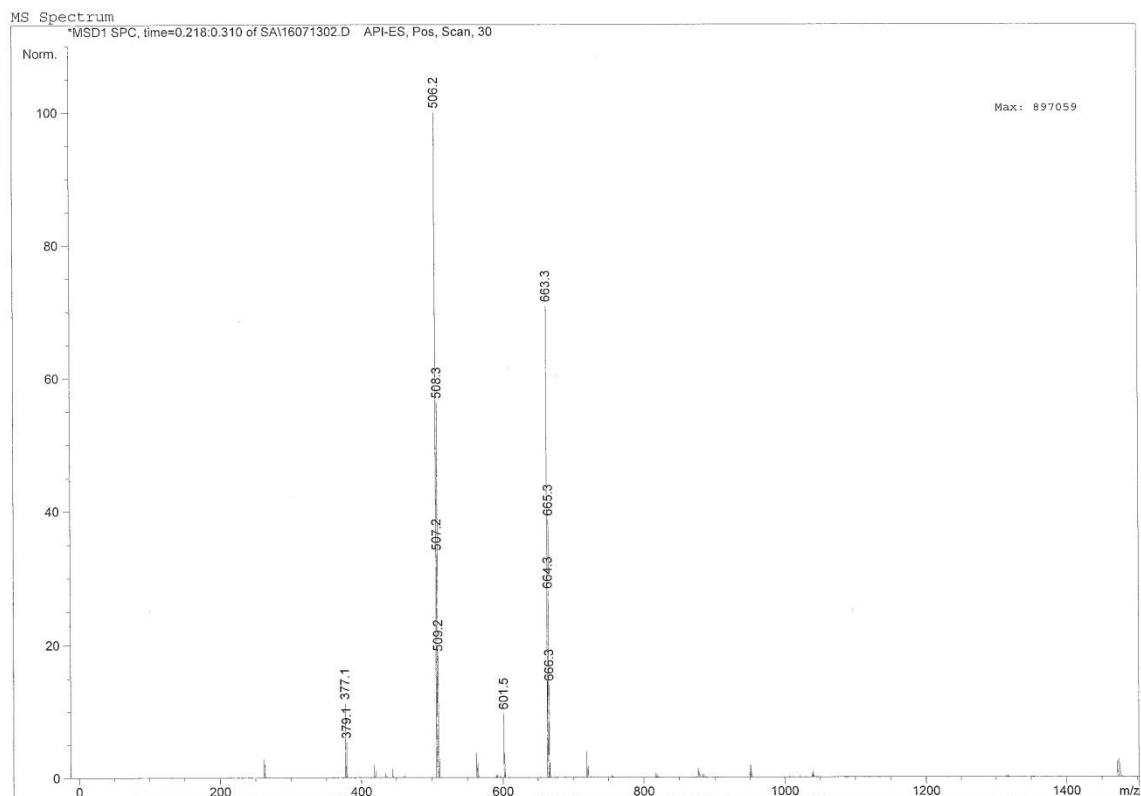
^{31}P NMR spectrum of $[(\text{L}^{\text{NMDA}})\text{Cu}(\text{PTA})_2]\text{PF}_6$ (**14**) in CD_3CN at 293K.



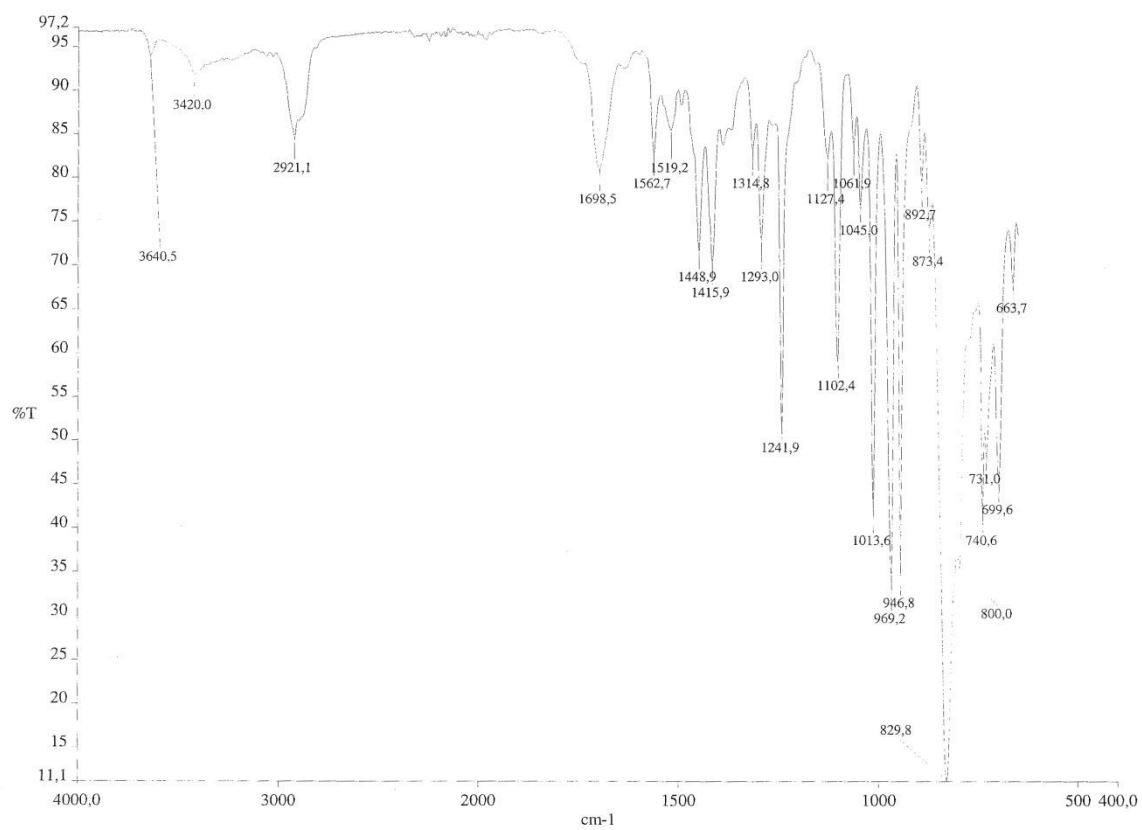
ESIMS (major negative-ions, CH_3OH) spectrum of $[(\text{L}^{\text{NMDA}})\text{Cu}(\text{PTA})_2]\text{PF}_6$ (**14**).



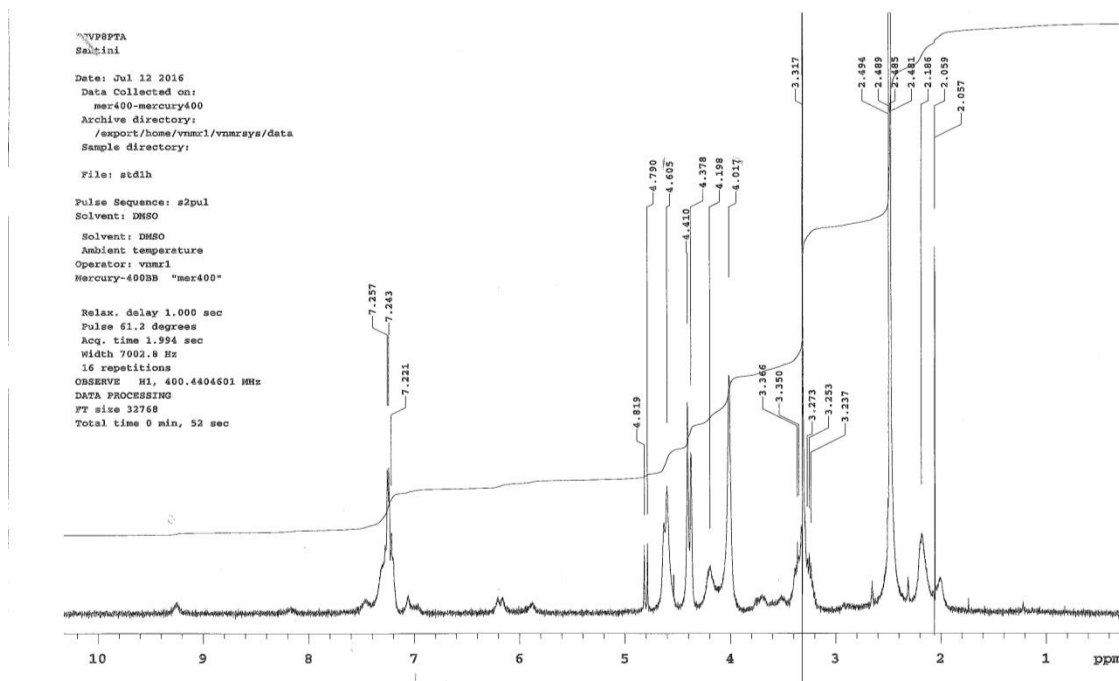
ESIMS (major positive-ions, CH₃OH) spectrum of [(L^{NMDA})Cu(PTA)₂]PF₆ (**14**).



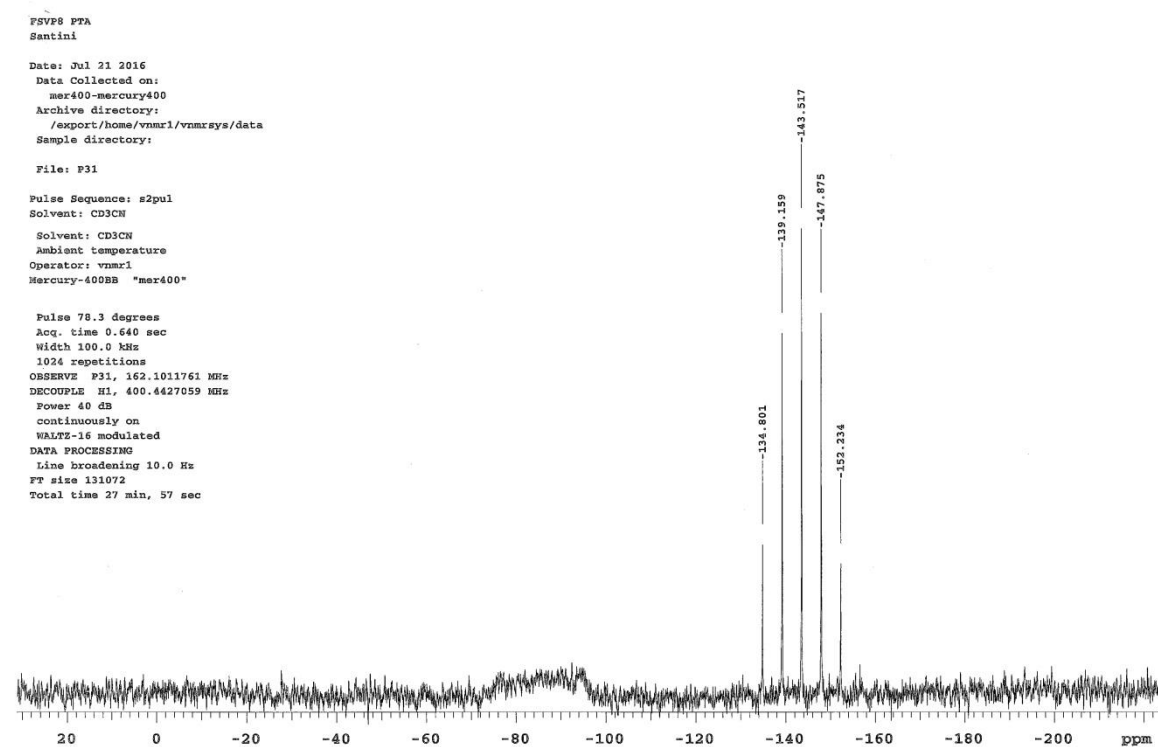
IR spectrum of [(L^{2NMDA})Cu(PTA)₂]PF₆ (**15**).



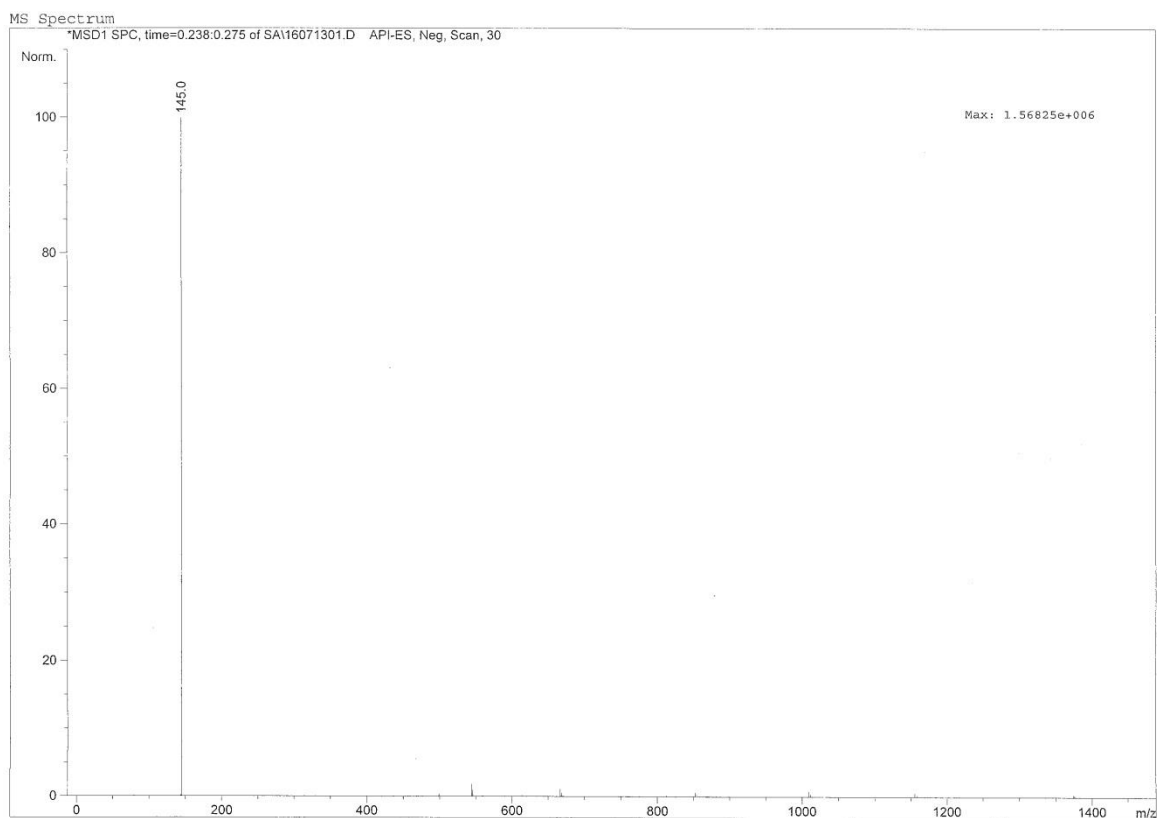
^1H NMR spectrum of $[(\text{L}^{2\text{NMDA}})\text{Cu}(\text{PTA})_2]\text{PF}_6$ (**15**) in DMSO.



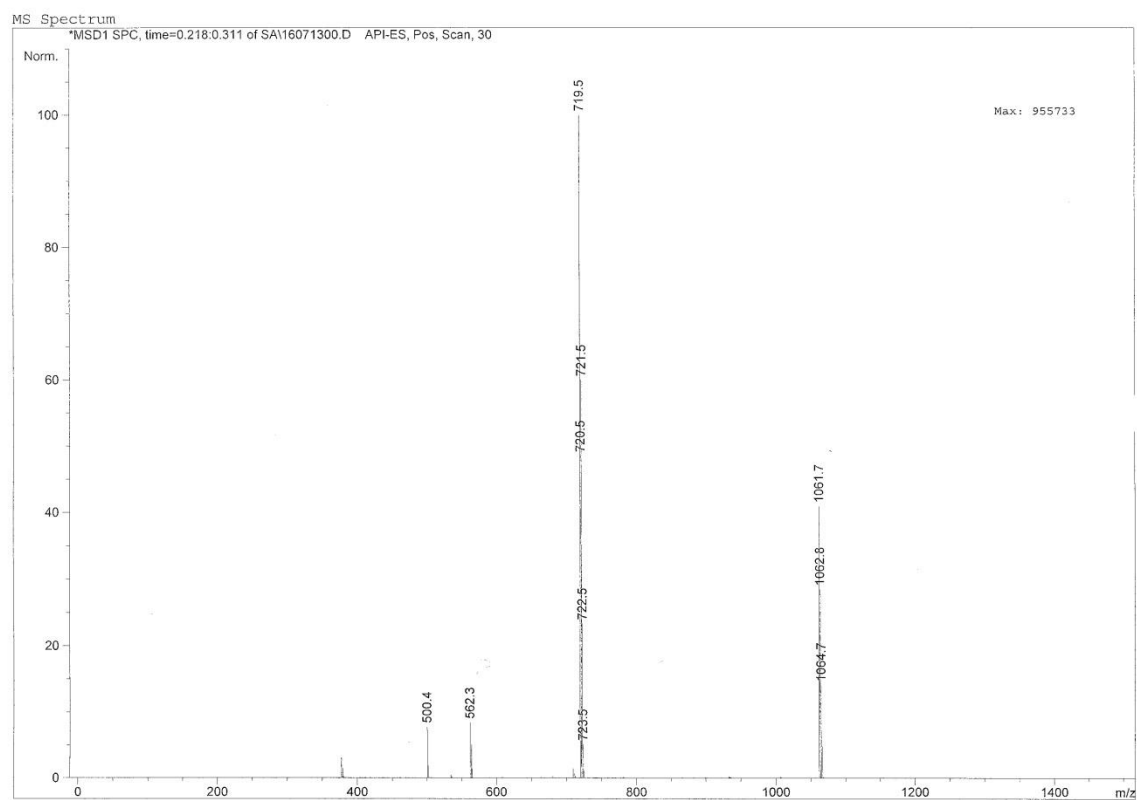
^{31}P NMR spectrum of $[(\text{L}^{2\text{NMDA}})\text{Cu}(\text{PTA})_2]\text{PF}_6$ (**15**) in CD_3CN at 293K.



ESIMS (major negative-ions, CH₃OH) spectrum of [(L^{2NMDA})Cu(PTA)₂]PF₆ (**15**).



ESIMS (major positive-ions, CH₃OH) spectrum of [(L^{2NMDA})Cu(PTA)₂]PF₆ (**15**).



V. References

1. Hambley, T. W., Developing new metal-based therapeutics: challenges and opportunities. *Dalton transactions* **2007**, (43), 4929-37.
2. Zhang, C. X.; Lippard, S. J., New metal complexes as potential therapeutics. *Current opinion in chemical biology* **2003**, 7 (4), 481-9.
3. Guo, Z.; Sadler, P. J., Metals in medicine. *Angewandte Chemie - International Edition* **1999**, 38 (11), 1513-1531.
4. Sessler, J. L.; Doctrow, S. R.; McMurry, T. J.; Lippard, S. J., *Medicinal Inorganic Chemistry* **2003**.
5. Gielen, M.; Tiekink, E. R. T., *Metallotherapeutic Drugs and Metal-Based Diagnostic Agents: The Use of Metals in Medicine*. 2005; p 1-598.
6. Sigel, H., *Metal Ions in Biological Systems*.
7. Keppler, B. K., *Metal Complexes in Cancer Chemotherapy* **1993**.
8. Orvig, C.; Abrams, M. J., Medicinal inorganic chemistry: introduction. *Chemical reviews* **1999**, 99 (9), 2201-4.
9. Thompson, K. H.; Orvig, C., Metal complexes in medicinal chemistry: new vistas and challenges in drug design. *Dalton transactions* **2006**, (6), 761-4.
10. Arnesano, F.; Natile, G., Mechanistic insight into the cellular uptake and processing of cisplatin 30 years after its approval by FDA. *Coordination Chemistry Reviews* **2009**, 253 (15-16), 2070-2081.
11. Rosenberg, B.; Vancamp, L.; Krigas, T., Inhibition of Cell Division in Escherichia Coli by Electrolysis Products from a Platinum Electrode. *Nature* **1965**, 205, 698-9.
12. Kauffman, G. B.; Pentimalli, R.; Doldi, S.; Hall, M. D., Michele Peyrone (1813‐1883), Discoverer of Cisplatin. *Platinum Metals Review* **2010**, 54 (4), 250-256.
13. Jung, Y.; Lippard, S. J., Direct cellular responses to platinum-induced DNA damage. *Chemical reviews* **2007**, 107 (5), 1387-407.
14. Boulikas, T.; Pantos, A.; Bellis, E.; Christofis, P., Designing platinum compounds in cancer: Structures and mechanisms. *Cancer Ther.* **2007**, 5, 537-583.
15. Van Zutphen, S.; Reedijk, J., Targeting platinum anti-tumour drugs: Overview of strategies employed to reduce systemic toxicity. *Coordination Chemistry Reviews* **2005**, 249 (24), 2845-2853.
16. Gust, R.; Beck, W.; Jaouen, G.; Schöenberger, H., Optimization of cisplatin for the treatment of hormone-dependent tumoral diseases. Part 2: Use of non-steroidal ligands. *Coordination Chemistry Reviews* **2009**, 253 (21-22), 2760-2779.
17. Gust, R.; Beck, W.; Jaouen, G.; Schöenberger, H., Optimization of cisplatin for the treatment of hormone dependent tumoral diseases. Part 1: Use of steroidal ligands. *Coordination Chemistry Reviews* **2009**, 253 (21-22), 2742-2759.
18. Bruijninx, P. C.; Sadler, P. J., New trends for metal complexes with anticancer activity. *Current opinion in chemical biology* **2008**, 12 (2), 197-206.

19. Petering, D. H., Carcinostatic copper complexes. *Metal Ions in Biological Systems* **1980**, *11*, 197-229.
20. Tisato, F.; Marzano, C.; Porchia, M.; Pellei, M.; Santini, C., Copper in diseases and treatments, and copper-based anticancer strategies. *Medicinal Research Reviews* **2010**, *30* (4), 708-749.
21. Marzano, C.; Pellei, M.; Tisato, F.; Santini, C., Copper complexes as anticancer agents. *Anti-Cancer Agents in Medicinal Chemistry* **2009**, *9* (2), 185-211.
22. Tardito, S.; Marchiò, L., Copper compounds in anticancer strategies. *Current Medicinal Chemistry* **2009**, *16* (11), 1325-1348.
23. Wang, T.; Guo, Z., Copper in medicine: Homeostasis, chelation therapy and antitumor drug design. *Current Medicinal Chemistry* **2006**, *13* (5), 525-537.
24. Duncan, C.; White, A. R., Copper complexes as therapeutic agents. *Metallomics* **2012**, *4* (2), 127-138.
25. Jung, Y.; Lippard, S. J., Direct cellular responses to platinum-induced DNA damage. *Chemical Reviews* **2007**, *107* (5), 1387-1407.
26. Kraatz, H. B.; Metzler-Nolte, N., *Concepts and Models in Bioinorganic Chemistry* **2006**.
27. Lippard, S. J.; Berg, J. M., *Principles of Bioinorganic Chemistry* **1994**.
28. Lönnerdal, B., Bioavailability of copper. *American Journal of Clinical Nutrition* **1996**, *63* (5), 821S-829S.
29. Frausto da Silva, J. J. R.; Williams, R. J. P., *The Biological Chemistry of the Elements* **1991**.
30. Bull, P. C.; Cox, D. W., Wilson disease and Menkes disease: new handles on heavy-metal transport. *Trends in Genetics* **1994**, *10* (7), 247-252.
31. Melník, M.; Kabešová, M., Copper(III) coordination compounds: classification and analysis of crystallographic and structural data. *Journal of Coordination Chemistry* **2000**, *50* (3-4), 323-338.
32. Mukherjee, R., Copper. In *Comprehensive Coordination Chemistry II*, 2004; Vol. 6, pp 747-910.
33. Kitajima, N.; Moro-oka, Y., Copper-dioxygen complexes. Inorganic and bioinorganic perspectives. *Chemical reviews* **1994**, *94* (3), 737-757.
34. Linder, M. C., *Biochemistry of Copper* **1991**.
35. Santini, C.; Pellei, M.; Gioia Lobbia, G.; Papini, G., Synthesis and properties of poly(pyrazolyl)borate and related boron-centered scorpionate ligands. Part A: Pyrazole-based systems. *Mini-Reviews in Organic Chemistry* **2010**, *7* (2), 84-124.
36. Bigmore, H. R.; Lawrence, S. C.; Mountford, P.; Tredget, C. S., Coordination, organometallic and related chemistry of tris(pyrazolyl) methane ligands. *Dalton transactions* **2005**, (4), 635-651.
37. Otero, A.; Fernández-Baeza, J.; Antiñolo, A.; Tejeda, J.; Lara-Sánchez, A., *Dalton Trans.* **2004**.

38. Otero, A.; Lara-Sánchez, A.; Fernández-Baeza, J.; Martínez-Caballero, E.; Márquez-Segovia, I.; Alonso-Moreno, C.; Sánchez-Barba, L. F.; Rodríguez, A. M.; López - Solera, I., New achiral and chiral NNE heteroscorpionate ligands. Synthesis of homoleptic lithium complexes as well as halide and alkyl scandium and yttrium complexes. *Dalton transactions* **2010**, 39 (3), 930-940.
39. Pellei, M.; Gioia Lobbia, G.; Papini, G.; Santini, C., Synthesis and properties of poly(pyrazolyl)borate and related boron-centered scorpionate ligands. part b: Imidazole-, triazole- and other heterocycle-based systems. *Mini-Reviews in Organic Chemistry* **2010**, 7 (3), 173-203.
40. Pellei, M.; Papini, G.; Trasatti, A.; Giorgetti, M.; Tonelli, D.; Minicucci, M.; Marzano, C.; Gandin, V.; Aquilanti, G.; Dolmella, A.; Santini, C., Nitroimidazole and glucosamine conjugated heteroscorpionate ligands and related copper(ii) complexes. Syntheses, biological activity and XAS studies. *Dalton transactions* **2011**, 40 (38), 9877-9888.
41. Santini, C.; Pellei, M.; Gandin, V.; Porchia, M.; Tisato, F.; Marzano, C., Advances in copper complexes as anticancer agents. *Chemical reviews* **2014**, 114 (1), 815-862.
42. Bowen, R. J.; Navarro, M.; Shearwood, A. M. J.; Healy, P. C.; Skelton, B. W.; Filipovska, A.; Berners-Price, S. J., 1: 2 Adducts of copper(I) halides with 1,2-bis(di-2-pyridylphosphino) ethane: Solid state and solution structural studies and antitumour activity. *Dalton transactions* **2009**, (48), 10861-10870.
43. Berners-Price, S. J.; Sadler, P. J., Phosphines and metal phosphine complexes: Relationship of chemistry to anticancer and other biological activity. *Struct. Bonding* **1988**, 70, 27-102.
44. Berners-Price, S. J.; Sant, M. E.; Christopherson, R. I.; Kuchel, P. W., ¹H and ³¹P NMR and HPLC studies of mouse L1210 leukemia cell extracts: The effect of Au(I) and Cu(I) diphosphine complexes on the cell metabolism. *Magnetic Resonance in Medicine* **1991**, 18 (1), 142-158.
45. Paterson, B. M.; Donnelly, P. S., Copper complexes of bis(thiosemicarbazones): From chemotherapeutics to diagnostic and therapeutic radiopharmaceuticals. *Chemical Society Reviews* **2011**, 40 (5), 3005-3018.
46. Tisato, F.; Refosco, F.; Porchia, M.; Tegoni, M.; Gandin, V.; Marzano, C.; Pellei, M.; Papini, G.; Lucato, L.; Seraglia, R.; Traldi, P., The relationship between the electrospray ionization behaviour and biological activity of some phosphino Cu(I) complexes. *Rapid Communications in Mass Spectrometry* **2010**, 24 (11), 1610-1616.
47. Marzano, C.; Gandin, V.; Pellei, M.; Colavito, D.; Papini, G.; Gioia Lobbia, G.; Del Giudice, E.; Porchia, M.; Tisato, F.; Santini, C., In vitro antitumor activity of the water soluble copper(I) complexes bearing the tris(hydroxymethyl)phosphine ligand. *Journal of Medicinal Chemistry* **2008**, 51 (4), 798-808.
48. Santini, C.; Pellei, M.; Papini, G.; Morresi, B.; Galassi, R.; Ricci, S.; Tisato, F.; Porchia, M.; Rigobello, M. P.; Gandin, V.; Marzano, C., In vitro antitumour activity of

- water soluble Cu(I), Ag(I) and Au(I) complexes supported by hydrophilic alkyl phosphine ligands. *Journal of Inorganic Biochemistry* **2011**, *105* (2), 232-240.
49. Porchia, M.; Benetollo, F.; Refosco, F.; Tisato, F.; Marzano, C.; Gandin, V., Synthesis and structural characterization of copper(I) complexes bearing N-methyl-1,3,5-triaza-7-phosphaadamantane (mPTA). Cytotoxic activity evaluation of a series of water soluble Cu(I) derivatives containing PTA, PTAH and mPTA ligands. *Journal of Inorganic Biochemistry* **2009**, *103* (12), 1644-1651.
 50. Gandin, V.; Pellei, M.; Tisato, F.; Porchia, M.; Santini, C.; Marzano, C., A novel copper complex induces paraptosis in colon cancer cells via the activation of ER stress signalling. *Journal of Cellular and Molecular Medicine* **2012**, *16* (1), 142-151.
 51. Zanella, A.; Gandin, V.; Porchia, M.; Refosco, F.; Tisato, F.; Sorrentino, F.; Scutari, G.; Rigobello, M. P.; Marzano, C., Cytotoxicity in human cancer cells and mitochondrial dysfunction induced by a series of new copper(I) complexes containing tris(2-cyanoethyl)phosphines. *Investigational New Drugs* **2011**, *29* (6), 1213-1223.
 52. Lazarou, K.; Bednarz, B.; Kubicki, M.; Verginadis, I. I.; Charalabopoulos, K.; Kourkoumelis, N.; Hadjikakou, S. K., Structural, photolysis and biological studies of the bis(μ -2-chloro)-tris(triphenylphosphine)-di-copper(I) and chloro-tris(triphenylphosphine)-copper(I) complexes. Study of copper(I)-copper(I) interactions. *Inorganica Chimica Acta* **2010**, *363* (4), 763-772.
 53. Sathyadevi, P.; Krishnamoorthy, P.; Butorac, R. R.; Cowley, A. H.; Dharmaraj, N., Synthesis of novel heterobimetallic copper(i) hydrazone Schiff base complexes: A comparative study on the effect of heterocyclic hydrazides towards interaction with DNA/protein, free radical scavenging and cytotoxicity. *Metallomics* **2012**, *4* (5), 498-511.
 54. Krishnamoorthy, P.; Sathyadevi, P.; Butorac, R. R.; Cowley, A. H.; Bhuvanesh, N. S. P.; Dharmaraj, N., Copper(i) and nickel(ii) complexes with 1:1 vs. 1:2 coordination of ferrocenyl hydrazone ligands: Do the geometry and composition of complexes affect DNA binding/cleavage, protein binding, antioxidant and cytotoxic activities? *Dalton transactions* **2012**, *41* (15), 4423-4436.
 55. Eichhorn, G. L.; Shin, Y. A., Interaction of metal ions with polynucleotides and related compounds. XII. The relative effect of various metal ions on DNA helicity. *Journal of the American Chemical Society* **1968**, *90* (26), 7323-7328.
 56. Takahara, P. M.; Frederick, C. A.; Lippard, S. J., Crystal structure of the anticancer drug cisplatin bound to duplex DNA. *Journal of the American Chemical Society* **1996**, *118* (49), 12309-12321.
 57. Kagawa, T. F.; Geierstanger, B. H.; Wang, A. H. J.; Ho, P. S., Covalent modification of guanine bases in double-stranded DNA. The 1.2-Å Z-DNA structure of d(CGCGCG) in the presence of CuCl₂. *Journal of Biological Chemistry* **1991**, *266* (30), 20175-20184.

58. Tan, J.; Wang, B.; Zhu, L., DNA binding and oxidative DNA damage induced by a quercetin copper(II) complex: Potential mechanism of its antitumor properties. *Journal of Biological Inorganic Chemistry* **2009**, *14* (5), 727-739.
59. Chakraborty, A.; Kumar, P.; Ghosh, K.; Roy, P., Evaluation of a Schiff base copper complex compound as potent anticancer molecule with multiple targets of action. *European Journal of Pharmacology* **2010**, *647* (1-3), 1-12.
60. Qiao, X.; Ma, Z. Y.; Xie, C. Z.; Xue, F.; Zhang, Y. W.; Xu, J. Y.; Qiang, Z. Y.; Lou, J. S.; Chen, G. J.; Yan, S. P., Study on potential antitumor mechanism of a novel Schiff Base copper(II) complex: Synthesis, crystal structure, DNA binding, cytotoxicity and apoptosis induction activity. *Journal of Inorganic Biochemistry* **2011**, *105* (5), 728-737.
61. Qin, Y.; Meng, L.; Hu, C.; Duan, W.; Zuo, Z.; Lin, L.; Zhang, X.; Ding, J., Gambogic acid inhibits the catalytic activity of human topoisomerase II α by binding to its ATPase domain. *Molecular Cancer Therapeutics* **2007**, *6* (9), 2429-2440.
62. Hall, I. H.; Taylor, K.; Miller, M. C.; Dothan, I. I. I.; Khan, X.; Bouet, M. A., F. M. *Anticancer Res.* **1997**, *17*, 2411.
63. Dou, Q. P.; Smith David, M.; Daniel Kenyon, G.; Kazi, A., Interruption of tumor cell cycle progression through proteasome inhibition: implications for cancer therapy. *Prog Cell Cycle Res FIELD Full Journal Title:Progress in cell cycle research* **2003**, *5*, 441-6.
64. Drexler, H. C. A., Activation of the cell death program by inhibition of proteasome function. *Proceedings of the National Academy of Sciences of the United States of America* **1997**, *94* (3), 855-860.
65. Daniel, K. G.; Gupta, P.; Harbach, R. H.; Guida, W. C.; Dou, Q. P., Organic copper complexes as a new class of proteasome inhibitors and apoptosis inducers in human cancer cells. *Biochemical Pharmacology* **2004**, *67* (6), 1139-1151.
66. Dou, Q. P.; Goldfarb, R. H., Bortezomib Millennium Pharmaceuticals. *IDrugs* **2002**, *5* (8), 828-834.
67. Chen, D.; Cui, Q. C.; Yang, H.; Barrea, R. A.; Sarkar, F. H.; Sheng, S.; Yan, B.; Reddy, G. P. V.; Dou, Q. P., Clioquinol, a therapeutic agent for alzheimer's disease, has proteasome-inhibitory, androgen receptor-suppressing, apoptosis-inducing, and antitumor activities in human prostate cancer cells and xenografts. *Cancer Research* **2007**, *67* (4), 1636-1644.
68. Daniel, K. G.; Chen, D.; Orlu, S.; Cui, Q. C.; Miller, F. R.; Dou, Q. P., Clioquinol and pyrrolidine dithiocarbamate complex with copper to form proteasome inhibitors and apoptosis inducers in human breast cancer cells. *Breast cancer research : BCR* **2005**, *7* (6), R897-R908.
69. Chen, D.; Peng, F.; Cui, Q. C.; Daniel, K. G.; Orlu, S.; Liu, J.; Dou, Q. P., Inhibition of prostate cancer cellular proteasome activity by a pyrrolidine dithiocarbamate-copper complex is associated with suppression of proliferation and induction of apoptosis. *Frontiers in Bioscience* **2005**, *10* (SUPPL. 3), 2932-2939.

70. Li, L.; Yang, H.; Chen, D.; Cui, C.; Ping Dou, Q., Disulfiram promotes the conversion of carcinogenic cadmium to a proteasome inhibitor with pro-apoptotic activity in human cancer cells. *Toxicology and Applied Pharmacology* **2008**, *229* (2), 206-214.
71. Pang, H.; Chen, D.; Cui, Q. C.; Ping Dou, Q., Sodium diethyldithiocarbamate, an AIDS progression inhibitor and a copper-binding compound, has proteasome-inhibitory and apoptosis-inducing activities in cancer cells. *International Journal of Molecular Medicine* **2007**, *19* (5), 809-816.
72. Frezza, M.; Hindo, S.; Chen, D.; Davenport, A.; Schmitt, S.; Tomco, D.; Dou, Q. P., Novel metals and metal complexes as platforms for cancer therapy. *Current Pharmaceutical Design* **2010**, *16* (16), 1813-1825.
73. Yu, Z.; Wang, F.; Milacic, V.; Li, X.; Cui, Q. C.; Zhang, B.; Yan, B.; Dou, Q. P., Evaluation of copper-dependent proteasome-inhibitory and apoptosis-inducing activities of novel pyrrolidine dithiocarbamate analogues. *International Journal of Molecular Medicine* **2007**, *20* (6), 919-925.
74. Tardito, S.; Bassanetti, I.; Bignardi, C.; Elviri, L.; Tegoni, M.; Mucchino, C.; Bussolati, O.; Franchi-Gazzola, R.; Marchiò, L., Copper binding agents acting as copper ionophores lead to caspase inhibition and paraptotic cell death in human cancer cells. *Journal of the American Chemical Society* **2011**, *133* (16), 6235-6242.
75. Xiao, Y.; Chen, D.; Zhang, X.; Cui, Q.; Fan, Y.; Bi, C.; Dou, Q. P., Molecular study on copper-mediated tumor proteasome inhibition and cell death. *International Journal of Oncology* **2010**, *37* (1), 81-87.
76. Costas, M.; Mehn, M. P.; Jensen, M. P.; Que, L., Dioxygen Activation at Mononuclear Nonheme Iron Active Sites: Enzymes, Models, and Intermediates. *Chemical reviews* **2004**, *104* (2), 939-986.
77. Parkin, G., Synthetic Analogues Relevant to the Structure and Function of Zinc Enzymes. *Chemical reviews* **2004**, *104* (2), 699-768.
78. Türkoglu, G.; Ulldemolins, C. P.; Müller, R.; Hübner, E.; Heinemann, F. W.; Wolf, M.; Burzla, N., Bis(3,5-dimethyl-4-vinylpyrazol-1-yl)acetic acid: A new heteroscorpionate building block for copolymers that mimic the 2-His-1-carboxylate facial triad. *European Journal of Inorganic Chemistry* **2010**, (19), 2962-2974.
79. Smith, J. N.; Hoffman, J. T.; Shirin, Z.; Carrano, C. J., H-Bonding Interactions and Control of Thiolate Nucleophilicity and Specificity in Model Complexes of Zinc Metalloproteins. *Inorganic Chemistry* **2005**, *44* (6), 2012-2017.
80. Conti, G.; Arribas, G.; Altomare, A.; Ciardelli, F., Influence of ligands and cocatalyst on the activity in ethylene polymerization of soluble titanium complexes. *Journal of Molecular Catalysis* **1994**, *89* (1), 41-50.
81. Doherty, S.; Errington, R. J.; Jarvis, A. P.; Collins, S.; Clegg, W.; Elsegood, M. R. J., Polymerization of ethylene by the electrophilic mixed cyclopentadienylpyridylalkoxide complexes [CpM{NC₅H₄(CR₂O)-₂}Cl₂] (M = Ti, Zr, R = Ph, Pri). *Organometallics* **1998**, *17* (16), 3408-3410.

82. Nomura, K.; Naga, N.; Miki, M.; Yanagi, K.; Imai, A., Synthesis of various nonbridged titanium(IV) cyclopentadienyl-aryloxy complexes of the type CpTi(OAr)X₂ and their use in the catalysis of alkene polymerization. Important roles of substituents on both aryloxy and cyclopentadienyl groups. *Organometallics* **1998**, *17* (11), 2152-2154.
83. Kopf, H.; Holzberger, B.; Pietraszuk, C.; Hübner, E.; Burzlaff, N., Neutral ruthenium carbene complexes bearing N,N,O heteroscorpionate ligands: Syntheses and activity in metathesis reactions. *Organometallics* **2008**, *27* (22), 5894-5905.
84. Ritter, T.; Hejl, A.; Wenzel, A. G.; Funk, T. W.; Grubbs, R. H., A standard system of characterization for olefin metathesis catalysts. *Organometallics* **2006**, *25* (24), 5740-5745.
85. Groves, J. T.; Quinn, R., Aerobic epoxidation of olefins with ruthenium porphyrin catalysts. *Journal of the American Chemical Society* **1985**, *107* (20), 5790-5792.
86. Türkoglu, G.; Tampier, S.; Strinitz, F.; Heinemann, F. W.; Hübner, E.; Burzlaff, N., Ruthenium carbonyl complexes bearing bis(pyrazol-1-yl)carboxylato ligands. *Organometallics* **2012**, *31* (6), 2166-2174.
87. Rhinehart, J. L.; Manbeck, K. A.; Buzak, S. K.; Lippa, G. M.; Brennessel, W. W.; Goldberg, K. I.; Jones, W. D., Catalytic arene H/D exchange with novel rhodium and iridium complexes. *Organometallics* **2012**, *31* (5), 1943-1952.
88. Tomek, E. S.; Lacrosse, L. A.; Nemirovsky, E. N.; Olive, F. M., NMDA Receptor Modulators in the Treatment of Drug Addiction. *Pharmaceuticals* **2013**, *6* (2).
89. Martin, W. R.; Eades, C. G.; Thompson, J. A.; Huppler, R. E.; Gilbert, P. E., The effects of morphine- and nalorphine- like drugs in the nondependent and morphine-dependent chronic spinal dog. *Journal of Pharmacology and Experimental Therapeutics* **1976**, *197* (3), 517.
90. Zukin, S. R.; Brady, K. T.; Slifer, B. L.; Balster, R. L., Behavioral and biochemical stereoselectivity of sigma opiate/PCP receptors. *Brain Res* **1984**, *294* (1), 174-177.
91. Quirion, R.; Bowen, W. D.; Itzhak, Y.; Junien, J. L.; Musacchio, J. M.; Rothman, R. B.; Su, T. P.; Tam, S. W.; Taylor, D. P., A proposal for the classification of sigma binding sites. *Trends in pharmacological sciences* **1992**, *13* (3), 85-6.
92. Bowen, W. D., Sigma receptors: recent advances and new clinical potentials. *Pharmaceutica acta Helvetiae* **2000**, *74* (2-3), 211-8.
93. Walker, J. M.; Bowen, W. D.; Walker, F. O.; Matsumoto, R. R.; De Costa, B.; Rice, K. C., Sigma receptors: biology and function. *Pharmacological Reviews* **1990**, *42* (4), 355.
94. Vilner, B. J.; John, C. S.; Bowen, W. D., Sigma-1 and Sigma-2 Receptors Are Expressed in a Wide Variety of Human and Rodent Tumor Cell Lines. *Cancer Research* **1995**, *55* (2), 408.
95. Guitart, X.; Codony, X.; Monroy, X., Sigma receptors: biology and therapeutic potential. *Psychopharmacology* **2004**, *174* (3), 301-319.

96. van Waarde, A.; Rybczynska, A. A.; Ramakrishnan, N. K.; Ishiwata, K.; Elsinga, P. H.; Dierckx, R. A. J. O., Potential applications for sigma receptor ligands in cancer diagnosis and therapy. *Biochim Biophys Acta* **2015**, *1848* (10 Pt B), 2703-2714.
97. Bonifazi, A.; Del Bello, F.; Mammoli, V.; Piergentili, A.; Petrelli, R.; Cimarelli, C.; Pellei, M.; Schepmann, D.; Wünsch, B.; Barocelli, E.; Bertoni, S.; Flammini, L.; Amantini, C.; Nabissi, M.; Santoni, G.; Vistoli, G.; Quaglia, W., Novel Potent N-Methyl-d-aspartate (NMDA) Receptor Antagonists or σ_1 Receptor Ligands Based on Properly Substituted 1,4-Dioxane Ring. *Journal of Medicinal Chemistry* **2015**, *58* (21), 8601-8615.
98. Porchia, M.; Papini, G.; Santini, C.; Gioia Lobbia, G.; Pellei, M.; Tisato, F.; Bandoli, G.; Dolmella, A., Novel Rhenium(V) Oxo Complexes Containing Bis(pyrazol-1-yl)acetate and Bis(pyrazol-1-yl) Sulfonate as Tripodal N,N,O-heteroscorpionate Ligands. *Inorganic Chemistry* **2005**, *44* (11), 4045-4054.